U.S. Department
of Transportation
**Federal Railroad
Administration**

Analytical Descriptions of Track Geometry Variations

Office of Research and
Development
Washington DC 20590

Volume I - Main Text

A. Hamid
K. Rasmussen
M. Baluja
T-L. Yang

ENSCO, Inc.
Transportation Technology Engineering Division
5400 Port Royal Road
Springfield VA 22151

DOT/FRA/ORD-83/03.1

December 1983

This document is disseminated under the sponsorship of the Department of Transportation in the interest of information exchange. The United States Government assumes no liability for its contents or use thereof.

The contents of this report reflect the view of ENSCO, Inc. who is responsible for the facts and the accuracy of the data presented herein. The contents do not necessarily reflect the official view or policy of the Department of Transportation. This report does not constitute a standard, specification, or regulation.

Technical Report Documentation Page

1. Report No.	2. Government Accession No.	3. Recipient's Catalog No.
DOT/FRA/ORD-83/03.1		

4. Title and Subtitle	5. Report Date
ANALYTICAL DESCRIPTIONS OF TRACK GEOMETRY VARIATIONS VOLUME I - MAIN TEXT	December 1983
	6. Performing Organization Code 1444-105-08
7. Author(s) A. Hamid, K. Rasmussen, M. Baluja & T-L. Yang	8. Performing Organization Report No. DOT-FR-82-03
9. Performing Organization Name and Address ENSCO, INC. TRANSPORTATION TECHNOLOGY ENGINEERING DIVISION 5400 Port Royal Road Springfield, VA 22151	10. Work Unit No. (TRAIS) 11. Contract or Grant No. DTFR53-80-C-00002
12. Sponsoring Agency Name and Address DEPARTMENT OF TRANSPORTATION FEDERAL RAILROAD ADMINISTRATION 400 SEVENTH ST., S.W. WASHINGTON, DC 20590	13. Type of Report and Period Covered FINAL REPORT MAY 1976-JULY 1981 14. Sponsoring Agency Code

15. Supplementary Notes

Volume II contains the appendices.

16. Abstract

Analyses of recorded track geometry measurements were conducted to develop analytical representations of track geometry variations that exist on the U.S. railroad track. These analytical representations include: 1) continuous stationary random variations described by power spectral density functions with a normalized frequency characteristic and a roughness amplitude; 2) randomly modulated periodic effects associated with rail length which are described by joint amplitude statistics and a shape function; and 3) isolated events described by a shape function, amplitude and characteristic length. The parameters of these representations are obtained as a function of current FRA track classes for gage, surface, crosslevel and alignment.

Analyses are also presented to establish the relationships and statistical correlations between the track geometry variables. The effects of curvature and superelevation on gage, alignment and surface variations are also discussed.

The results of the work presented here are expected to be applied to vehicle track interaction simulation studies related to rail car safety, performance and lading damage. A current application being conducted under concurrent efforts is the development of performance based limits on permissible track geometry variations that can be directly related to the railroad operational safety.

17. Key Words	18. Distribution Statement
Track Geometry Track Irregularities Analytical Descriptions Track Geometry Models	This document is available to the public through the National Technical Information Service, Springfield, VA 22161

19. Security Classif. (of this report)	20. Security Classif. (of this page)	21. No. of Pages	22. Price
Unclassified	Unclassified	148	

Form DOT F 1700.7 (8-72) Reproduction of completed page authorized

PREFACE

Analytical descriptions of track geometry variations are necessary to conduct design and simulation studies intended to improve the performance, reliability and safety of the rail transportation system. Accordingly, this report gives the analytical descriptions of geometric variations of the United States track in a form suitable for these studies.

The work described in this report was conducted under the track characterization program. This program was directed by the Transportation Systems Center (TSC) in support of the Improved Track Structures Research program of the Federal Railroad Administration's (FRA) Office of Rail Safety Research. These efforts were carried out under contracts DOT-TSC-1211; DOT-TSC-1631; DOT-FR-64113, Task 462; and DTFR53-80-C-00002, Task 105.

The authors wish to acknowledge the contribution of Dr. Herbert Weinstock of TSC in the technical direction of the program. The authors also wish to thank Messrs. W. B. O'Sullivan and R. Krick of FRA for their support and comments.

Appreciation is also expressed to ENSCO co-workers Messrs. E. Cunney, E. Howerter, K. Kesler and Drs. M. Kenworthy and R. Owings for a thorough review which greatly improved the quality of this report. The efforts of Mrs. C. McAlee in typing, editing and assembly of this report are greatly appreciated.

METRIC CONVERSION FACTORS

Approximate Conversions to Metric Measures

Symbol	When You Know	Multiply by	To Find	Symbol
		LENGTH		
in	inches	*2.5	centimeters	cm
ft	feet	30	centimeters	cm
yd	yards	0.9	meters	m
mi	miles	1.6	kilometers	km
		AREA		
in^2	square inches	6.5	square centimeters	cm^2
ft^2	square feet	0.09	square meters	m^2
yd^2	square yards	0.8	square meters	m^2
mi^2	square miles	2.6	square kilometers	km^2
	acres	0.4	hectares	ha
		MASS (weight)		
oz	ounces	28	grams	g
lb	pounds	0.45	kilograms	kg
	short tons (2000 lb)	0.9	tonnes	t
		VOLUME		
tsp	teaspoons	5	milliliters	ml
Tbsp	tablespoons	15	milliliters	ml
fl oz	fluid ounces	30	milliliters	ml
c	cups	0.24	liters	l
pt	pints	0.47	liters	l
qt	quarts	0.95	liters	l
gal	gallons	3.8	liters	l
ft^3	cubic feet	0.03	cubic meters	m^3
yd^3	cubic yards	0.76	cubic meters	m^3
		TEMPERATURE (exact)		
°F	Fahrenheit temperature	5/9 (after subtracting 32)	Celsius temperature	°C

*1 in. = 2.54 cm (exactly). For other exact conversions and more detail tables see NBS Misc. Publ. 286, Units of Weight and Measures. Price $2.25 SD Catalog No. C13 10 286.

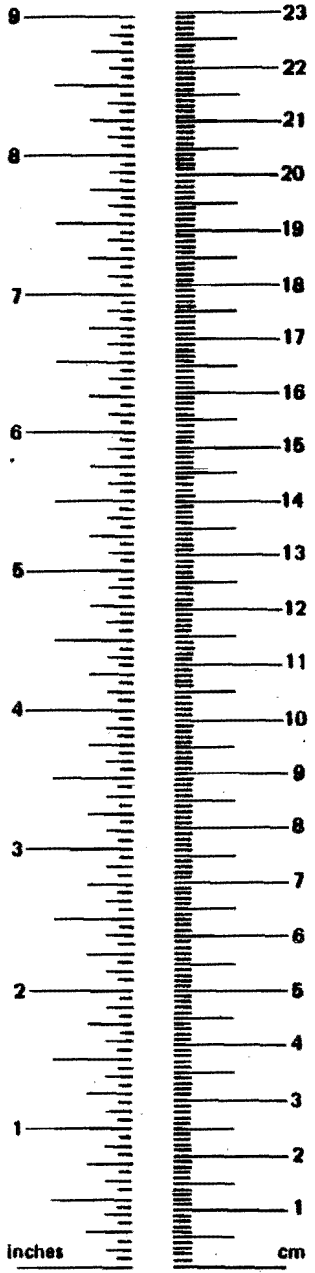

Approximate Conversions from Metric Measures

Symbol	When You Know	Multiply by	To Find	Symbol
		LENGTH		
mm	millimeters	0.04	inches	in
cm	centimeters	0.4	inches	in
m	meters	3.3	feet	ft
m	meters	1.1	yards	yd
km	kilometers	0.6	miles	mi
		AREA		
cm^2	square centimeters	0.16	square inches	in^2
m^2	square meters	1.2	square yards	yd^2
km^2	square kilometers	0.4	square miles	mi^2
ha	hectares (10,000 m^2)	2.5	acres	
		MASS (weight)		
g	grams	0.035	ounces	oz
kg	kilograms	2.2	pounds	lb
t	tonnes (1000 kg)	1.1	short tons	
		VOLUME		
ml	milliliters	0.03	fluid ounces	fl oz
l	liters	2.1	pints	pt
l	liters	1.06	quarts	qt
l	liters	0.26	gallons	gal
m^3	cubic meters	36	cubic feet	ft^3
m^3	cubic meters	1.3	cubic yards	yd^3
		TEMPERATURE (exact)		
°C	Celsius temperature	9/5 (then add 32)	Fahrenheit temperature	°F

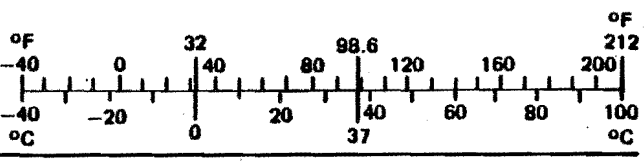

TABLE FOR METRIC CONVERSION OF PSD LEVELS

Given:	To find: $in^2/cy/ft$ — Multiply by:	To find: $cm^2/cy/m$ — Multiply by:
$ft^2/cy/ft$	144.	2.83×10^2
$in^2/cy/ft$	1.00	1.97
$in^2/cy/in$	8.33×10^{-2}	0.164
$ft^2/rad/ft$	9.05×10^2	1.78×10^3
$in^2/rad/ft$	6.28	12.4
$in^2/rad/in$	0.524	1.03
$m^2/cy/m$	5.09×10^3	1.00×10^4
$cm^2/cy/m$	0.509	1.00
$cm^2/cy/cm$	5.09×10^{-3}	1.00×10^{-2}
$m^2/rad/m$	3.20×10^4	6.28×10^4
$cm^2/rad/m$	3.20	6.28
$cm^2/rad/cm$	3.20×10^{-2}	6.28×10^{-2}

TABLE FOR METRIC CONVERSION OF SPATIAL FREQUENCY

Given:	To find: cy/ft — Multiply by:	To find: cy/m — Multiply by:
cy/ft	1.00	3.28
cy/in	12.0	39.4
rad/ft	0.159	4.85×10^{-2}
rad/in	1.91	4.04×10^{-3}
cy/m	0.305	1.00
cy/cm	30.5	1.00×10^2
rad/m	4.85×10^{-2}	0.159
rad/cm	4.85	15.9

TABLE FOR METRIC CONVERSION OF ROUGHNESS PARAMETER UNITS

Given:	To find: in^2-cy/ft (Multiply by:)	To find: cm^2-cy/m (Multiply by:)
ft^2-cy/ft	144.	3.05×10^{-3}
in^2-cy/ft	1.00	21.2
in^2-cy/in	12.0	254.
ft^2-rad/ft	22.9	485.
in^2-rad/ft	0.159	3.37
in^2-rad/in	1.91	40.4
m^2-cy/m	472.	1.00×10^4
cm^2-cy/m	4.72×10^{-2}	1.00
cm^2-cy/cm	4.72	100.
m^2-rad/m	75.2	1.59×10^3
cm^2-rad/m	7.52×10^{-3}	0.159
cm^2- rad/cm	0.752	15.9

TABLE OF CONTENTS

TABLE OF CONTENTS

LIST OF ILLUSTRATIONS

LIST OF ILLUSTRATIONS

LIST OF ILLUSTRATIONS

LIST OF ILLUSTRATIONS

LIST OF TABLES

SUMMARY

Track geometry variations are the primary inputs to rail vehicles. In order to study vehicle/track interaction, it is essential to provide quantitative descriptions of track geometry variations. Analytical descriptions of track geometry variations are necessary for performing simulation studies for improved rail safety. Such descriptions are also needed for evaluation of track quality, vehicle performance, passenger comfort and lading damage.

Most track can be separated into segments that are constructed and maintained in a uniform manner. These segments exhibit similar track geometry variations which consist of random waviness and relatively large amplitudes at joints and welds. Such variations are called "typical" variations in this report.

Track geometry variations not covered by typical variations will be called "isolated" track geometry variations. Isolated variations usually occur at special track work or physical features such as switches, turnouts, crossings, and bridges. These variations occur occasionally but do have regular patterns.

A track geometry data base consisting of 30 zones which reflect a range of railroad operating conditions and maintenance practices of the United States track was established for the analytical characterization of track geometry variations. A statistical approach was used in the characterization of track geometry variations. This report gives the analytical descriptions of typical and isolated track geometry variations along with the parameters of these descriptions. This report also discusses the relationships between track geometry parameters and the effect of curvature and superelevation on gage, alignment and surface variations. The reader is referred to Section 1.0 for the terminology used in this report.

TYPICAL TRACK GEOMETRY VARIATIONS

Typical track geometry variations can be described by periodically modulated random process. This process consists of a stationary random process which accounts for the random irregularities in the rail, and a process associated with regularly spaced rail joints having a non-zero mean amplitude. The amplitude of joints varies randomly while the wavelength stays the same.

The power spectral density (PSD) is a useful tool for analyzing the periodically modulated random process. In track geometry PSD's, the stationary random process produces the smooth continuum and non-zero mean joint amplitude causes the spectral peaks.

The PSD continuum representing the stationary random process can be modeled as a normalized function of frequency and a roughness parameter representing the amplitude. The normalized function of frequency for a given track geometry parameter does not change significantly with track class. However, the normalized functions are significantly different for different track geometry parameters. On the other hand, the roughness parameter is directly related to the track class since it is indicative of the roughness of track. Models based on PSD were developed for all track geometry parameters, i.e., gage, alignment, crosslevel and profile. These models along with the values of parameters for all current track classes are given in Section 2.

The joint shape can be modeled by an exponential function characterized by joint amplitude and joint duration. The mean amplitude and the joint duration can be estimated from spectral peaks. Both the mean amplitude and joint duration increase with track degradation.

Values of these parameters for all the six track classes are also included in Section 2.

The power spectral density function provides a complete analytic description of a random variable having a normal distribution whose statistical parameters are independent of position and invariant with time. The track geometry variations of railroad track satisfy this requirement only partially. The mathematics of the calculation of the PSD is such that with appropriate precautions computations made using a PSD formulation for random variables which do not satisfy the above requirements will provide accurate predictions of mean squared values of vibration levels of linear systems. However,

- Rail vehicles exhibit strongly nonlinear behavior
- Lower classes of track are dominated by joint effects
- Isolated variations are obscured by averaging properties of PSD formulations.

The isolated variations represent special cases which occur occasionally but do have regular patterns. These variations are often the causes of hazardous responses and should be included in vehicle analyses.

ISOLATED TRACK GEOMETRY VARIATIONS

Eight key signatures have been identified in isolated track geometry variations. These are designated as cusp, bump, jog, plateau, trough, sinusoid, damped sinusoid and sin x/x. These signatures can be described as a function of two parameters; amplitude, A and a duration related parameter, k. Analytical descriptions of the key signatures along with the values of A and k are given in Section 3. Note that the values of these parameters are a function of track class, track goemetry parameter, and the signature itself. In general the values of A and k decrease as the track class increases. However, the ranges of values overlap considerably between different track classes.

Isolated track geometry variations usually occur in spirals, at special track work and other track anomalies such as soft subgrade or poor drainage areas. Isolated variations have been identified at such track features as road crossings, turnouts, interlockings and bridges. Their frequency of occurrence depends upon the number of curves and special track features.

The key signatures occur as single events, in combination with each other and in a periodic fashion. Furthermore, isolated track geometry defects can occur simultaneously in more than one track geometry parameter.

The periodic variations have been observed in the form of cusp, bump, jog and sinusoid signatures. The most common periodic forms are found in crosslevel and mean alignment (average of left and right rail alignment). The most common wavelengths of such periodic forms are 39 feet for crosslevel and 78 feet for alignment. A periodic cuspy type behavior is also commonly observed in gage and single rail alignment in curves. The mean profile (average of left and right rail profile) can also develop quasi-periodic bumps at mud spots and periodic jogs in spirals.

RELATIONSHIPS BETWEEN TRACK GEOMETRY PARAMETERS

A vehicle receives simultaneous input from gage, line and surface irregularities. In order to provide reasonable experimental and analytic simulations of actual railroad operating conditions, it is therefore necessary to investigate the relationships between track geometry parameters.

Track geometry data typical of U.S. track were analyzed to determine the relationships and statistical correlations between track geometry parameters. These analyses were conducted in the frequency domain by generating auto-spectral densities, cross-spectral densities, coherence functions and transfer functions. Results of these analyses are described in Section 4.0. It was found that some track geometry parameters are correlated at certain wavelengths. These correlations should be taken into account in vehicle analyses.

Based on the results of this study, it can be concluded that variations in the left and right alignment are the same for wavelengths longer than 100 feet. For wavelengths typically shorter than 70 feet, there is a strong linear relationship between gage and single rail alignment. Left and right rail alignments are more or less independent for these wavelengths.

Mixed results were obtained for wavelengths between 70 and 100 feet. In general, gage shows strong linear relationship with single rail alignment for wavelengths up to 100 feet. However, in some cases, there are strong 78 foot alignment perturbations in both the rails. In such cases left and right rail alignment are highly correlated and gage shows poor correlation with the single rail alignment.

If one rail is consistently subjected to more lateral load than the other in curves, it may exhibit more alignment variations than those of the other rail. In such cases gage shows stronger relationship with the rail having more alignment activity.

A rail can either go in (towards track center line) or out, (towards the field side) at joints. In curves the low rail has more tendency to go in and the high rail has more tendency to go out.

The alignment at joints can be modeled by exponential rectified inverted sinusoidal, or triangular cusps. The amplitude of these cusps varies randomly from one joint to the other.

Surface variations of the two rails have strong linear relationship for wavelengths longer than 20 feet. The crosslevel at a joint is predominantly due to a low joint on one rail. This gives a strong coherence between crosslevel and single rail profile at 39 feet wavelength for bolted track.

The profile exhibits negative cusps at joints. This can be characterized by an exponential model as a function of joint amplitude and a decay factor. The joint amplitude varies randomly from one joint to the other. Relatively large amplitude variations on joints can give significant coherence between crosslevel and alignment at 39-foot wavelength. Large long wavelength variations can also occur simultaneously in crosslevel and alignment in some track zones. In such cases, crosslevel shows strong coherence with alignment at some discrete wavelengths typically between 50 and 90 feet.

Simultaneous degradation of track geometry parameters may result in significant coherence between all track geometry parameters at certain wavelengths. The bolted track sections analyzed in this study exhibited strong coherence between the gage and profile and between the profile and alignment at a wavelength equal to one-half the rail length.

RMS* VARIATIONS

Track geometry data were analyzed to determine the effect of curvature and superelevation on gage and alignment variations. Analyses were also conducted to determine the difference between the surface variations of the low and high rail. Results of these analyses are given in Section 5.0.

The curvature showed insignificant effect on gage variations in the body of curves. The curvature did not show any consistent effect on the magnitude of either rail alignment variations. On the average the alignment variations of the low and high rail were of the same order of magnitude.

In isolated cases, one rail may have more alignment variations than the other which can be associated with operation at unbalanced speed. However, no definite conclusions can be made from the analyses conducted in this study regarding the differences between the alignment variations of the low and high rail as a function of superelevation.

The rms value calculated by using a 200-foot moving point window can distinguish between the typical and isolated variations. The average values of this descriptor both for the typical and isolated variations are given for Class 2 and 3 track.

The surface variations of left and right rail are generally the same for the tangent track. In curves, there is no significant difference between the surface variations of the low and high rail for the welded track. However, for Class 2 and 3 bolted track, the low rail tends to have more surface variations than the high rail. Furthermore, the surface variations of the low rail tend to increase with the degree of curvature.

*Root mean square

1.0 INTRODUCTION

Analytical characterizations of track geometry variations are essential for design and simulation studies intended to improve the track safety. This chapter describes the background and objectives of the track characterization program, scope of the report and terminology used. A discussion on the origin and formation of track geometry variations is also provided.

1.1 BACKGROUND

Track geometry variations are the primary input to the rail vehicle. In order to study the vehicle/track interaction, it is essential to provide quantitative descriptions of track geometry variations. Analytical descriptions of track geometry variations are essential for simulation studies designed to improve rail safety and for evaluation of track quality, vehicle performance, passenger comfort and lading damage.

An infinite number of track geometry variations can occur in the railway track. Therefore, the only way the universe of the track can be characterized is through the statistics of the population.

The program for statistical characterization of track geometry variations was initiated in 1976. Statistical representations of randomly varying track geometry variations were developed during the first phase of this program. This phase was concluded in April 1978 with the submission of an interim report entitled "Statistical Representations of Track Geometry." (1)

During the first phase, it was found that large amplitude variations occurred more frequently than would be predicted by the stationary random process characterization of typical track goemetry variations. Large amplitude variations represent isolated cases which can produce large amplitude vehicle responses and thus should be included in vehicle analyses. Therefore, the second phase of the track characterization program was initiated in December 1978. Analytical descriptions of isolated track geometry variations were developed during this phase. This phase was concluded in October 1979 with the submission of another interim report.(2)

A vehicle receives simultaneous input from gauge, line and surface irregularities. Therefore, the analytical characterization of track geometry variations should include the relationships between track geometry parameters. This was the major objective of the third phase of the track characterization program. This phase was initiated in May 1980 and was concluded by the submission of this report.

This report documents the results of all three phases of the track characterization program.

1.2 OBJECTIVES

The main objective of the track characterization program is to provide analytical characterization of track geometry variations in a form suitable for various simulation and design studies. The specific objectives can be summarized as follows:

- Develop analytical descriptions of variations of alignment, profile, crosslevel and gauge with distance along the track for both typical and isolated conditions.

- Provide tabulations and plots of the parameters of analytical representations for the United States railroad track.

- Develop analytical descriptions of the relationships between track geometry variables and determine the parameters of these relationships.

1.3 SCOPE OF THE REPORT

The analyses and results given in this report are mainly based on the data collected by automated track geometry cars. Traditionally gage and alignment measurements are made 5/8th of an inch below the railhead and the railhead wear is not measured by these cars.

Federal Railroad Administration (FRA) track geometry cars usually record the data at a sample interval of one foot. Therefore, the Nyquist cut off wavelength is two feet and no information can be obtained for wavelengths shorter than two feet. There is also a long wavelength cut off in the inertial alignment and profile measurements due to accelerometer signal-to-noise ratio (1). Generally, crosslevel and gage do not experience the long wavelength noise problem. It is believed that the most critical wavelength range for vehicle dynamics is between 3 to 300 feet.(2) Therefore, this wavelength range is emphasized in this report.

This report is intended to be a handbook of track geometry variations of the United States track and is written for researchers, designers and field personnel. The report is written in two volumes. Volume I is the main text and Volume II contains more detailed data to support the results described in Volume I.

The remaining part of this chapter gives a synopsis on the formation of track geometry variations. The next chapter of this volume (Volume I) deals with the typical track geometry variations. Analytical descriptions of isolated track geometry variations are given in Chapter 3. The relationships between track geometry parameters are discussed in Chapter 4. This is followed by the effect of curvature and superelevation of rms variations of alignment and profile in Chapter 5. References and the report of new technology are given at the end.

1.4 TERMINOLOGY

Before proceeding further, it is important to define the terminology used in this report. Terms used have popular meaning in most cases. However, some of the terms are used in a limited sense within the context of this report.

Track Geometry Parameters

Track geometry parameters include gage, alignment, profile and crosslevel. Definitions of terms related to these parameters are as follows.(3,4)

Gage: The distance between the rails measured 5/8th of an inch below the top surfaces of rails.

Space Curve: This is a representation for track alignment and profile in which any slow and steady variations (i.e., curves for alignment and grades for profile) have been removed.

Alignment: The space curve representation of the lateral variations of rail. Single rail alignment is the alignment of either left or right rail. Mean alignment is the average of left and right rail alignments. A positive value refers to an offset to the left.

Profile: The space curve representation of the running surface variations of rail. Single rail profile refers to the profile of either left or right rail. Mean profile is the average of left and right profiles. A positive value represents a bump.

Crosslevel: The difference in elevation of the running surfaces between the left and right rails. Crosslevel variations refer to high pass filtered (mean-removed) crosslevel. A positive value indicates that the left rail is high.

Correlation: A linear relationship exists between two parameters x and y.

Coherence: $\hat{\gamma}^2_{xy}(f)$ between x and y is computed from a data sample by

$$\hat{\gamma}^2_{xy}(f) = \frac{|\bar{G}_{xy}(f)|^2}{\bar{G}_x(f)\bar{G}_y(f)} \qquad (1\text{-}1)$$

where

$\bar{G}_{xy}(f)$ = Average cross spectral density of x and y

$\bar{G}_x(f)$ = Average auto-spectral density of the parameter x

$\bar{G}_y(f)$ = Average auto-spectral density of the parameter y

The values of $\hat{\gamma}^2_{xy}(f)$ lie between zero and one. A value of zero indicates no linear relationship between the two parameters. On the other hand, a value of unity indicates a perfect linear relationship. For intermediate values, such as $\hat{\gamma}^2_{xy}(f) = 0.75$, we may interpret that 75 percent of variations in the parameter x are related linearly to the variations in y.

1.5 CAUSES OF TRACK GEOMETRY VARIATIONS

This section discusses the origin and mechanisms of track geometry variations. It is not intended to be an exhaustive presentation of either track structures or the mechanisms of track deterioration. However, this section provides introductory material on the sources and progressive development of various types of track geometry variations. This material is based on existing literature and experience of authors and other co-workers.

Track irregularities or variations in track geometry are the result of cumulative forces that have shaped the track structure during its life time. These variations begin with small imperfections in materials and tolerances and errors in the manufacture of rail and other track components. Terrain variations and survey errors during the design and construction of track add to this. Various deformations are induced by the maintenance operations. The progressive deterioration of track geometry occurs under traffic and environmental factors.

These processes induce the track geometry variations of different wavelengths. Short wavelength variations can be associated with the manufacturing process, the intermediate wavelengths with track degradation and long wavelengths with the terrain and track construction.

Variations caused by the rail manufacturing process are typically shorter than 5 feet although other wavelengths such as 13 feet may be induced during the rail straightening process. Very short wavelength

variations such as 0.2 inch to 10 feet may also be caused by wear mechanism under the traffic loads. Examples of such variations are engine burns, rail corrugation, and rail wear.

Variations of wavelengths longer than 300 feet usually result from terrain and track construction. Design and track construction may also cause localized variations of shorter wavelengths. For example, the structural weakness at joints or welds results in peridoic variations of a wavelength equal to the rail length. Track variations of wavelengths 100 to 300 feet may be created during design and construction of curves and spirals or during the surfacing and line operations.

The intermediate wavelength variations are typically caused by track deformation due to traffic and environmental factors. Discrete wavelength defects may develop in the wavelength region of 5-25 feet under the action of vehicles with a high natural frequency. Accelerated track degradation at joints can cause track geometry variations equal to one half or the full rail length. The heterogeneous compaction of ballast under the action of traffic results in general track deterioration in the wavelength range of 25 to 125 feet. (6) Localized geometric variations of wavelengths between 90 and 140 feet are often caused by the dynamic vehicle/track interaction and have been observed in the track geometry data. The following paragraphs give further details of causes of track geometry variations.

1.5.1 MATERIALS AND MANUFACTURE

Small inclusions of slag and other impurities in the melt and piping that may occur when the steel is cast and rolled, result in small localized weaknesses in rails and other track components. Later, under traffic, rail surface depressions, spalls and other defects tend to develop at these weak spots.

Newly rolled rails tend to bend as they cool, because the relatively thick railhead cools at a slower rate than the web and flange, and the rail tends to curl upwards. In many cases, the deviations of the rails from straight lines are reduced by controlled cooling and, in other cases, by straightening the rails after they cool. In the latter cases, the 39-foot rails are commonly straightened by bending them at the one-third points. When these straightened rails are fastened end-to-end, distinct kinks are found at joints and at intervals of about 13 feet between joints. The ends of rails that are to be welded together into continuous welded rail (CWR) are usually straightened additionally to minimize the irregularity that will result at the joint.

Peak vertical accelerations have been observed corresponding to the forced spatial excitation of a 5.6 foot wavelength. (6) This rail defect is believed to be caused during the manufacturing process. The influence of this defect, which is not noticeable at low speed, increases as the induced frequency approaches the resonance frequency in a vehicle and often becomes predominant at speeds above 125 mph.

1.5.2 DESIGN AND CONSTRUCTION

Inadequacies in the design of drainage, embankment soil strength, embankment depth and width, filter layer or subballast, ballast quality and gradation, tie size, strength and tie spacing, can all lead to rapid deterioration of a track under traffic and result in large irregularities in the track. Usually the deterioration is seen first as large vertical deflections under traffic loads, but lateral deviations may also result.

Small deviations from perfectly smooth space curves are built into a track during construction as a result of survey errors and errors in measurements and workmanship. Inadequate compliance with plans and specifications (such as filters for drainage systems and the moisture content of embankment soils during compaction) lowers the resistance of the track structure to degradation under traffic. Design and construction of spirals and curves is especially difficult and larger deviations may be introduced during construction.

Special track work such as turnouts and crossings have irregularities and tolerance built into them. Under traffic these irregularities become sites of accelerated degradation. Changes in track stiffness and alignment at turnouts, road crossings, and rigid bridge abutments, all may increase the magnitude of dynamic forces resulting in further track deterioration.

Bolted joints are generally the weakest points in the track construction since free plays develop at joints which introduce discrete soft spots in rails of continuous stiffness. As a result of this variation in stiffness, the traffic loads on the track at joints are higher and track degrades more rapidly at joints than elsewhere.

Small irregularities occur where rails that are not perfectly aligned are welded together. The welding also changes the hardness of the steel, so that the steel adjacent to the welds may wear and deform under traffic at a faster rate than elsewhere in the track.

1.5.3 TRAFFIC

Traffic loads are by far the major cause of progressive deformation of track geometry. The rolling stock interacts dynamically with the track and deteriorates the track geometry through the mechanisms of stress, wear and differential settlement. The physical factors such as track subsidence, mud pumping, ballast contamination and loosening of track components accelerate the track deterioration under traffic loads.

Track irregularities acting dynamically with the rolling stock can further develop into severe track geometry variations. When a car wheel passes a track irregularity, it is accelerated laterally and/or vertically, which increases the forces between the wheel and rail.

The dynamic interaction is most pronounced at locations of abrupt changes in stiffness, surface and alignment as may occur at bridges, turnouts, road crossings, and when entering or leaving curves. Permanent alignment deviations of wavelengths corresponding to the truck centers of locomotives have been observed at such locations.

The frictional or creep forces caused by the longitudinal or lateral wheel slip cause the direct abrasion of the rail surface. Examples of very short wavelength irregularities are engine burns and rail corrugations. Engine burn is caused by spinning of wheels under rapid application of power. Extensive braking or slipping of wheels can create a wavy running surface known as corrugations. (7) Corrugation often develops on the inner rail of sharp curves, however, it has also been observed at other locations and there are many different theories on its cause.

Rail wear is especially a problem in curves. Mixed traffic tends to cause gage side wear that results in long wavelength deviations in the effective alignment and gage widening in curves. Unit train operations tend to increase the amount of wear since the cars have similar characteristics and dynamic response. Operation at unbalanced speeds is another cause of excessive wear in curves.

Wear produces shorter wavelength deviations at track features that have built-in irregularities which increase wheel-rail forces. These features include frogs, switch points, joints, bridge abutments and spirals.

The stress mechanism arises from overstressing the track structure by the rolling stock passing over it. Bending and twisting moments are created which can seriously damage the track structure. Rails may be kinked, surface bent or broken from excessive loadings. The concentrated loads may stress the metal beyond its elastic limit and cause the actual flow of metal.(5) Car defects, such as wheel irregularities and flats, add to the forces at the wheel rail interface and increase the rate of degradation of track.

High lateral forces can cause lateral shifts and gage widening. The lateral shifts reduce the lateral restraint of the ballast which increases the likelihood of additional shifts. This may even result in track buckling if large longitudinal stresses develop due to thermal expansion of rail at high temperatures.

The lateral shift of rails from the track center results in gage widening, which is most often observed on curves if the outer rail is subjected constantly to high lateral forces. Inadequate spiking and damaged ties increase the likelihood of rail shift. Even if the spikes and ties are sufficiently strong to hold the lateral force, rail rollover may occur due to the overturning torque produced by the combined lateral and vertical load. Worn ties with the bearing surface cut in by tie plate tends to allow outward cant of the rail contributing to gage widening.

A classic example of stress mechanism is observed at bolted joints which are weak points in the track structure. Heavy loads are transferred to the ballast and subgrade at the joints and deterioration occurs faster than it does between joints. In many cases, ballast is pounded down beneath the joint ties, so that gaps develop between them and the ballast. The ties are then left suspended from the rail.

The lateral weakness at joint bars makes bolted rail less effective in distributing lateral forces along the track, so that it tends to deflect laterally more at joints then elsewhere and transfers more load to ties near joints than to other ties. Ties near joints are then more likely to shift laterally in the ballast. This effect may change a smooth curve to a series of short tangents with lateral kinks at the joints.

Gaps between rail ends at bolted joints permit expansion of the rails in hot weather to avoid the development of large longitudinal forces and possible buckling of the track. The gaps also permit battering of the rail ends, as the wheels of moving cars drop into them. The battering causes metal to flow towards the ends of the rails, so that the rails are closer together at the surface than they are further down in the gap between the rail ends. Unless the surface protuberances are cut back, very high stress concentrations will develop when the rails expand in hot weather,and the work hardened rail surface may spall off for a distance of several inches from the joint, thus producing a profile irregularity of short wavelength.

Subsidence is a common problem in track on low lying grounds and marshy areas. It tends to produce long wavlength profile deviations except where it occurs adjacent to a rigid structure such as a cut through a rock outcrop or a bridge abutment. It is often associated with obstruction of drainage or repeated heavy loadings, such as the impacts on ballasted track that occur adjacent to rigid bridge abutments. It produces vertical settlement of the track and vertical deviations with wavelengths that may range from 20 to 300 feet, except adjacent to rigid structures where the wavelengths are short. In side hill cuts and fills, subsidence may also result in lateral movement of the track over short to long wavelengths.

Mud pumping occurs when traffic vibrations mix water with the soil under track, and the wheels of passing cars press the rails and ties down so that the pressure pulses force muddy water up through the interstices of the ballast. Mud and water serve as lubricants which reduce the friction between aggregates in the ballast thereby reducing the resistance to movement under load. Poor drainage is usually a contributing factor, but mud pumping may start even with a good drainage system, when the ballast itself becomes clogged with fine materials that retain water. Mud pumping results in fouled ballast and accelerated track degradation under traffic.

1.5.4 ENVIRONMENT

Even if there were no traffic loads, the track structure will deteriorate due to environmental factors such as rain and temperature. The environmental factors deteriorate the track geometry through the mechanisms of corrosion, rot, ballast contamination, frost action and track buckling.

Corrosion is simply a chemical reaction between the rail and the environment. It may be as simple as metallic oxidation (rust) or it may be caused by the introduction of some caustic material resulting from local industry or freight traffic. Corrosion by itself is of little consequence but in conjunction with the wear mechanism it can greatly accelerate the deterioration of the railhead. The corrosion has been known to cause irregularities in rail surface and alignment in a few cases where corrosive water dripped continuously on the rails. More commonly, failures have occurred in the webs of rails installed for long periods in corrosive environments.

Rot attacks the ties rather than the rail. Rotten ties do not distribute the vertical loads as designed and accelerate rail damage due to over-stressing. Rot also diminishes the overall ability of the track to maintain lateral loads, which creates the derailment potentials known as gage widening and rail rollover.

Rot and other tie defects produce irregularities with a wavelength double the tie spacing and longer where defective ties are grouped together. As a result, the traffic loads on adjacent ties are increased and they tend to overload the ballast and embankment and increase the rate of track deterioration.

Significant levels of rot are found more usually in moderate climates such as the Southeastern United States. In contrast, rot does not pose a problem in desert areas or where hard freezing maintains an ecological lid on destructive bacteria.

The ballast contamination caused by rain water lowers its ability to distribute load. Water pockets under the track or in the roadbed cause soft sinking spots. In addition, the mud may start working upward destroying the drainage property of ballast.

Rail expands and contracts as its temperature changes. If the external restraints prevents this, the thermal stresses are set up. The thermal stresses may result in "pull-apart" of rails in cold weather and track buckling or "panel shift" in hot weather. These stresses are more of a problem in continuous welded rail since the gaps between joints relieves these stresses in bolted rail.

Both the vertical and lateral track buckling have been observed in warm summer months. In some tests conducted on vertical track buckling, the observed length of the lift-off region was about 98 feet and upward deflection was 2.6 feet.(8) The recorded length in the lateral buckling mode was 62 feet and the largest deflection was approximately one foot. In all these tests, the total axial force was approximately 200 tons at the onset of buckling.

Frost action or "heaving" is likely to come in cold weather. This can cause lateral displacement of track and is also a common cause of rough track in the winter. Heaving is caused by the direct volumetric increase of free moisture freezing in the soil and from swelling caused by the ice layers.

1.5.5 MAINTENANCE

Maintenance requirements develop as track deteriorates because of traffic and envionmental conditions. Survey errors, measurement errors and machine tolerances may introduce additional track deviations during a maintenance operation. The basic or spot maintenance is traditionally performed by non-mechanized gangs. Such maintenance operations while correcting one condition may introduce other defects. During the lining operations, swings and false tangents may be introduced into the straight track and dog legs, hooks and compound curvature may occur in curves. (5)

Maintenance operations usually take place at a temperature different than that at which the track was originally laid. This may relieve the built-in stresses and later on the track might be subjected to severe thermal stresses.

1.6 TYPICAL AND ISOLATED VARIATIONS

A brief description of various causes of track geometry variations was given in the previous section. For the purpose of this report, these variations can be divided into two broad categories; the typical variations and isolated variations.

Most track segments are constructed and maintained in a uniform manner. These segments exhibit similar track geometry variations. These variations consist of random waviness with relatively severe amplitudes at joints and welds. These variations are called "typical" variations in this report. Typical variations are the subject of the next section.

Track geometry variations not covered by typical variations will be called "isolated" track geometry variations. These variations occur occasionally but do have regular patterns, usually large amplitudes or long wavelengths. Isolated variations usually occur at special track work or physical features such as switches, turnouts, crossings, and bridges, etc. Isolated variations are discussed in Section 3.

2.0 TYPICAL TRACK GEOMETRY VARIATIONS*

2.1 INTRODUCTION

An observation of track geometry data reveals that a majority of track exhibits typical track geometry variations. Track is generally constructed by welding or bolting together many short pieces of rail all having the same length. Typical track geometry variations consist of regularly occurring patterns superimposed on a background of apparently random behavior. The regularly occurring patterns in track geometry are normally caused by joints and welds.

Typical track geometry variations are indicative of the average quality of the track. A statistical characterization of these variations is important for the evaluation of the average vehicle responses. This can also be used for evaluation of the degradation of average track quality.

Most track segments are constructed in a uniform manner and are maintained to provide the same performance levels. These segments produce the track geometry traces that exhibit the same features observed in the individual segments of track. Therefore, it is possible to describe these variations statistically as a function of a few parameters.

Analytical representations of typical track geometry variations were developed in Phase I of the track characterization program. Results of this study are given in Reference (1). This section summarizes the methodology and findings of this study pertaining to typical track geometry variations.

2.2 METHODOLOGY

2.2.1 PROCESS IDENTIFICATION

Time series analysis techniques were applied to track geometry data to obtain analytical representations of track geometry variations. It was shown that a periodically modulated random process provided an adequate representation of typical track geometry variations.(8) This process includes two subset processes which can be used to represent typical track geometry behavior.

- o A stationary random process which accounts for the random irregularities in the rail.
- o A periodic process that describes the regularly spaced rail joints having non-zero mean amplitude. The amplitude of joints varies randomly from one joint to the other.

A stationary random process is the one for which all moments are constant, i.e., the mean, standard deviation, etc., are independent of the position along the rail. The stationary random deviations represent the cumulative history of forces that have shaped the track structure during its lifetime. This force-induced waviness begins with rail manufacture, cooling and straightening. Terrain variations

---

*This section is extracted from Reference (1), Corbin, J.C., "Statistical Representation of Track Geometry, Volume II," Report No. FRA/ORD-80/22, 1980.

and survey errors add to this. Various deformations are induced by lining and surfacing operations, traffic and the environment.

The periodic process is the result of rolling rails in relatively short but constant length, e.g., 39 feet and then bolting or welding them into longer sections. This process is characterized by a non-zero periodic mean associated with randomly varying amplitude of joints or welds.

2.2.2 STATIONARY RANDOM PROCESS (SRP)

Most stationary random processes are well defined by their probability distributions and correlation functions. In the case where the SRP is a normally distributed random variable, the auto-correlation function, or equivalently, the Power Spectral Density (PSD), completely describes the process. Therefore, the applicable analytical techniques for the SRP are histograms and PSD's.

The PSD is a useful tool for estimating some properties of the processes described in Section 2.2.1. Application of the PSD to data that includes many rail lengths produces graphs that exhibit a relatively smooth continuum punctuated by sharp, harmonically spaced spikes. The continuum is an estimator of the covariance function (auto-correlation) of the parent random process. The pronounced peaks are estimators of the periodic process.

Figure 2-1 shows a typical PSD of the profile geometry of the bolted track. The power density is plotted as a function of spatial frequency (1/wavelength). Note the pronounced peaks on a relatively smooth continuum. These peaks appear at wavelengths corresponding to the rail length (about 39 feet) and its harmonics indicating the existence of a periodic component.

As seen in Figure 2-1, the PSD supplies too many data points in a form which does not define the component processes. Also it is not particularly useful for the comparative evaluation and classification of track deviations and the vehicle responses to these deviations. What is needed is a process model for the two simplified processes identified in the previous section. Then the model can be applied to develop a short parameter list that describes all salient features of the rail deviations.

Track geometry PSD's are often presented as power density versus frequency often in a log-log form. As a result, a power law relationship for a continuum appears as a straight line. Review of PSD's from railroads in many parts of the world indicates a consistent pattern of distinct frequency bands wherein the PSD is well modeled by an even-powered straight line segment. Power laws -2 and -4 have been commonly observed. A PSD model for profile reflecting these observations is illustrated in Figure 2-2.

The individual segments of the PSD represented in Figure 2-2 can be linked to manufacture, installation and subsequent degradation of the rail. Several distinct regions can be identified in Figure 2-2. These are summarized in Table 2-1 and their physical causes are also discussed starting at the short wavelength end of the spectrum.

Analysis of profile geometry PSD's was performed over the frequency range of 10^{-3} cy/ft to 0.2 cy/ft. For these frequencies the following even power law approximation to empirical PSD's could be fitted universally to the continuum with a residual of less than 10 percent:

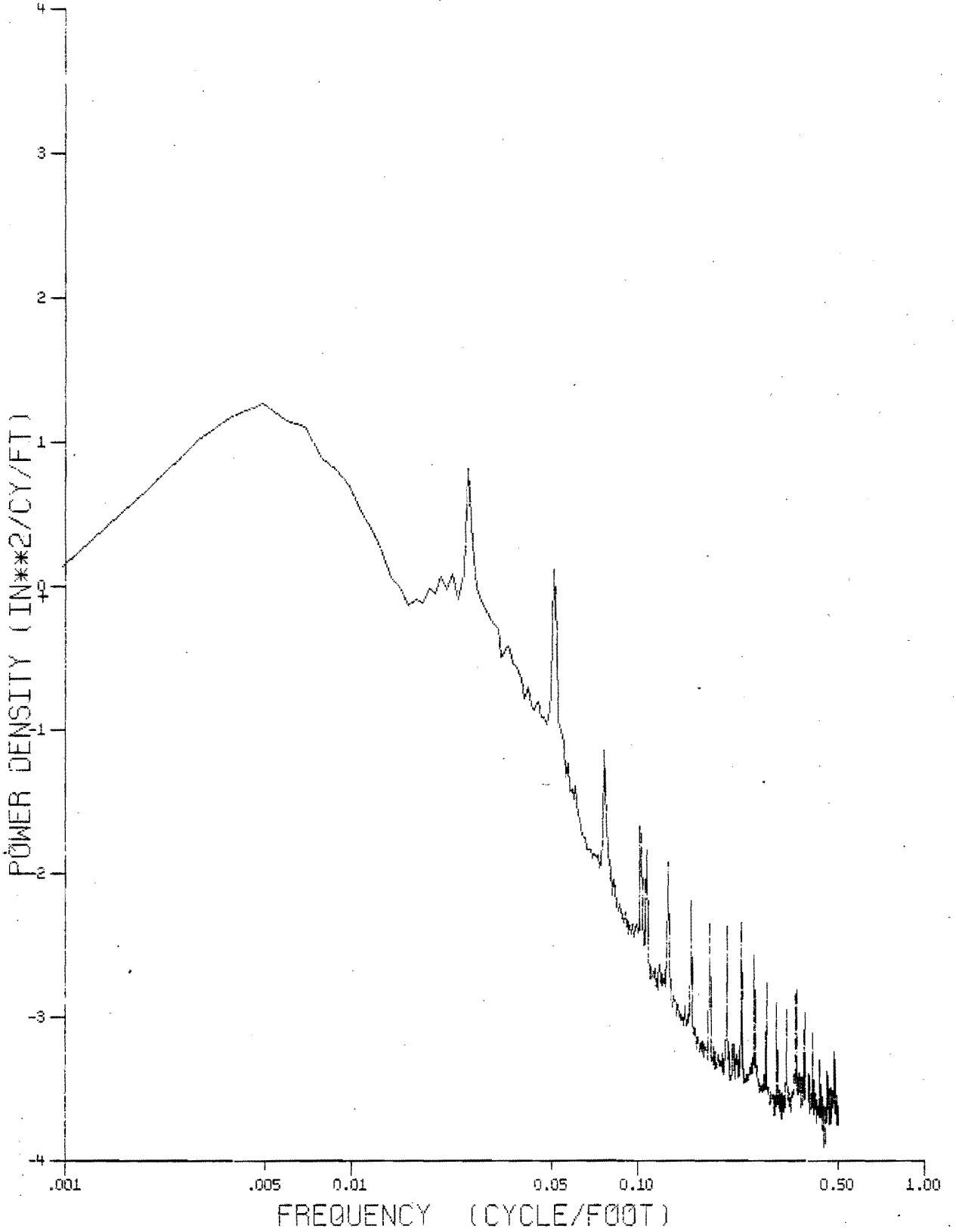

Figure 2-1. Typical PSD of Profile

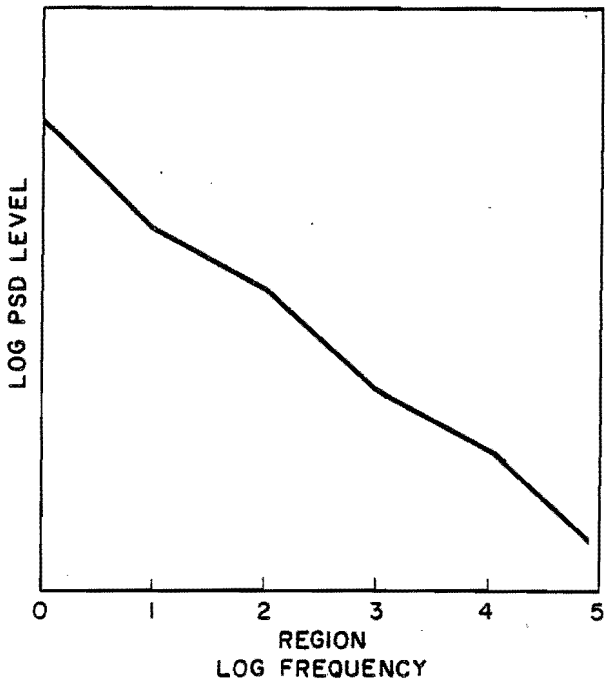

Figure 2-2. PSD Regions for Profile

TABLE 2-1
REGIONS OF RAIL PROFILE PSD'S

Region	Spectral Behavior	Wavelength Range	Cause
5	ϕ^{-4}	2 Inches $\leq\lambda\leq$ 1 Foot	Roughness in the rollers
4	ϕ^{-2}	1 Foot $\leq\lambda\leq$ 5 Feet	Grinding operations which are used to effect smoothing of the surface geometry
3	ϕ^{-4}	5 Feet $\leq\lambda\leq$ 25 Feet	Track degradation
2	ϕ^{-2}	25 Feet $\leq\lambda\leq$ 125 Feet	In the new construction, ϕ^{-2} behavior established in Region 4 continues through Regions 3 and 2
1	ϕ^{-4}	$\lambda \geq$ 125 Feet	Terrain

ϕ = Spatial Frequency (cycles/foot).
λ = Wavelength = $1/\phi$

$$\hat{S}_1(\phi) \begin{cases} \dfrac{A_1{}^2{}_{13}}{\phi^4}, & 10^{-3} \text{ cy/ft} \quad \phi \leq \phi_{13}; \\ \dfrac{A_1}{\phi^2}, & \phi_{13} \leq \phi \leq \phi_{14}; \text{ and} \\ \dfrac{A_1 \phi_{14}}{\phi^4}, & \phi_{14} \leq \phi \leq 0.2 \text{ cy/ft}. \end{cases} \tag{2-1}$$

where

ϕ = spatial frequency;

$\hat{S}_1(\phi)$ = discontinuous analytical PSD;

A_1 = profile roughness for ϕ^{-2} range;

and ϕ_{13}, ϕ_{14} = break frequencies.

Since this PSD model is not continuous, a smooth functional fit was sought. This is given by:

$$S_1(\phi) = \frac{A_1 \phi_{14}^2 (\phi^2 + \phi_{13}^2)}{\phi^4 (\phi^2 + \phi_{14}^2)} \tag{2-2}$$

Both $\hat{S}_1(\phi)$ and $S_1(\phi)$ are shown in Figure 2-3 along with raw profile PSD data.

For track that is in regular commercial service, ϕ_{13} and ϕ_{14} are both constant with values of 6.3×10^{-3} cy/ft and 4.0×10^{-2} cy/ft, respectively. Therefore, over the range of wavelengths most critical to vehicle dynamics, the continuous portion of the profile PSD is adequately specified by the single remaining constant, A_1.

Similar models were developed for other track geometry parameters. These models are given in Section 2.3.

2.2.3 PERIODIC PROCESS

The predominant North American practice is to roll rail in the shorter, more manageable lengths of 39 feet. Then it is bolted or welded into the longer strings to form the track. Both bolted and welded joints are sites of structural weakness and accelerated degradation of geometry. Additionally, the inability to straighten vertical deflections at the ends of the rail segments is incorporated into the profile geometry of the weld.(9)

Physical observation of track geometry and stiffness measurements indicate that joints and welds are locations in the track where conditions differ significantly in character from those found between joints and welds. The regular occurrence of joints or welds results in a periodic process in the track geometry.

A cuspy behavior is observed in the track geometry at joints. Analyses of track geometry data indicate that the rail profile or alignment at a joint can be adequately represented by a cusp shape of the form:

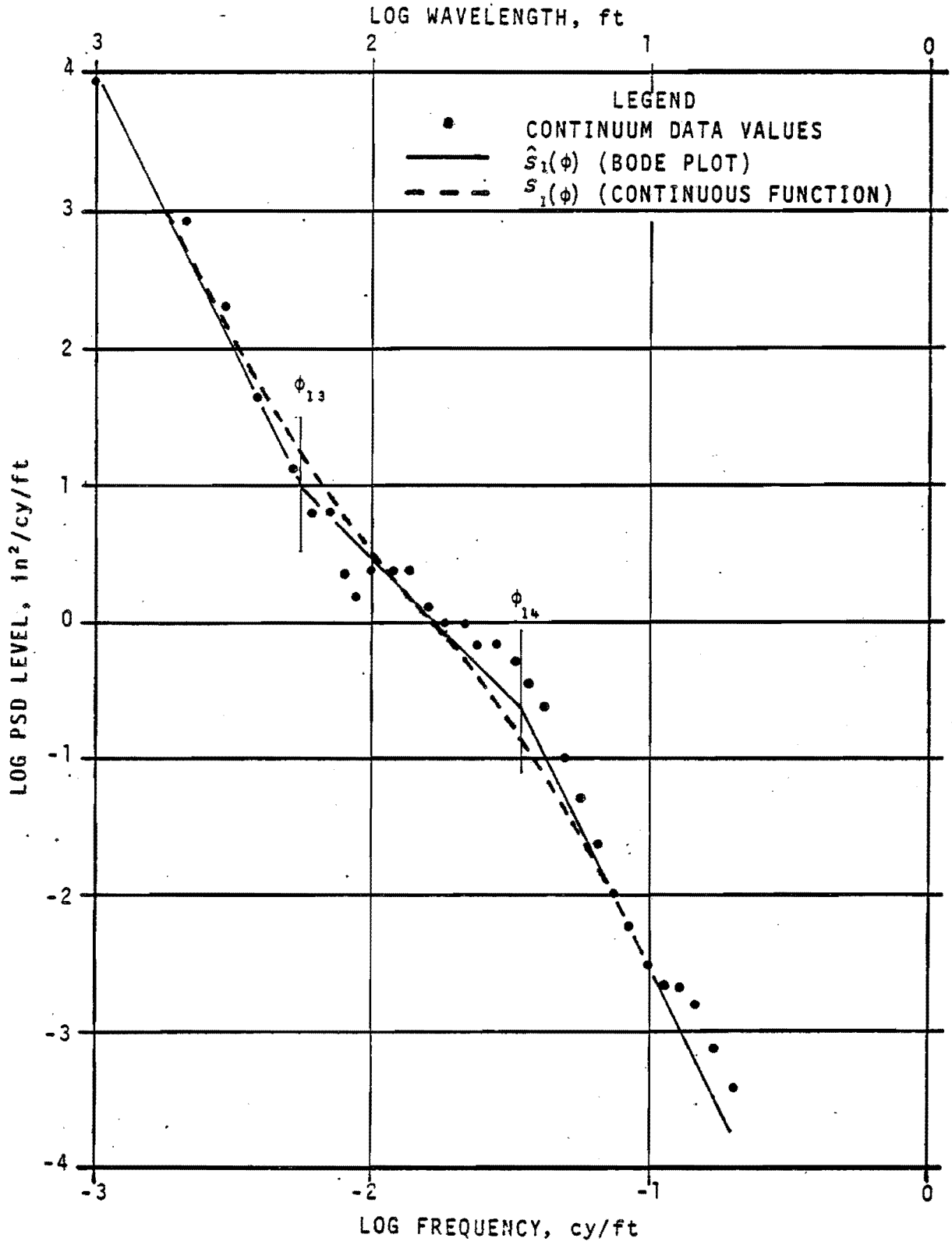

Figure 2-3. Comparison of Typical Profile Continuum Values, Bode Plot Fit, and Continuous Function Fit

$$y(x) = Ce^{-k|x|} \qquad (2\text{-}3)$$

where

x = distance along the rail,

$y(x)$ = rail profile or alignment,

C = joint cusp amplitude, and

and k = decay rate, assumed constant on a particular section of track.

Thus, the shape of a joint is defined by its amplitude and its decay rate. The values of joint amplitude were found to be represented by a stationary random process governed by distribution with a non-zero mean, $\bar{C}$.

On bolted rail and on some CWR fabricated from relay bolted rail, the cusp is downward. Its duration (inverse decay rate) is on the order of 2 to 10 feet long and its amplitude generally falls between 0 and 3 inches. Both duration and amplitude increase with degradation, which results from the structural weakness of the joint and is accelerated by loosening and wear of the joint bars.

On CWR fabricated from new rail, the cusp is usually upward and much shorter, 2 to 4 feet long, and its amplitude may be as great as 0.3 inch. It is caused by the rolling-cooling process during which the rail bends upward. Even though the rail is straightened after this process, straightening does not totally remove the curvature from the ends and a cusp occurs at the location of the weld at the CWR string.(9) CWR joint degradation consists of the development of a depression around the upward cusp, rather than in the cusp itself.

2.2.4 DATA PROCESSING

Twenty-nine zones of track geometry data representing a total of 150 miles of track were selected to characterize the typical track geometry variations. These sections were broadly distributed throughout the United States and covered the full range of track classes as defined in the Track Safety Standrds.(10) These zones reflect various types of operating conditions and maintenance practices of different railroads. Typically, the zones vary in length from one to ten miles. Characteristics of these zones are given in Appendix A.

Empirical PSD's were generated for the track profile, crosslevel, alignment and gage data. On the basis of these, analytical models of the continuum portion of PSD's were developed for all the track geometry parameters. Various parameters of the models such as the roughness constant, break frequencies, mean joint amplitude and decay rate were estimated from the empirical PSD's. Appendix B.2 describes the method used to extract these parameters.

2.2.5 STATISTICAL PROPERTIES

It has been shown in Reference (1) that the stationary random process (SRP) is a Markov process. By virtue of the Markov property of SRP's, track measures such as high-pass space curve, mid-chord offset (MCO), warp, gage and crosslevel variations are given as weighted sum of many consecutive values of a sequence of white noise values. Therefore, according to the central limit theorem, these measures will be normally distributed. Therefore, if only the SRP is present in the geometry, the track measurement is a normally distributed random variable that is adequately described by its mean and variance.

Profile and alignment measurements are often specified in terms of an MCO of half-length, S. An MCO measuring a SRP produces a fluctuating random variable having zero mean and correlation function, R(x,S). The expression for R(x,S) is given as:

$$R(x,S) = 1/4U(x-2S) - U(x-S) + 3/2U(x) - U(x+S) + 1/4U(x+2S) \quad (2\text{-}4)$$

where U(x) is a function of the process PSD.

The variance of the mid-chord is given by R(0,S) which is a function of the chord length. Expected values of standard deviations (square root of variance) for 62-foot MCO are given in Section 2.3.

Two track sections were analyzed to characterize the distribution of joint amplitudes for the profile geometry. Data were processed to include the following representations of the profile.

- o Space curve.*
- o An MCO of length equal to twice the rail length.
- o An MCO of length equal to the rail length.
- o An MCO of length equal to one-half the rail length.

A regression analysis was performed to determine which of these representations would provide the best information on the location and amplitude of a joint. The space curve was found to be the best indication of a joint. The half rail length MCO was the second best choice.

Another section of track geometry data was used to determine the distribution of joints. This track zone was estimated at Class 3. The construction was bolted with rail length equal to 39 feet.

Joints were located by their characteristic cusp signature in the space curve. Then, using a 16-foot MCO, the amplitudes of joints were measured.

The magnitude of joint amplitude are plotted in the histogram shown in Figure 2-4. The results display a skewed distribution having a mean amplitude, $\bar{C}$ of 0.284 inches. This distribution is highly suggestive of a Γ-distribution which can be described as:

$$P_2(C) = \left(\frac{4}{\bar{C}}\right)^4 \frac{C^3 e^{-4C/\bar{C}}}{6} \quad (2\text{-}5)$$

values of $\bar{C}$ for various track classes are given in the next section.

2.3 RESULTS

2.3.1 ANALYTICAL MODELS

Typical PSD's for track geometry parameters ar given in Appendix B. On the basis of these, models for SRP were developed for all track geometry parameters. These models are given in Table 2-2.

*Space curve is a pseudo-reconstruction of track in space without the effect of local topography.

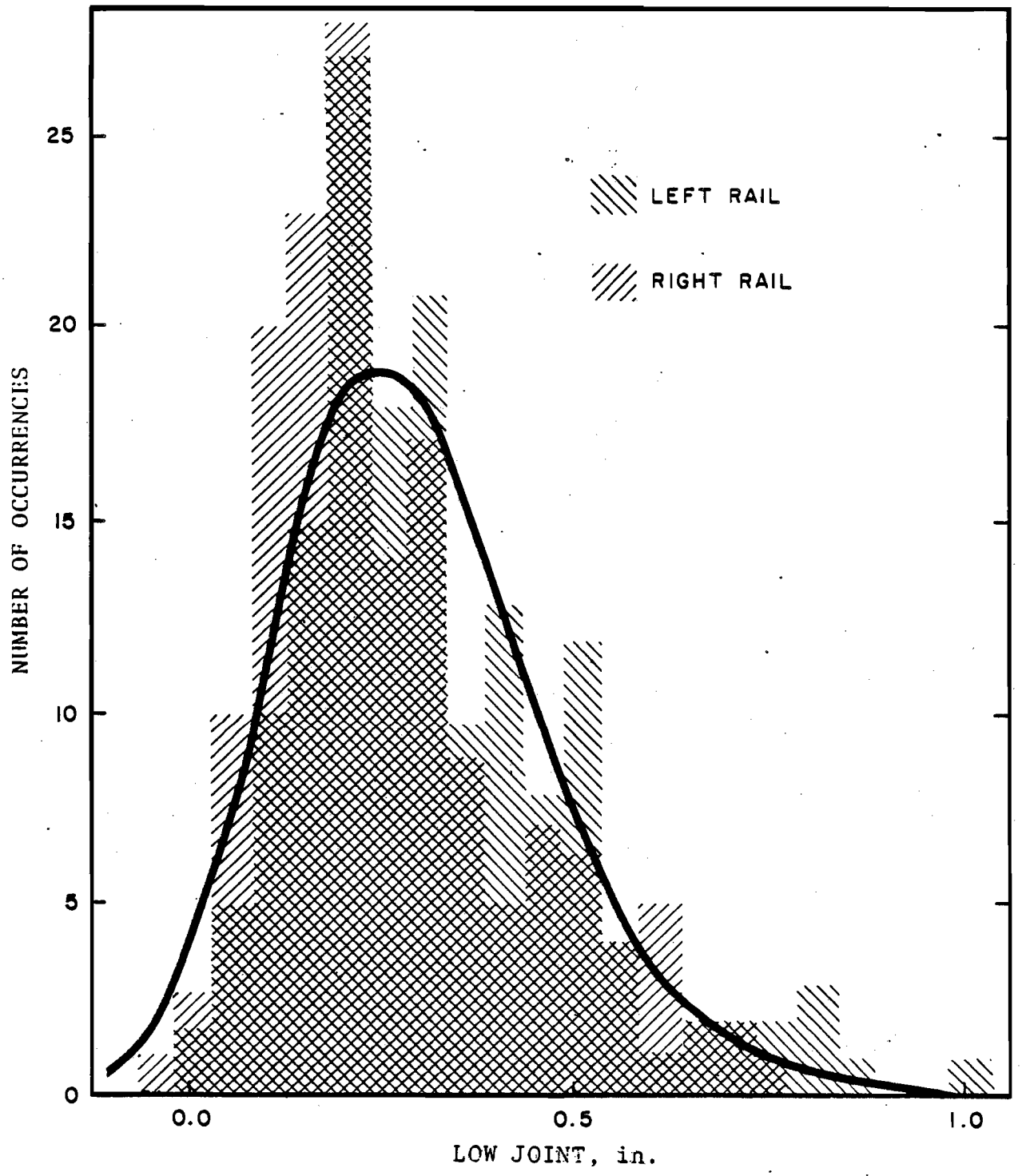

Figure 2-4. Histogram for 156 Left Rail and 156 Right Rail Bolted Joints

TABLE 2-2

MODELS FOR PSD CONTINUUM

For wavelength coverage from 10 to 1000 ft, omit the term in [ ].
To extend wavelength coverage to 0.2 ft, include the term in [ ].

ϕ = spatial frequency (cy/ft)

λ = wavelength (ft) = ϕ^{-1}

$S_n(\phi)$ = PSD (in^2/cy/ft)

n = a geometry variable designator:

n = 1 → Left rail profile
2 → Right rail profile
3 → Mean profile
4 → Crosslevel

ϕ_{nm} = mth corner frequency of nth track geometry PSD

$\lambda_{nm} = \phi_{nm}^{-1}$

PROFILE (n = 1,2,3)

$$S_n(\phi) = \frac{A_n \phi_{n4}^2 (\phi^2 + \phi_{n3}^2)}{\phi^4 (\phi^2 + \phi_{n4}^2)} \left[\frac{\phi_{n6}^2 (\phi^2 + \phi_{n5}^2)}{\phi_{n5}^2 (\phi^2 + \phi_{n6}^2)} \right]$$

with:

$\lambda_{n3} \cong$ 140 ft
$\lambda_{n4} \cong$ 25 ft
$\lambda_{n5} \cong$ 5 - 10 ft
$\lambda_{n6} \cong$ 1.0 ft

CROSSLEVEL (n = 4)

$$S_4(\phi) = \frac{A_4 \phi_{44}^2 (\phi^2 + \phi_{42}^2)}{(\phi^2 + \phi_{41}^2)(\phi^2 + \phi_{43}^2)(\phi^2 + \phi_{44}^2)} \left[\frac{\phi_{46}^2 (\phi^2 + \phi_{45}^2)}{\phi_{45}^2 (\phi^2 + \phi_{46}^2)} \right]$$

with:

$\lambda_{41} \cong$ 200 - 1000 ft
$\lambda_{42} \cong$ 40 - 200 ft
$\lambda_{43} \cong$ 25 - 50 ft
$\lambda_{44} \cong$ 18 ft
$\lambda_{45} \cong$ 5 - 10 ft
$\lambda_{46} \cong$ 1.0 ft

$\hat{\lambda}_{43} = \lambda_{43}$ (effective combination of λ_{41}, λ_{42}, λ_{43})

$\hat{\lambda}_{43}$ = 140 ft (Use with $\lambda_{41} = \lambda_{42} = \infty$)

TABLE 2-2 (CONT)

MODELS FOR PSD CONTINUUM

For wavelength coverage from 10 to 1000 ft, omit the term in [ ].
To extend wavelength coverage to 1.0 ft, include the term in [ ].

ϕ = spatial frequency (cy/ft)

λ = wavelength (ft) = ϕ^{-1}

$S_n(\phi)$ = PSD (in^2/cy/ft)

n = a geometry variable designator:

- n = 5 → Left rail alignment
- 6 → Right rail alignment
- 7 → Mean alignment
- 8 → Gage

ϕ_{nm} = mth corner frequency of nth track geometry PSD.

$\lambda_{nm} = \phi_{nm}^{-1}$

ALIGNMENT (n = 5,6,7)

$$S_n(\phi) = \frac{A_n \phi_{n4}^2 (\phi^2 + \phi_{n3}^2)}{\phi^4 (\phi^2 + \phi_{n4}^2)} \left[\frac{\phi^2 + \phi_{n5}^2}{\phi_{n5}^2} \right]$$

with:

$\lambda_{n3} \cong 100$ ft

$\lambda_{n4} \cong 18$ ft

$\lambda_{n5} = 5 - 10$ ft

GAGE (n = 8)

$$S_8(\phi) = \frac{A_8 \phi_{84}^2 (\phi^2 + \phi_{82}^2)}{(\phi^2 + \phi_{81}^2)(\phi^2 + \phi_{83}^2)(\phi^2 + \phi_{84}^2)} \left[\frac{\phi^2 + \phi_{85}^2}{\phi_{85}^2} \right]$$

with:

$\lambda_{81} \cong 200 - 1000$ ft

$\lambda_{83} \cong 25 - 50$ ft

$\hat{\lambda}_{83} \cong 40 - 200$ ft

$\hat{\lambda}_{83} = \lambda$ (effective combination of λ_{81}, λ_{82} and λ_{83})

$\hat{\lambda}_{83} = 120$ ft (Use with $\lambda_{81} = \lambda_{82} = \infty$)

$\lambda_{84} \cong 14$ ft

$\lambda_{85} \cong 5 - 10$ ft

The empirical PSD's were separated by track speed classification as identified in the current FRA Track Safety Standards. The amplitudes and break frequencies of the continuum portion of the spectra were evaluated. These are also summarized in Appendix B.

A regression analysis of parameters versus track class was performed to determine how the parameters were related to the track class.

It was found that the break frequencies were more or less constant and were not dependent on the speed classification of track. However, the parameters related to the roughness of the track were strongly related to the track class. Results of this regression analysis are presented in Table 2-3 and in Figure 2-5. The reader is cautioned that these tabulated values are means of the regression and scatter of data values about mean regression lines is of the order of ±1 track class.

It should be noted that the following simple models can be used over the wavelength range of 10 to 1,000 feet:

Profile, Alignment:

$$S(x)\phi = \frac{A\phi_b^2 \, (\phi^2 + \phi_a^2)}{\phi^4(\phi^2 + \phi_b^2)} \qquad (2\text{-}6)$$

Crosslevel, Gage:

$$S(\phi) = \frac{A\phi_b^2}{(\phi^2 + \phi_a^2)(\phi^2 + \phi_b^2)} \qquad (2\text{-}7)$$

where:

A = roughness parameter,

ϕ = spatial frequency (cy/ft),

$S(\phi)$ = PSD (in^2/cycles/ft),

ϕ_a, ϕ_b = break frequencies,

λ = wavelength = $1/\phi$,

and λ_a, λ_b = break wavelengths

The values of break frequenices (or equivalently break wavelengths) are independent of track class and are functions of only the track geometry parameters. Values of break wavelengths for the simple models are given in Table 2-4.

TABLE 2-4

VALUES OF BREAK WAVELENGTHS

Parameter	λ_a (feet)	λ_b (feet)
Surface*	140	25
Alignment	100	18
Gage	112	14

*Profile and crosslevel.

TABLE 2-3

SUMMARY OF SPECTRAL MODELS AS A FUNCTION OF TRACK CLASS

Continuum: Units: A_n: in^2-cy/ft, ϕ_{mn}: cy/ft; All σ's (standard errors) in inches			Track Class by Geometry	** "8"	** "7"	6	5	4	3	2	1
		Profile	$A_3 \times 10^{-4}$	0.06	0.18	0.45	0.79	1.4	2.5	4.5	7.9
			$\phi_{33} \times 10^{-3}$	11.2	8.9	7.1	7.1	7.1	7.1	7.1	7.1
			$\phi_{34} \times 10^{-2}$	(†)	4.0	4.0	4.0	4.0	4.0	4.0	4.0
			$\phi_{35} \times 10^{-1}$	(†)	0.71	1.2	1.4	1.6	1.8	2.1	2.4
			σ, 62' MCO	0.07	0.10	0.15	0.20	0.26	0.35	0.47	0.62
		Crosslevel	$A_4 \times 10^{-4}$	0.12	0.20	0.34	0.50	0.74	1.1	1.6	2.3
			$\phi_{43} \times 10^{-3}$	7.1	7.1	7.1	7.1	7.1	7.1	7.1	7.1
			$\phi_{44} \times 10^{-2}$	(†)	4.0	4.0	4.0	4.0	4.0	4.0	4.0
			$\phi_{45} \times 10^{-1}$	(†)	0.84	1.0	1.1	1.1	1.2	1.2	1.3
			σ, X-lev	0.05	0.07	0.09	0.11	0.13	0.16	0.20	0.23
			σ, 31'Warp	0.06	0.08	0.11	0.13	0.16	0.19	0.23	0.28
		Alignment	$A_7 \times 10^{-4}$	0.06	0.13	0.28	0.50	0.89	1.6	2.8	5.0
			$\phi_{73} \times 10^{-3}$	15.8	12.6	10.0	10.0	10.0	10.0	10.0	10.0
			$\phi_{74} \times 10^{-2}$	(†)	5.6	5.6	5.6	5.6	5.6	5.6	5.6
			$\phi_{75} \times 10^{-1}$	(†)	0.71	0.97	1.8	1.3	1.5	1.7	2.0
			σ, 62' MCO	0.09	0.11	0.13	0.18	0.24	0.32	0.42	0.57
		Gage	$A_8 \times 10^{-4}$	0.20	0.22	0.28	0.50	0.89	1.6	2.8	5.0
			$\phi_{83} \times 10^{-3}$	8.9	8.9	8.9	8.9	8.9	8.9	8.9	8.9
			$\phi_{84} \times 10^{-2}$	(†)	(†)	7.1	7.1	7.1	7.1	7.1	7.1
			$\phi_{85} \times 10^{-1}$	(†)	(†)	0.87	1.00	1.15	1.30	1.5	1.8
			σ, Gage	0.04	0.06	0.07	0.09	0.13	0.17	0.22	0.30
Periodic Deterministic Process (Individual Rail)		Profile	Joint Ampl. $\bar{C}$ (in)	0.06	0.08	0.11	0.14	0.19	0.25	0.33	0.45
			Decay Rate, k (ft^{-1})	0.42	0.33	0.25	0.20	0.15	0.14	0.13	0.13
		Alignment	Joint Ampl. $\bar{C}$ (in)	0.04	0.06	0.08	0.11	0.15	0.20	0.27	0.35
			Decay Rate, k (ft^{-1})	*	*	0.57	0.46	0.35	0.20	0.15	0.12

* Reliable estimators not currently available.
† Degenerate pair of corner frequencies.
** Hypothetical track classes

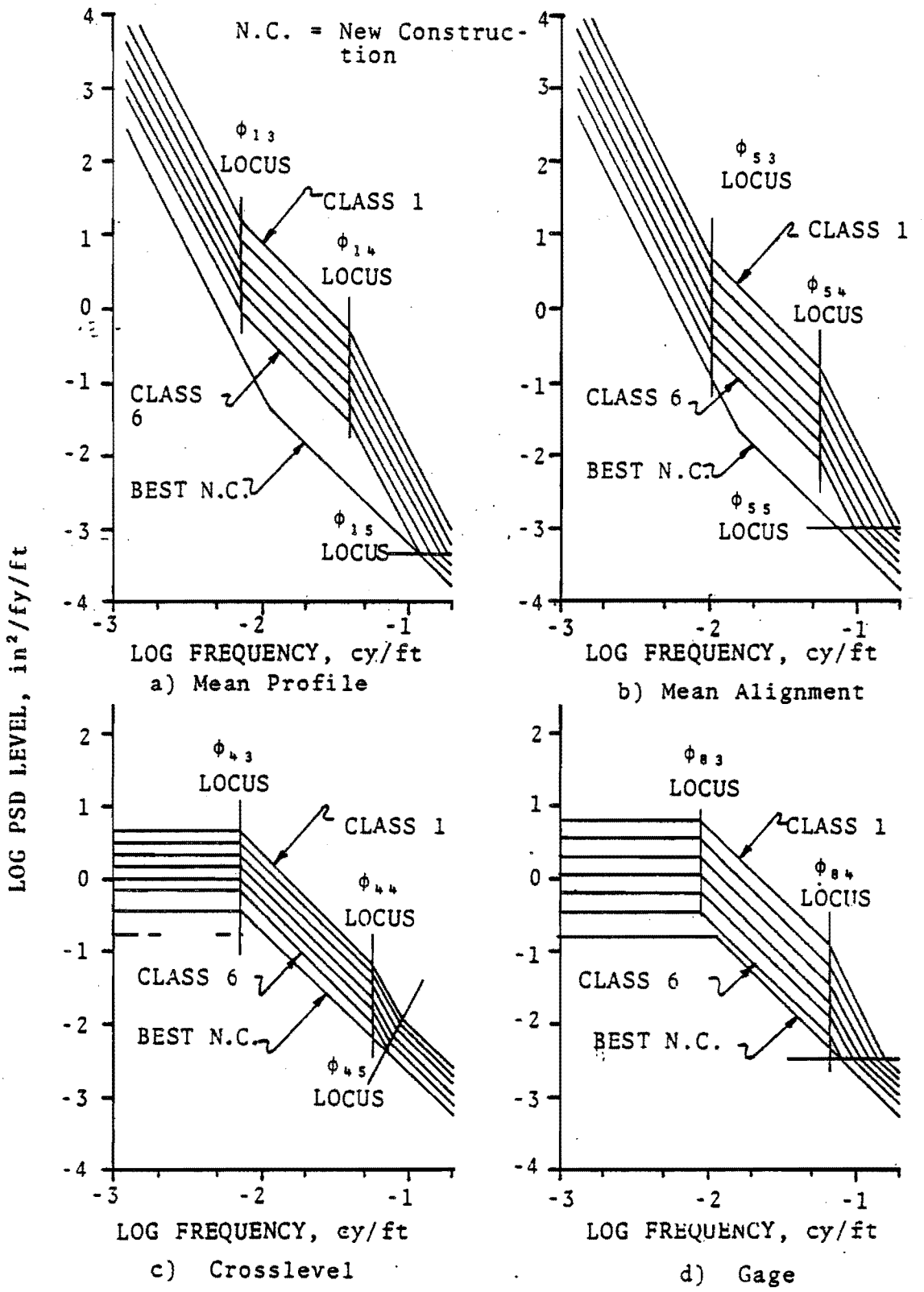

Figure 2-5. Spectral Models as a Function of Track Class as Defined in Current Track Safety Standards

As mentioned earlier, the roughness parameter, A, is strongly dependent on track class. This is illustrated in Figure 2-6 for the roughness parameter of mean profile.

Through the regression analysis, it was first established that the standard deviations of the measures specified in the track safety standards were closely related to the roughness parameter. For example, the empirical relationships for profile was given by:

$$\sigma = 21 \sqrt{A_1} \tag{2-8}$$

where

σ = standard deviation of 62-foot MCO of profile, and

A_1 = roughness parameter for profile.

Next it was shown that the standard deviations of the 62-foot MCO were directly proportional to the track class. This relationship for profile was given by:

$$\sigma = 10^{-(0.6 + v)/8} \tag{2-9}$$

From equations (2-8 and (2-9)

$$A_1 = 0.002310^{-(0.6 + v)/4} \tag{2-10}$$

Thus, the roughness parameter is functionally related to the track class.

The regression analysis was also performed among the roughness parameters of various track geometry parameters. The following least square relationship was found to exist between these parameters:

$$A_3 = 200\ A_4^{3/2} = \sqrt{2}\ A_7 = \sqrt{2}\ A_8 \tag{2-11}$$

where

A_3 = roughness parameter for mean profile,

A_4 = roughness parameter for crosslevel,

A_7 = roughness parameter for mean alignment,

and A_8 = roughness parameter for gage.

The curve fitting procedure was applied to the spectral line components of the empirical PSD's. The mean amplitude, $\bar{C}$, and the decay rate, k, were thus evaluated. A regression against track class produced the results summarized in the bottom part of Table 2-3. There are significant variations of both $\bar{C}$ and k as a function of track class with both the amplitude and the duration (k^{-1}) growing with degradation. Also, the scatter in $\bar{C}$ about the regression lines increases significantly for the lower classes of track.

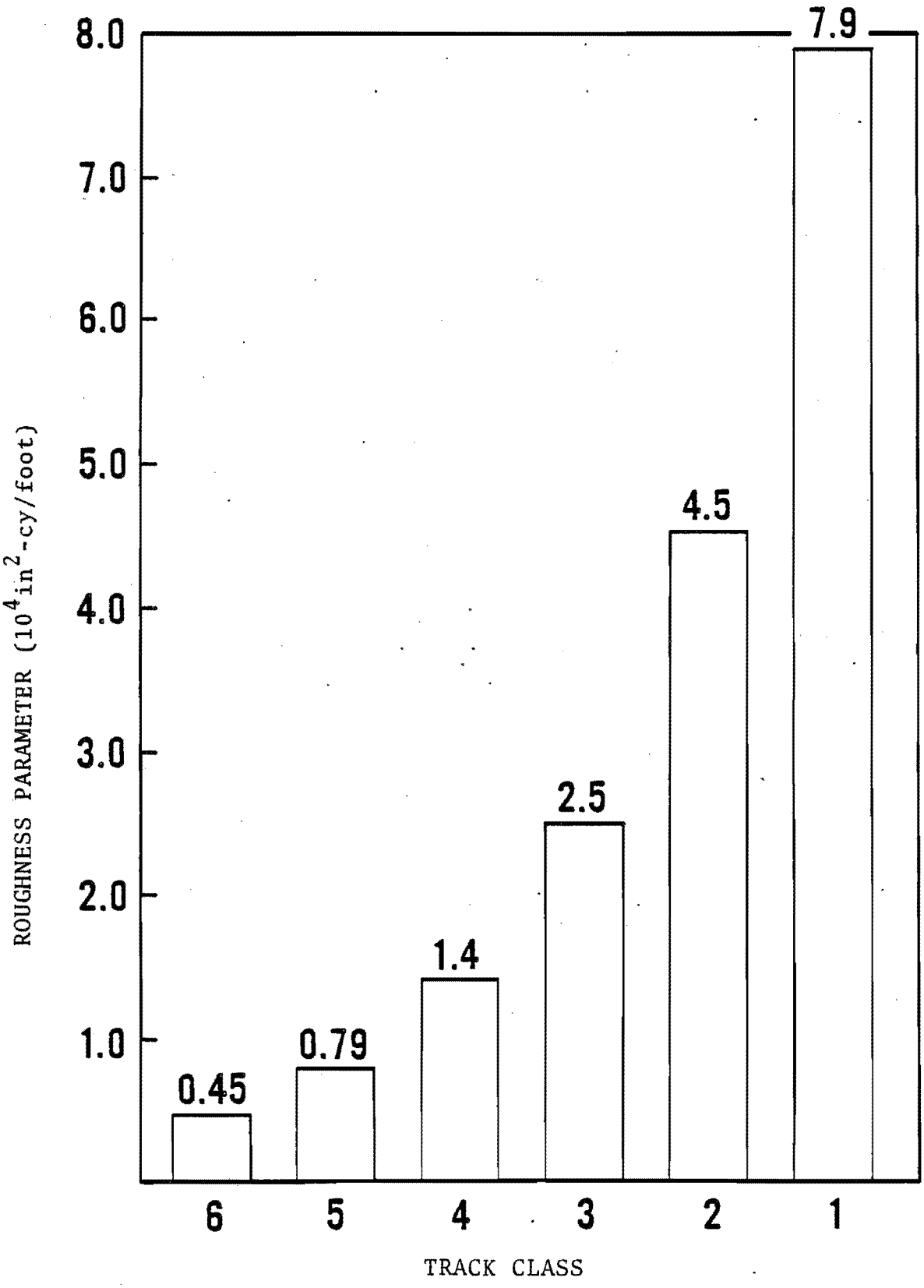

Figure 2-6 Roughness Profile Parameter Versus Track Class

Regressions were performed to determine how the mean joint amplitude varied with the exception thresholds for surface variables as prescribed in the track safety standards. The following least square relationship was found between the mean amplitude and the track class:

$$\bar{C}_1 = 10^{-2(2.0 + \nu)/8} \qquad (2\text{-}12)$$

where

$\bar{C}_1$ = mean joint amplitude (profile),

and ν = track class.

An increase of scatter was found with decreasing track class.

Regressions were also performed to determine how $\bar{C}_1$ for profile and $\bar{C}_5$ for alignment varied with the corresponding roughness parameters, A_1 and A_5, and with decay rates, k_1, for profile and k_5 for alignment. The mean joint amplitudes were found to increase with the increase in the roughness parameters with the following least square relationships:

$$\bar{C}_1^2 = 200\ A_1$$
$$\text{and} \qquad \bar{C}_5^2 = 250\ A_5 \qquad (2\text{-}13)$$

Decay rates showed inverse relationships with mean amplitude. Thus, while the mean amplitudes decrease with the increase in track class, the values of decay rates increase with the increase in the track class. In the case of profile, the decay rates start at relatively high values for undegraded track and as the track degrades, it eventually settles to a value of 0.14/ft. Alignment decay rates approach the same value but not so quickly.

2.3.2 EXTREMELY LONG AND SHORT WAVELENGTHS

Extremely long wavelengths (approximately 100,000 feet) PSD's were generated from the track charts using the procedure described in Appendix B.3. Extremely short wavelength (0.01 foot) PSD were generated by using some data contained in Remington, et al.(11) Results are shown in Figures 2-7, 2-8 and 2-9. These figures establish confidence that the trends exhibited by the intermediate wavelength PSD's are indeed valid and not biased by processing techniques.

2.3.3 STATISTICAL DISTRIBUTION

As discussed in Section 2.2.5, for typical track geometry measures, the stationary random process is a normally distributed random variable with a mean of zero. Thus, the probability density function, $p_1(y)$, is represented by:

$$p_1(y) = \frac{1}{\sqrt{2\pi}\ \sigma} e^{-1/2(y/\sigma)^2}, \qquad (2\text{-}14)$$

where y is a geometry variables, and σ is its standard deviation.

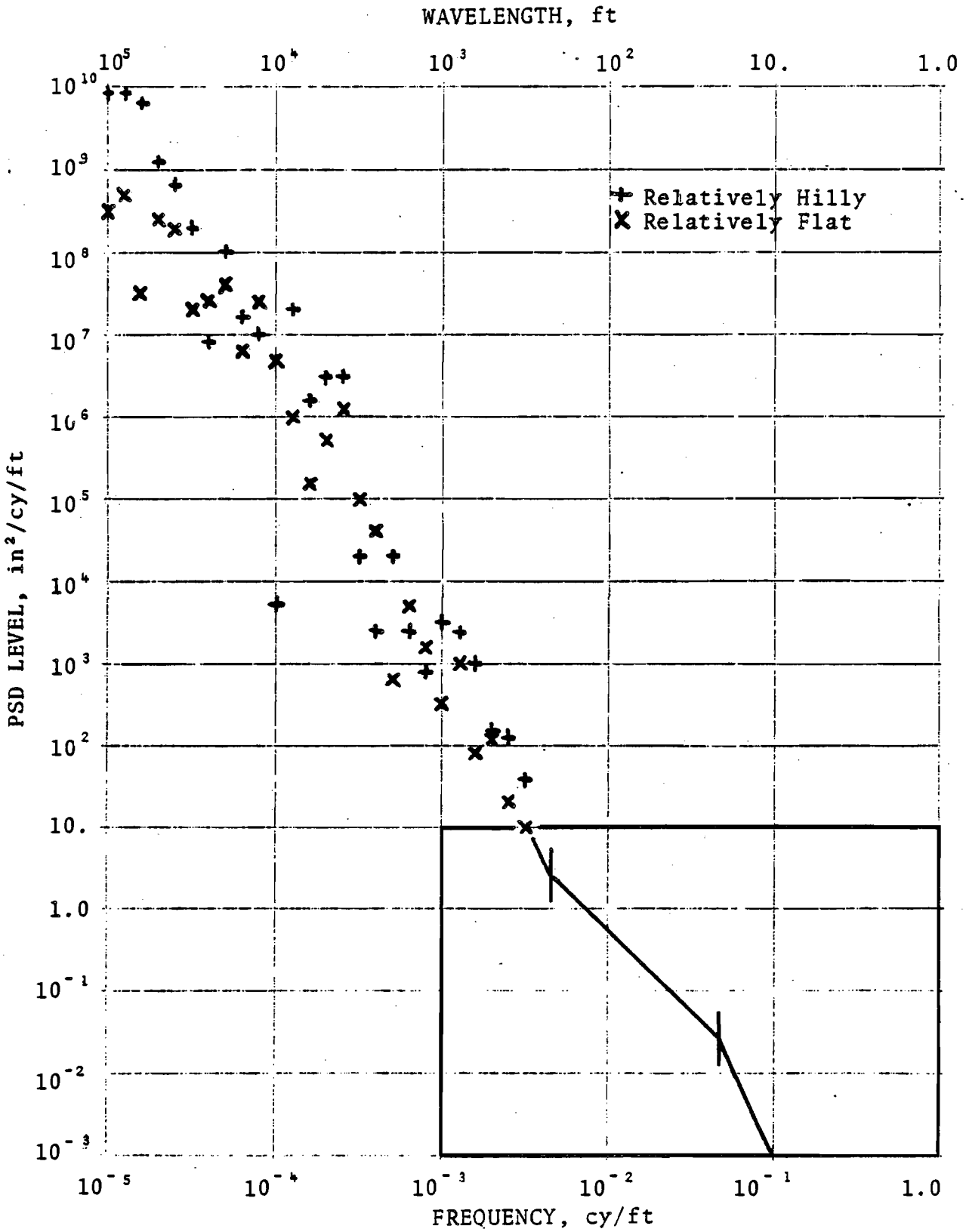

Figure 2-7. Extremely Long Wavelength Profile PSD's

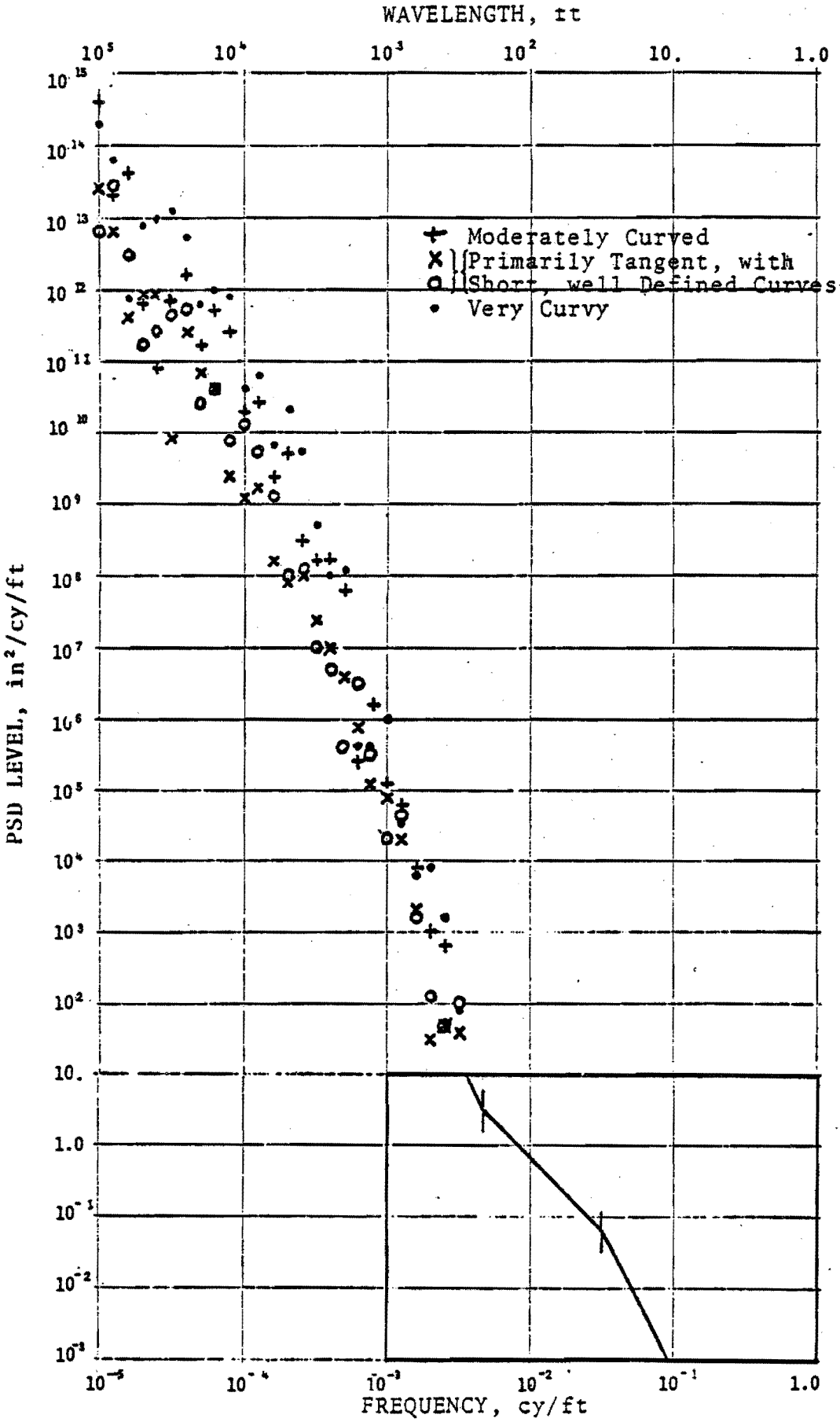

Figure 2-8. Extremely Long Wavelength Alignment PSD's

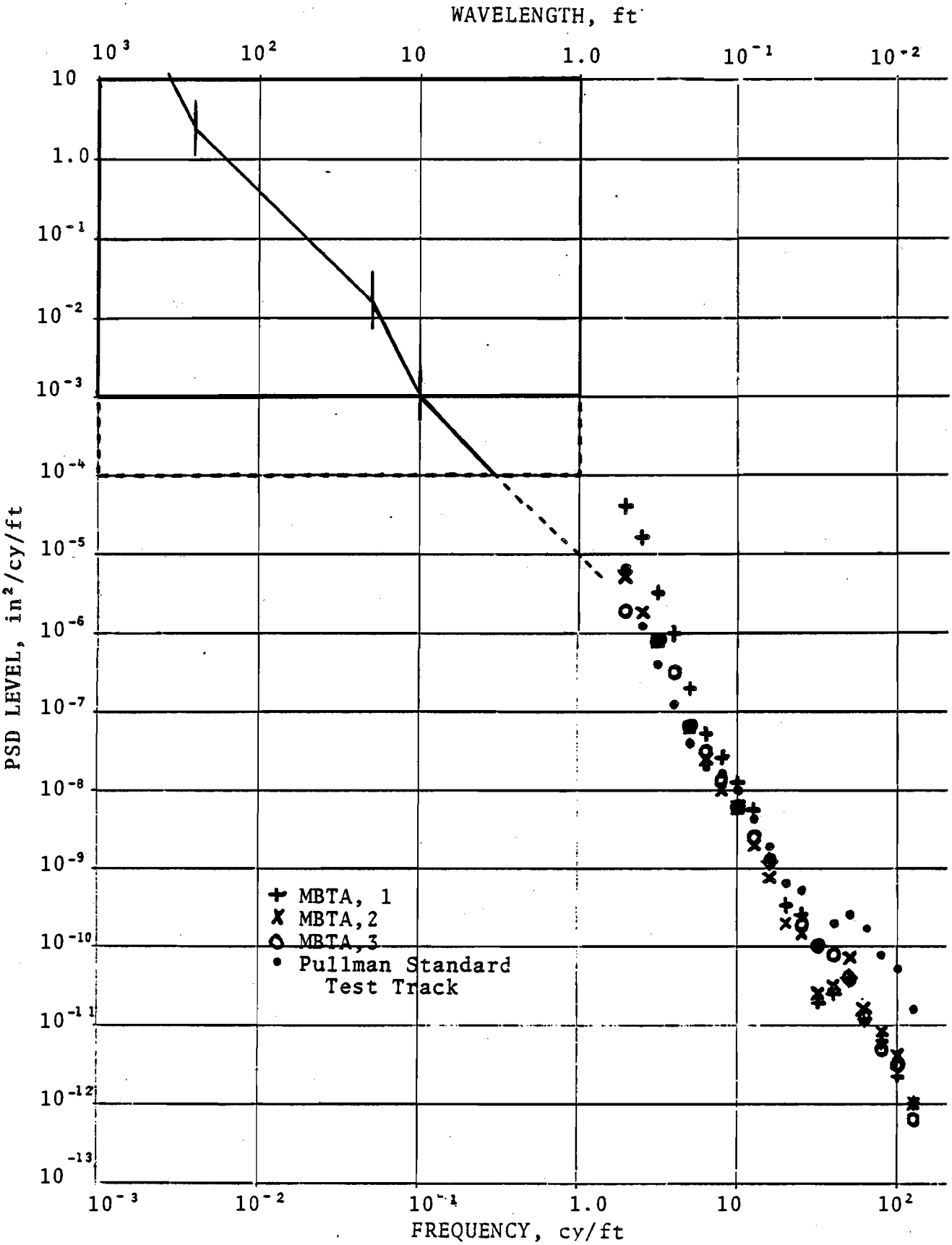

Figure 2-9. Extremely Short Wavelength Profile PSD's

It was further determined that the periodic process is distributed according to the Γ-distribution given by:

$$P_2(C) = \begin{cases} 0, & -\infty < C < 0; \\ \left(\frac{4}{\bar{C}}\right)^4 \frac{C^3 e^{-4C/\bar{C}}}{6}, & 0 \leq C < \infty \end{cases} \qquad (2\text{-}15)$$

where $\bar{C}$ is the mean of C.

The stationary random process and the periodic joint process occur simultaneously. The density function for this combined process is given by:

$$P_3(y) = Ke^{-1/2(y/\sigma)^2} \left(1 + \ell^2\right) + \frac{\sqrt{\pi}}{2}\left(3\ell + 2\ell^3\right) \left[1 + \text{erf}(\ell)\right] e^{\ell^2} \qquad (2\text{-}16)$$

where $K = \frac{1}{3\sigma\sqrt{2\pi}} \left(\frac{4\sigma}{\bar{C}}\right)^4$,

and $\ell = \frac{1}{\sqrt{2}} \left(\frac{y}{\sigma} - \frac{4\sigma}{\bar{C}}\right)$.

The densities $p_1(y)$, $p_2(y)$ and $p_3(y)$ are graphed in Figure 2-10.

Using the PSD models and the associated parameters given in Tables 2-2 and 2-3, standard deviations (σ) of the stationary random component were generated for the track measures cited in the FRA Track Safety Standards. This included gage, crosslevel, 31-foot warp*, and 62-foot mid-chord offsets of both profile and alignment. Comparing these results with threshold in the Track Safety Standards reveals that:

- In the lower classes of track (1 to 4) gage requires as little as 3- or 4-σ event to exceed an exception level.
- Other geometry measurements for Classes 1 to 4 require 5-σ or even higher multiples of σ to produce an exception.

To better understand the implications of this result, the correlation properties of gage, crosslevel, and 62-foot midchords of alignment and profile were computed, assuming a stationary random input described by the model PSD's. The results are shown in Figure 2-11. A correlation distance, x_0, describes how far along the track one must travel to obtain an independent measurement of geometry. Values of x_0 are on the order of 20 feet for the above track measures. Using the normal distribution and the 20-foot distance between independent measurements a +5σ level is exceeded once every 6,600 miles per geometry variable. A +4-σ exception is exceeded once every 60 miles. A +3-σ value occurs once every 1.4 miles. Therefore, for Class 4 through 1,

*The standard deviation for 62-foot warp is close to 1.41 times the standard deviation of crosslevel.

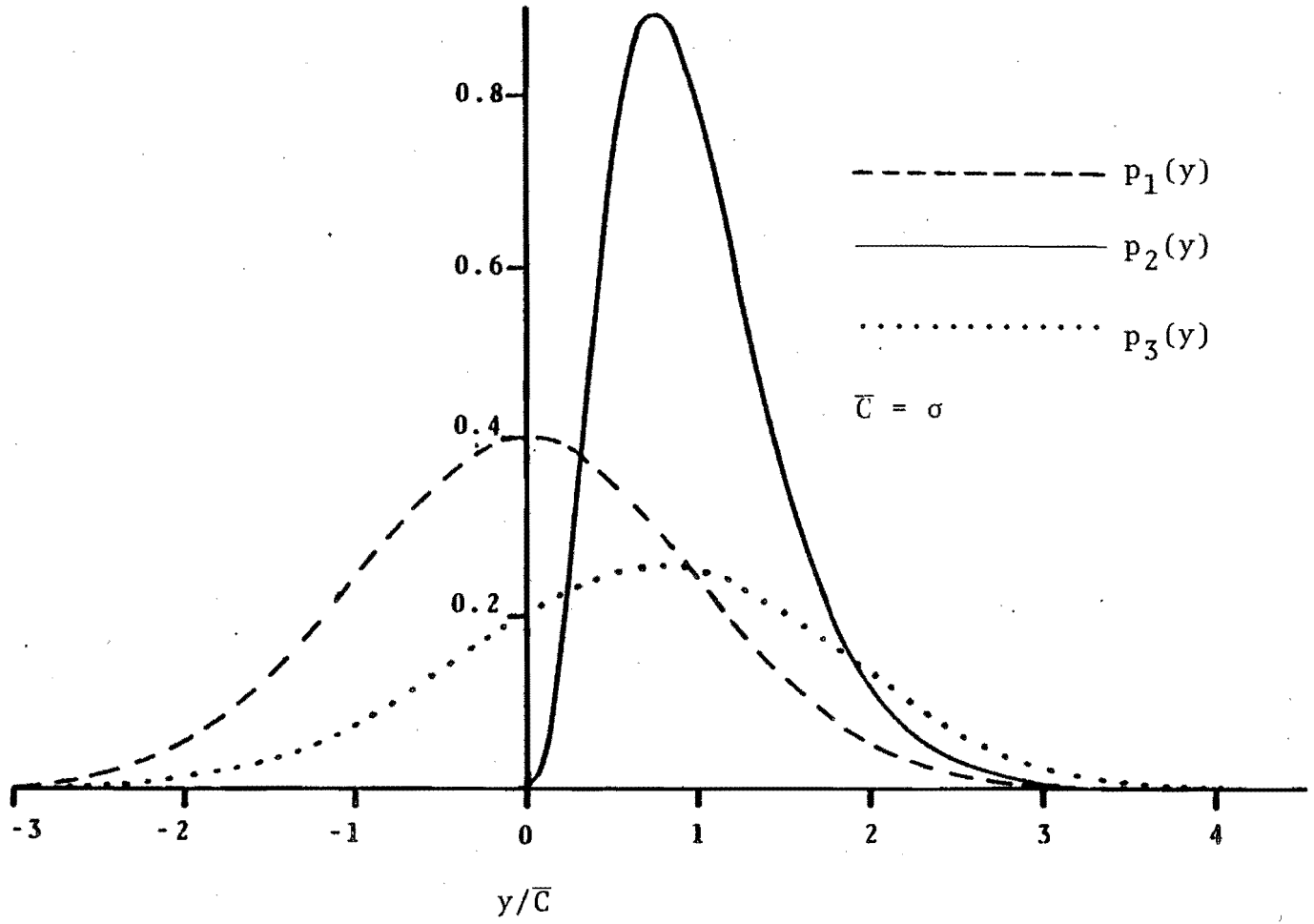

Figure 2-10. Comparison of Probability Densities $p_1(y)$, $p_2(y)$ and $p_3(y)$

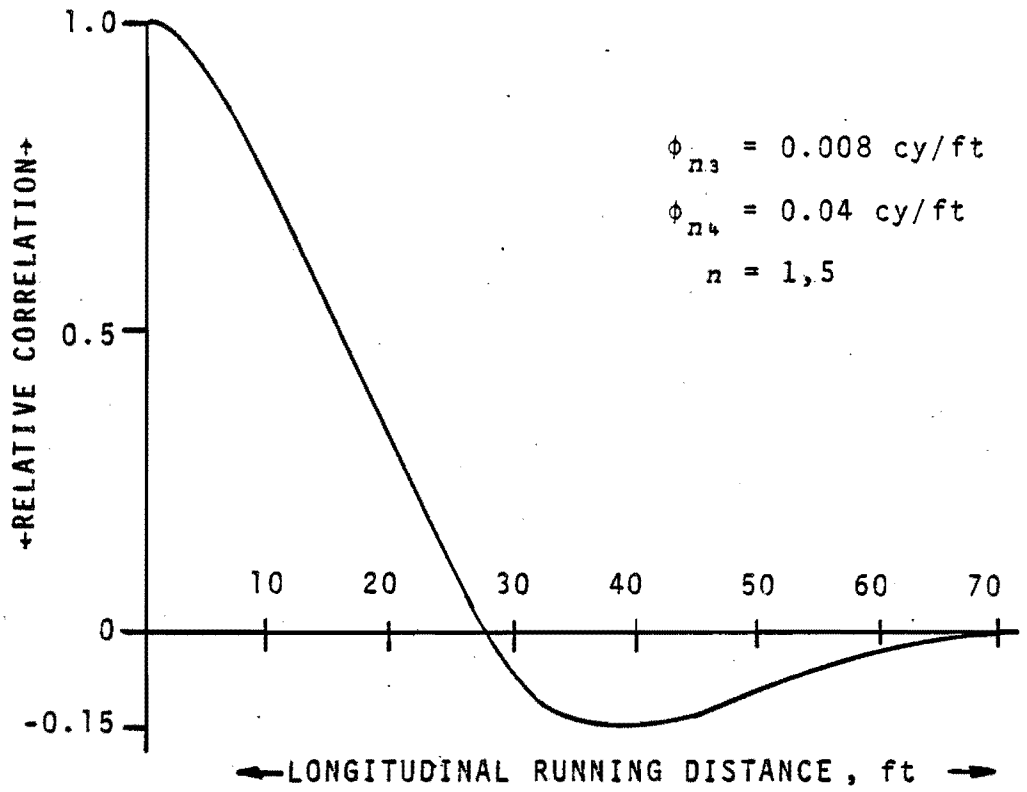

a) 62 FOOT MID-CHORD ON MODEL SPECTRUM, $A_n(\phi)$

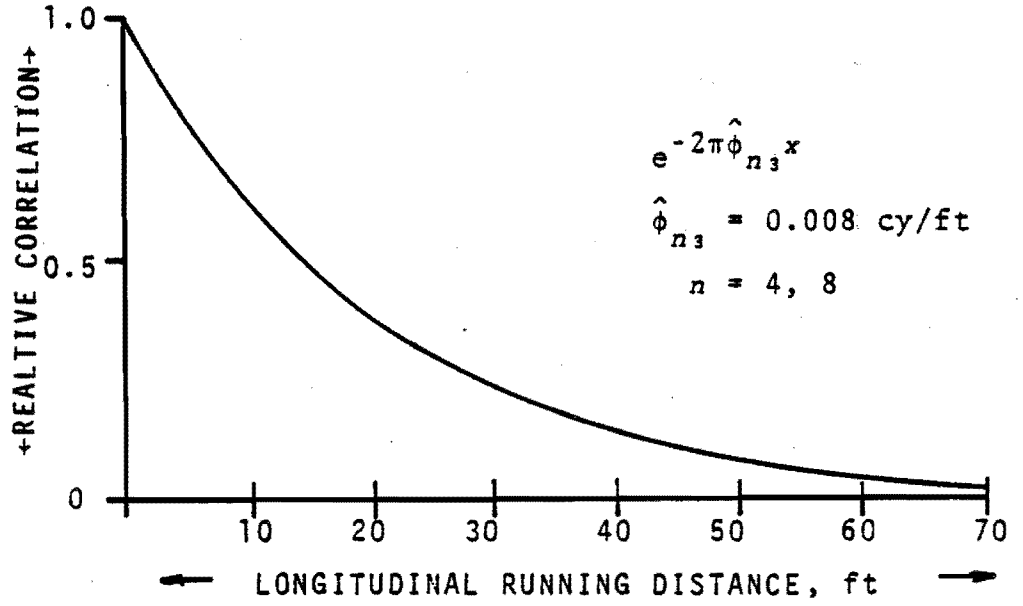

b) CROSSLEVEL AND GAGE ON MODEL SPECTRUM, $A_n(\phi)$

Figure 2-11. Correlation Properties of Current Track Geometry Measurements

the stationary random process acting by itself is unlikely to produce exceptions to the safety standards for geometry variations other than gage.

As mentioned earlier, the joint amplitudes are distributed according to a Γ-distribution. This process is more likely to produce an exception in crosslevel. Also, crosslevel is more likely to produce an exception than is profile. The crosslevel exception requires a low joint of amplitude $\sigma\bar{C}$ in classes 1 through 4. The probability that a single low joint will exceed a level of $\sigma\bar{C}$ is on the order of 10^{-7}. With each joint acting independently and spaced on the average of 19.5 feet, a $\sigma\bar{C}$ joint will happen once every 38,000 miles.

In actual track, the randomly distributed joints are superimposed on the stationary random process. If the random joint process ($\sigma\bar{C}$ equals exception level) is combined with the stationary random process (5σ equals exception level), then the combined process produces a crosslevel exception once every 60 miles. The history of crosslevel data collection reveals that crosslevel exceptions occur much more frequently than this. Therefore, it is concluded that the typical track geometry variations as described in this section cannot account for the observed frequency of geometry exceptions.

2.4 CONCLUSIONS

Time series analyses were conducted to obtain an analytical representation of typical track geometry variations. It is concluded that a periodically modulated random process provides a necessary and sufficient representation of typical track geometry variations. This process consists of a stationary random process and a periodic process having random amplitudes.

The power spectral density (PSD) is a useful tool for estimating the properties of such a process. In track geometry PSD's, it is found that the stationary random process produces the smooth continuum and that a non-zero mean in joint amplitudes (periodic process) causes the spectral peaks.

The PSD continuum representing the stationary random process can be modeled by even-powered laws as a function of break frequencies and a roughness parameter. The break frequencies do not change significantly for different track classes. Thus, the stationary random process is well represented by a single roughness parameter that is strongly related to track class.

The periodic process or joint shape can be modeled by an exponential function characterized by joint amplitude and joint duration. The mean amplitude and the joint duration (inverse decay rate) can be estimated from spectral peaks. Both the mean amplitude and joint duration increase with track degradation.

Track geometry models given in this chapter are very useful in determining the average vehicle responses to track inputs. The models based on PSD provide relatively inexpensive computer processing tools for frequency domain analyses of rail and vehicles. The PSD's can be used to calculate mean square values of rail deviations, rail curvatures, vibration levels in the vehicle, forces at wheel/rail interface and relative displacements between vehicle components. The mean square values are averaged over many rail lengths and they do not single out responses at specific locations within the averaging window.

The PSD is, however, a limited analysis tool for several reasons. Without detailed knowledge of the parent probability distributions governing each input and each response mode, mean square values cannot predict peak values. Another deficiency of the PSD concerns its

averaging property. Identical PSD's result from a wide variety of time histories. Therefore, track geometry PSD's do not give unique vehicle response for nonlinear vehicles. The PSD also destroys phase information so that the periodic deterministic waveshape cannot be reconstructed by using just the magnitudes of the peaks.

The stationary random component of typical track goemetry variations is a normally distributed random variable. The periodic process is represented by the I-distribution. The stationary random process and the periodic joint process occur simultaneously in typical track geometry variations. It has been shown that typical track geometry variations can produce one exception to the FRA Track Safety Standards every 66 miles. This is less than three percent of the observed rate of exceptions. Thus, the typical variations cannot account for the observed frequencies of peak amplitudes in the track geometry variations. The peak geometry values are normally associated with track anomalies such as switches, road crossings, turnouts, bridges, etc. Because of its averaging property, the PSD cannot isolate such variations. The analytical description of such isolated variations is, therefore, the subject of the next chapter.

3.0 ISOLATED TRACK GEOMETRY VARIATIONS

Typical track geometry variations include the random waviness in the rail and the periodic process at joints or welds. As discussed in the previous chapter, the PSD characterization of typical track geometry variations cannot account for the occurrences of large amplitude track irregularities. Isolated geometric variations in the track are obscured by the averaging property of the statistical processes used to characterize the typical track geometry variations. The isolated variations represent the spatial irregularities which occur occasionally and have regular patterns. These variations can produce large amplitude vehicle responses and thus should be included in vehicle analyses.

This chapter deals with the analytical description of isolated track geometry variations. The key signatures are first identified. The mathematical functions which can be used to describe these signatures are given along with the parameters of these fucntions. Typical occurrences of isolated track geometry variations are then discussed as single events, periodic variations and combined irregularities in track geometry parameters.

The information presented in this chapter was partially obtained from the personnel experienced in track structures, railroad operations and track geometry data. This was augmented by the analysis conducted on existing track geometry data. This also included the work done in Phases I and II.

Note that the track geometry data for alignment and profile were analyzed in the space curve form. The space curve is a pseudo reconstruction of track as a curve in space without the effects of local terrain.

3.1 KEY SIGNATURES

The following key signatures have been identified in the track geometry data:

- Cusp
- Bump
- Jog
- Plateau
- Trough
- Sinusoid
- Damped Sinusoid
- Sin(x)/x

These signatures can occur as single events, in combination with each other and in a periodic fashion. The following paragraphs give the shape and mathematical description of these signatures.

The shape of a typical cusp is shown in Figure 3-1. The cusp is a pointed end signature with a distinct discontinuity in the first derivative at the center. It has its peak amplitude at the center and returns to the baseline on either end. The cusp can be described by any of the following analytical forms:

$$\text{(a)}\quad y = Ae^{-k|x|}$$

$$\text{(b)}\quad y = A(1 - |\sin \pi kx|) \qquad (3\text{-}1)$$

$$\text{(c)}\quad y = A(1 - 2k|x|) \text{ -- triangular cusp.}$$

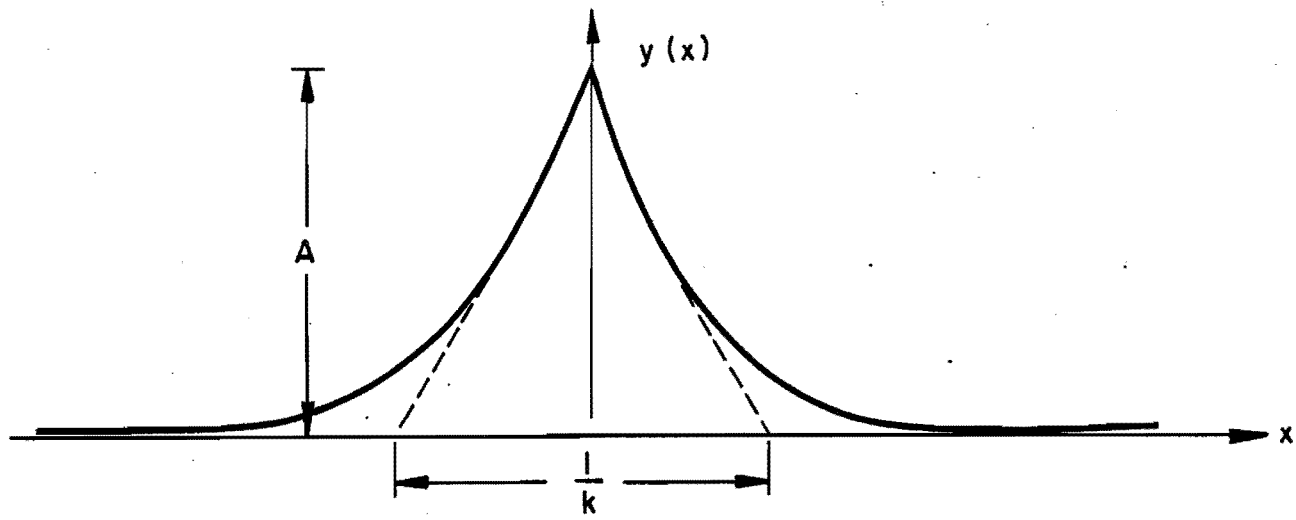

(a) ABSOLUTE SURVEY

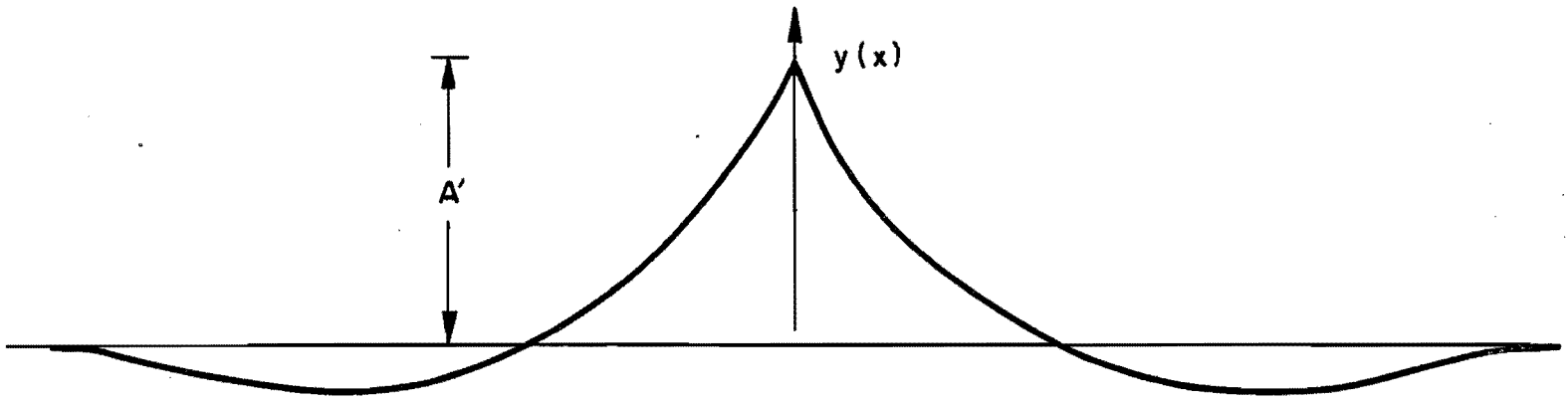

(b) RESPONSE OF SPACE CURVE

Figure 3-1. Cusp Signature

Where A is the peak amplitude and k is the duration (in distance) related parameter.

A typical bump signature is shown in Figure 3-2. This is a bell shaped curve which usually occurs at a depression in the rail or track. This signature also attains the peak amplitude at the center and returns to the baseline on either side. The function and at least its first derivative are continuous throughout the disturbance. The possible descriptive analytical forms for bump are:

$$\text{(a)}\quad y = A \operatorname{sech}(kx)$$

$$\text{(b)}\quad y = Ae^{-1/2(kx)^2} \tag{3-2}$$

$$\text{(c)}\quad y = \frac{A}{1 + k^2x^2}$$

Where A is the amplitude at x = 0, and k is the duration related parameter.

A typical jog signature is shown in Figure 3-3. This is a very critical signature and can occur in both the profile and alignment. In the case of jog, the disturbance reaches its maximum amplitude away from the center. The candidate analytical forms for jog are:

$$\text{(a)}\quad y = 1/2\ A \tanh(2kx) \tag{3-3}$$

$$\text{(b)}\quad y = A/\pi \tan^{-1}(\pi kx)$$

$$\text{(c)}\quad y = \frac{Akx}{\sqrt{1 + 4k^2x^2}}$$

Where A is the maximum amplitude and k is the duration related parameter.

A typical plateau signature is shown in Figure 3-4. This is like a step function with smooth rise and fall. The analytical form for a plateau can be obtained from the mathematical descriptions of jog by the following relation:

$$y = 0.5\left(y'(x + 1/k) - y'(x - 1/k)\right) \tag{3-4}$$

Where y'(x) is a functional description of a jog. For example, from equation 3.3(c), the analytical form for plateau is as follows:

$$y = 0.5\left[\frac{Ak(x + 1/k)}{\sqrt{1 + 4k^2(x + 1/k)^2}} - \frac{Ak(x - 1/k)}{\sqrt{1 + 4k^2(x - 1/k)^2}}\right] \tag{3-5}$$

A simpler analytical form for the plateau can be as follows:

$$y = \sqrt{\frac{A^2}{1 + (kx)^8}} \tag{3-6}$$

Another possible form for a plateau is given by a rectangular window with a 10% taper at each end.(12)

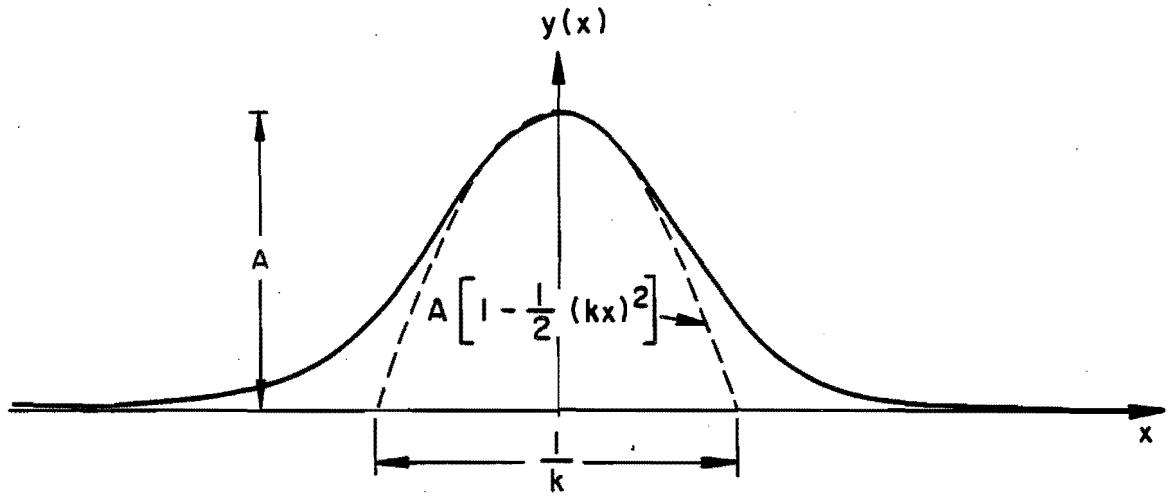

(a) ABSOLUTE SURVEY

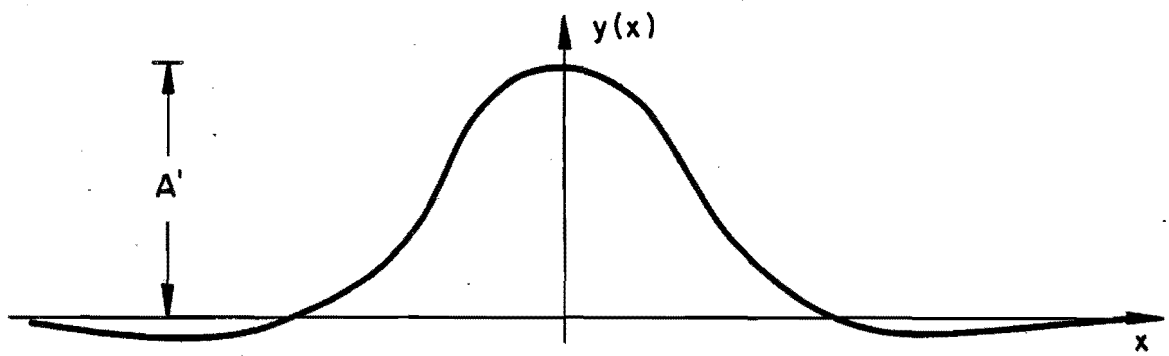

(b) RESPONSE OF SPACE CURVE

Figure 3-2. Bump Signature

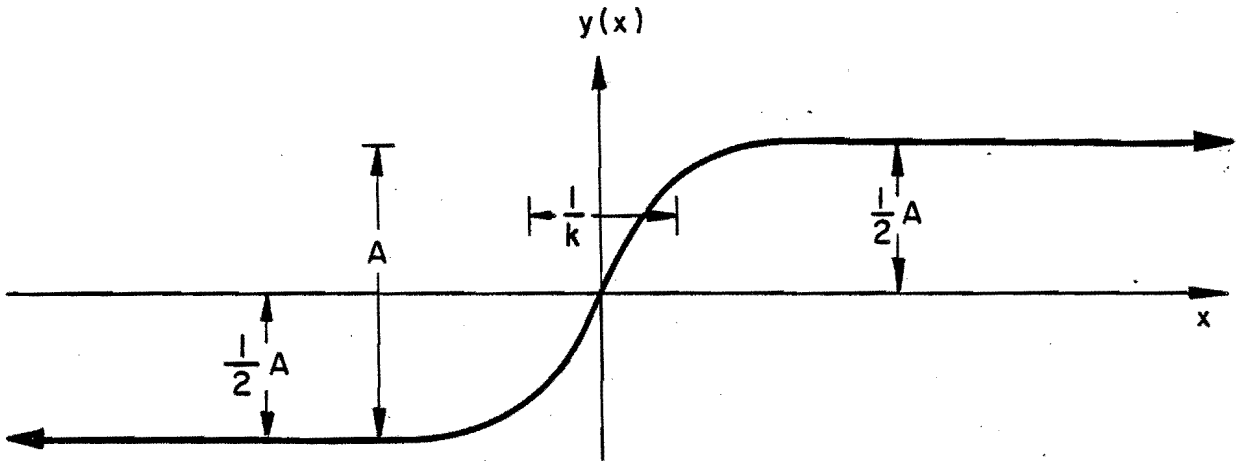

(a) ABSOLUTE SURVEY

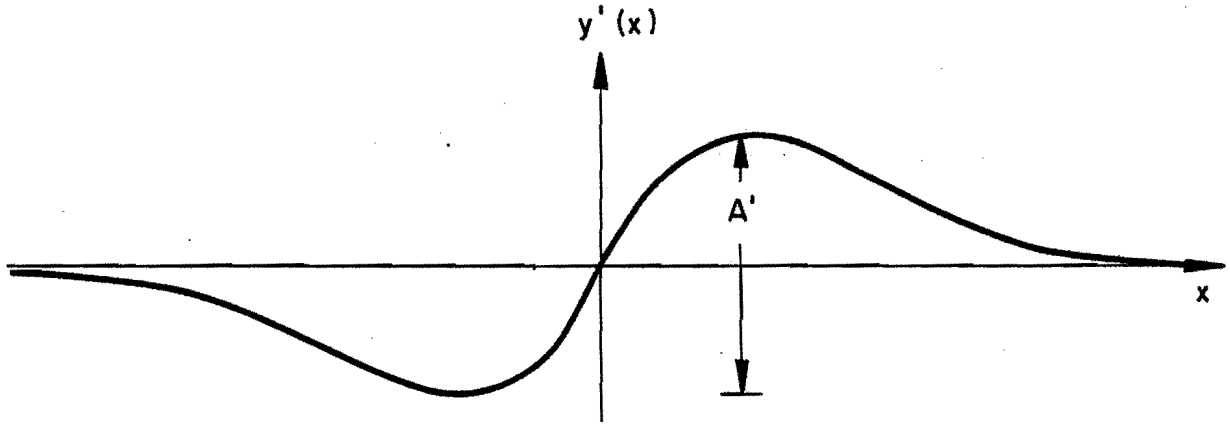

(b) RESPONSE OF SPACE CURVE

Figure 3-3. Jog Signature

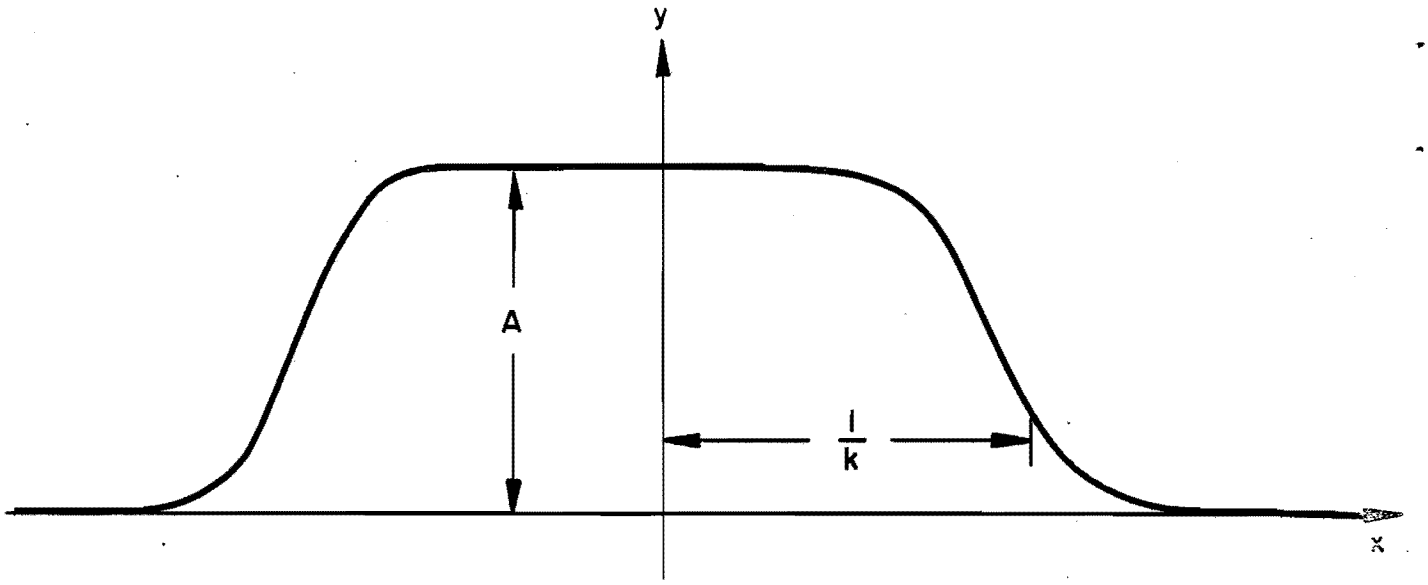

Figure 3-4. Plateau Signature

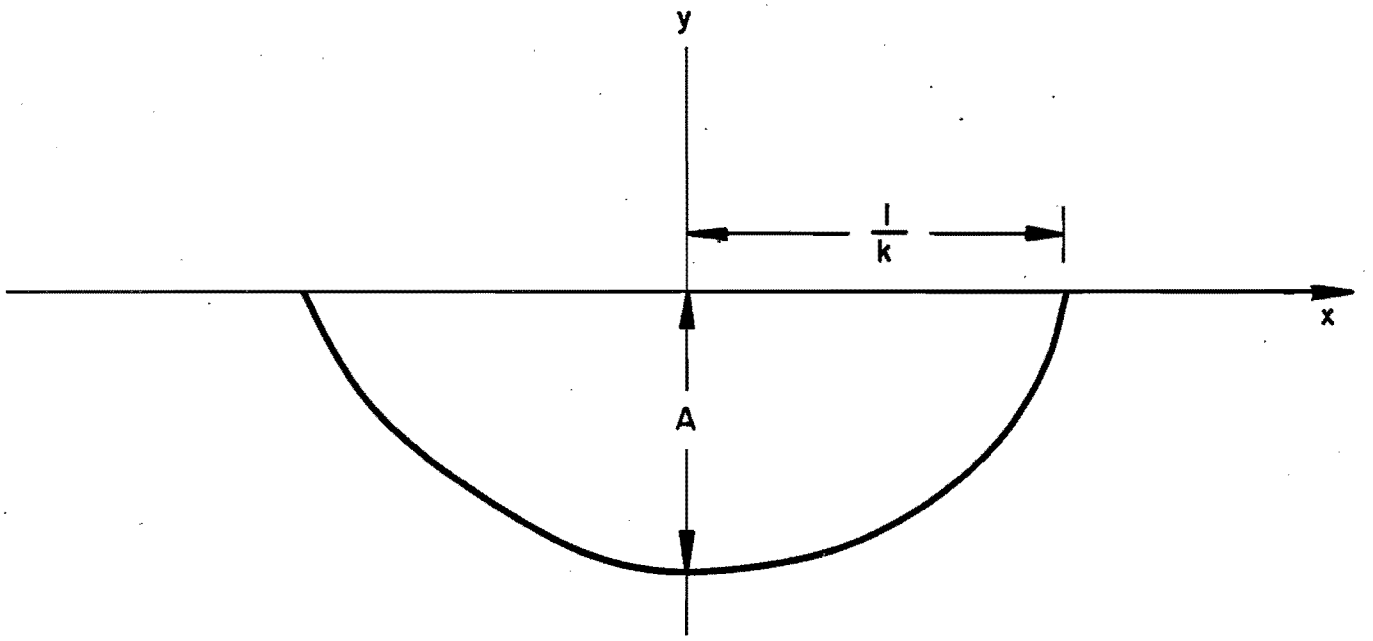

Figure 3-5. Trough Signature

$$Y = \begin{cases} A\cos^2 \frac{5\pi x}{D} & -\frac{D}{2} \leq x \leq -\frac{4D}{10} \\ A & -\frac{4D}{10} \leq x \leq \frac{4D}{10} \\ A\cos^2 \frac{5\pi x}{D} & \frac{4D}{10} \leq x \leq \frac{D}{2} \\ 0 & \text{otherwise.} \end{cases} \quad (3\text{-}7)$$

Where D is the total duration which is approximately equal to 2/k.

A typical trough signature is shown in Figure 3-5. A possible mathematical form for this signature is as follows:

$$y = Ak\sqrt{\left(\frac{1}{k}\right)^2 - x^2} \quad (3\text{-}8)$$

Figures 3-6 through 3-8 show different sinuosidal signatures. These include a sinusoid, a damped sinusoid and a sin (x)/x signature. The mathematical forms for these signatures are as follows:

Sinusoid: $y = A \sin \pi kx$ (3-9)

Damped Sinusoid: $y = Ae^{-kx} \cos \pi kx$ (3-10)

Sin (x)/x: $y = \frac{A \sin kx}{\pi kx}$ (3-11)

Table 3-1 shows how the key signatures are associated with various track geometry parameters. The possiblity of existence of key signatures is given in four levels. This is based on how often a key signature was seen in a track geometry parameter.

The analytical forms of key signatures are functions of two parameters, i.e., amplitude A and a duration related parameter k. Note that the duration of a signature is proportional to 1/k. Table 3-2 gives the relationships which can be used to approximate the duration of a signature.

TABLE 3-2
DURATION OF KEY SIGNATURES AS A FUNCTION OF k PARAMETER

Signature	Duration
Cusp	1.23/k
Bump	1.57/k
Jog	2.00/k
Plateau	2.00/k
Trough	2.00/k
Sinusoid	2.00/k
Damped Sinusoid	2.00/k
(Sin x)/x	2.00/k

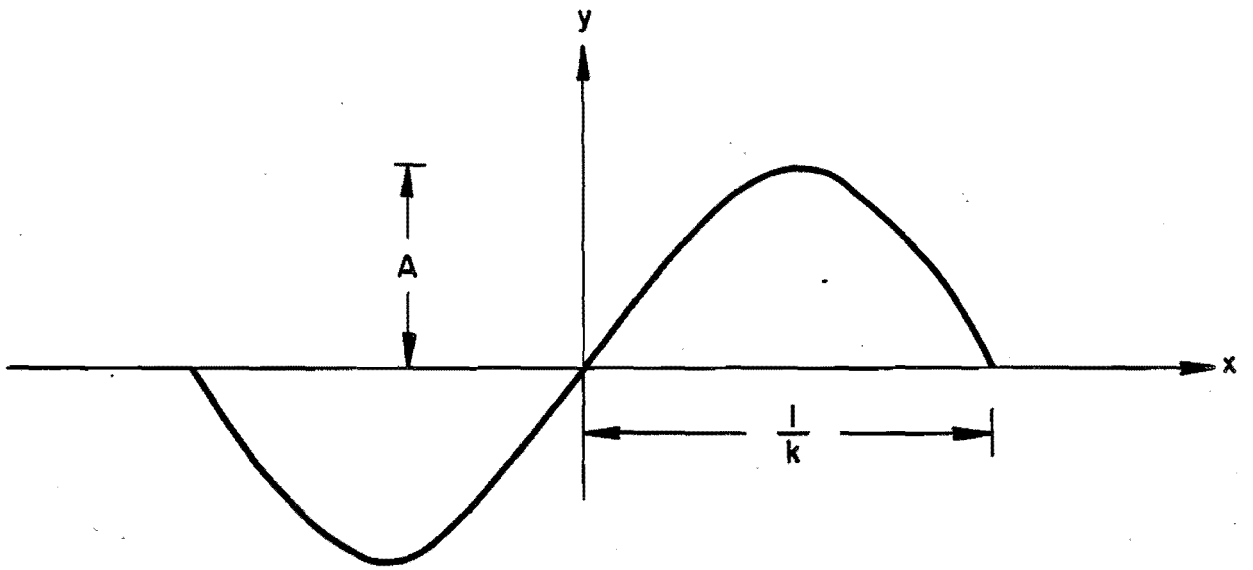

Figure 3-6. Sinusoid Signature

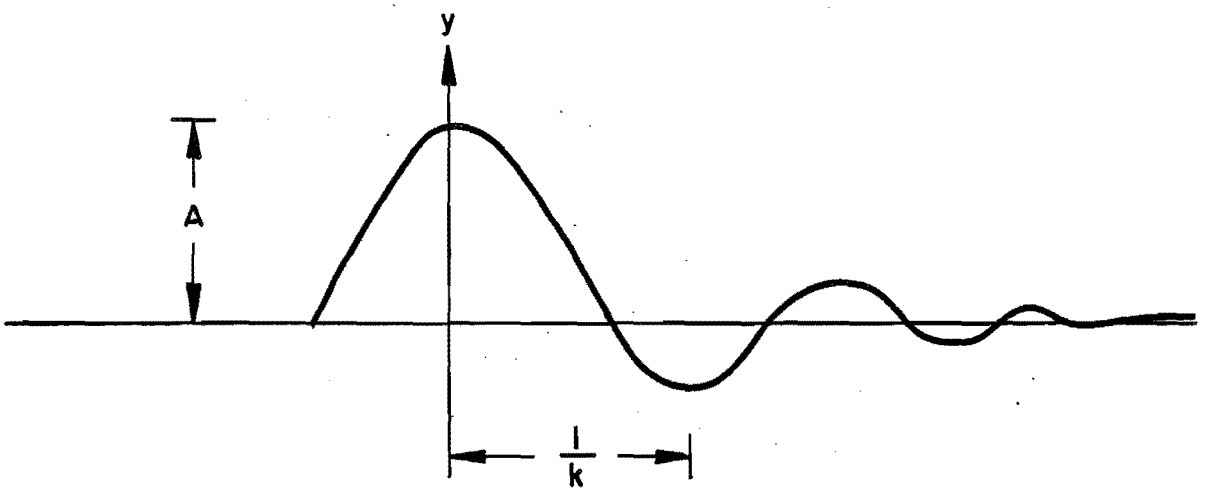

Figure 3-7. Damped Sinusoid Signature

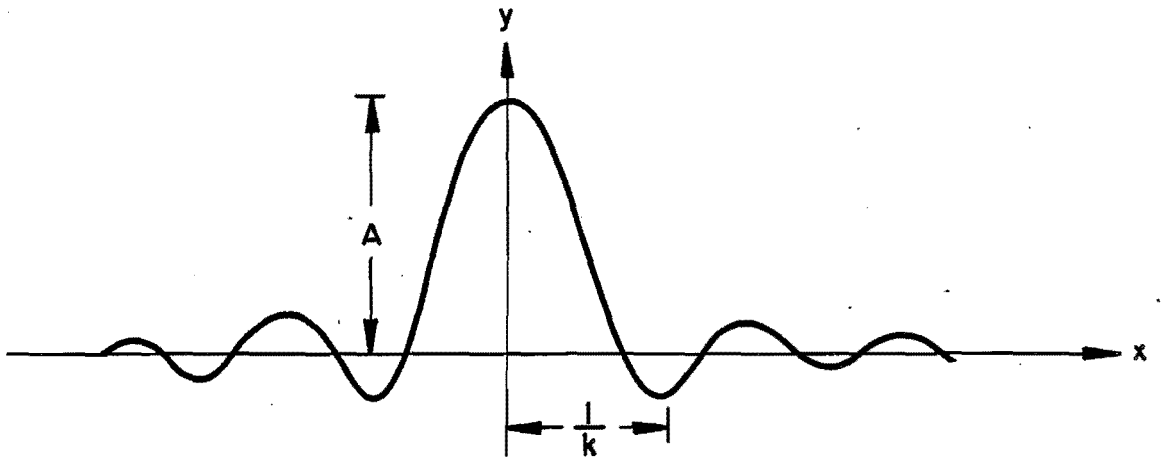

Figure 3-8. Sin x/x Signature

TABLE 3-1. IDENTIFICATION OF KEY SIGNATURES IN VARIOUS TRACK GEOMETRY PARAMETERS.

Signature	Possibility of Existence					
	Gage	Single Rail	Mean Alignment	Single Rail Profile Only	Mean Profile	Crosslevel
Cusp	High	Medium	Medium	Medium	Low	High
Bump	Medium	Medium	High	Medium	High	Low
Jog	None	Low	High	None	High	Low
Plateau	Medium	Low	Medium	Low	High	Low
Trough	Low	Low	Medium	Low	Medium	None
Sinusoid	None	Low	High	Low	Medium	None
Damped Sinusoid	Low	None	Low	Low	Low	Low
(Sin x)/x	None	None	None	None	Low	Low

Table 3-3 gives a range of values of A and k as found in the track geometry data analyzed in this study. Note that the values of these parameters are a function of track class, track geometry parameter, and the signature itself. In general the values of A and k decrease as the track class increases. However, no clear distinction can be made between different track classes as to the range of values of these parameters.

3.2 TYPICAL OCCURRENCES

The isolated track geometry variations most frequently occur at special track work, in spirals and in areas where track stiffness changes. Special track work such as switches, road crossings and bridges are stiffer than the surrounding track structure. It is difficult to maintain and align the track vertically and laterally with the surrounding track structure, especially when cuts, fills and abutments induce pronounced changes in the foundation and drainage characteristics in the area. Thus isolated track geometry variations tend to develop at such locations.

Table 3-4 lists the typical locations where the key signatures have been seen. These signatures occur as single events, in combination with each other and in a periodic fashion. Furthermore, isolated track geometry defects can occur simultaneously in more than one track geometry parameter. Appendix C contains examples of track geometry data showing the key signatures. The following section provides a discussion of typical occurrence of these signatures.

3.2.1 SINGLE EVENTS

Single events provide transitory input to vehicles and can cause severe dynamic interaction. Large amplitude single events are observed in track geometry data at isolated locations. Examples of single events are given in Figures contained in Appendix C.

A single cusp usually occurs at expansion or insulated joints in Continuous Welded Rail (CWR). This is most common in profile where cusp in one rail is usually accompanied by a depression on the opposite rail. Isolated cusps in gage and alignment can occur at joints with loose joint bars. An example of a single cusp in profile is shown in Figure 3-9.

A bump in one rail is also normally accompanied by a bump in the opposite rail. Bumps of large duration are almost always found simultaneously in the two rails. However, a bump in single rail profile may occur due to localized soft spots. A bump in mean profile can occur at bridge abuttments or under overpasses. Single bumps in mean alignment are usually observed in curves. A single bump in gage has been observed 100 to 200 feet away from spiral exits. Figures 3-10 through 3-12 show examples of single bumps in mean profile, mean alignment and gage.

The jog signature is commonly found in mean alignment. A typical example is a dogleg spiral. Spirals are laid out as transition regions to ease the movement of vehicles from tangent sections into curves and vice versa. However, under megatons of traffic over many years, the curve body moves outward and develops into a dogleg spiral. Single jogs in both the mean alignment and mean profile are found in spirals. A single jog can also occur due to change in track stiffness. This happens, for example, going from a solid track to a bridge or going from one weight rail to another. This can also occur due to improper maintenance techniques. Figures 3-13 and 3-14 show examples of single jogs in mean alignment and profile respectively.

A single plateau is commonly seen in mean profile and alignment. This has typically been observed at grade crossings and bridges and is

TABLE 3-3. PARAMETERS OF ANALYTICAL REPRESENTATIONS OF ISOLATED VARIATIONS.

Signature	Range of Values							
	Gage		Alignment		Crosslevel		Profile	
	A (inch)	k (ft^{-1})	A (inch)	k (ft^{-1})	A (inch)	k (ft^{-1})	A (inch)	k (ft^{-1})
Cusp	0.8-1.4	0.016-0.061	0.5-3.0	0.011-0.103	0.9-3.0	0.031-0.095	0.9-3.0	0.016-0.095
Bump	0.8-1.4	0.031-0.040	0.5-2.8	0.009-0.083	1.0-3.0	0.017-0.031	0.5-4.0	0.013-0.065
Jog	*	*	0.5-3.3	0.006-0.025	1.6-2.8	0.020-0.050	0.5-5.0	0.008-0.045
Plateau	0.8-1.3	0.029-0.08	1.2-1.6	0.025-0.027	0.6-1.0	0.026-0.04	0.9-3.0	0.009-0.033
Trough	*	*	1.4-2.2	0.013-0.029	*	*	0.7-2.0	0.020-0.025
Sinusoid	*	*	0.8-1.2	0.033-0.020	*	*	1.0-1.5	0.020-0.025
Damped Sinusoid	0.5-1.0	*	1.0-2.2	0.013-0.015	0.9-1.2	0.051-0.061	*	*
Sin x/x	*	*	*	*	*	*	1.0-1.2	0.031-0.033

*Signature not observed in the data.

TABLE 3-4. TYPICAL OCCURRENCES OF ISOLATED VARIATIONS

Signature	Occurrence
Cusp	joints, turnouts, interlockings, sun kinks, buffer rail, insulated joints in CWR, splice bar joint in CWR, piers at bridge
Bump	soft spots, washouts, mud spots, fouled ballast, joints, spirals, grade crossings, bridges, overpasses, loose bolts, turnouts, interlockings
Jog	spirals, bridges, crossings, interlockings, fill-cut transitions
Plateau	bridges, grade crossings, areas of spot maintenance
Trough	soft spots, soft and unstable subgrades, spirals
Sinusoid	spirals, soft spots, bridges
Damped Sinusoid	spirals, turnouts, localized soft spot
Sin x/x	localized soft spots, insulated joints

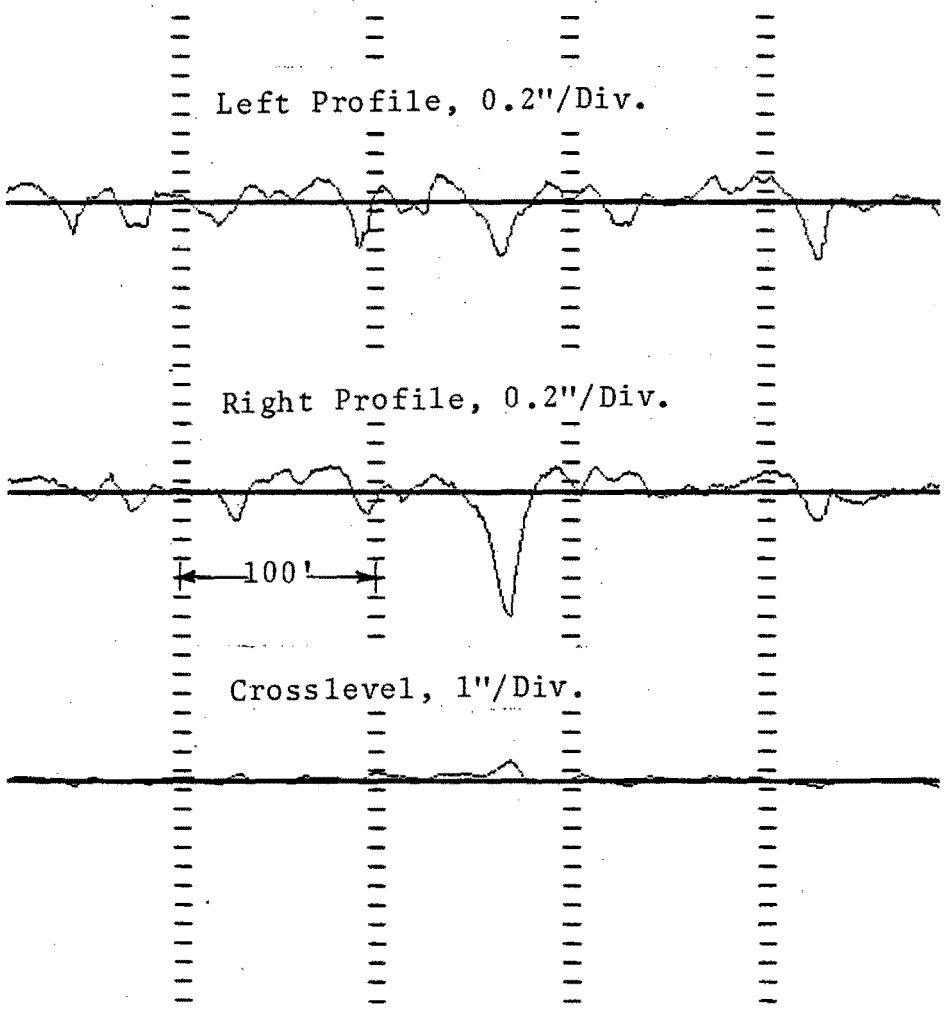

Figure 3-9. Single Cusp in Profile (Class 4, Tangent).

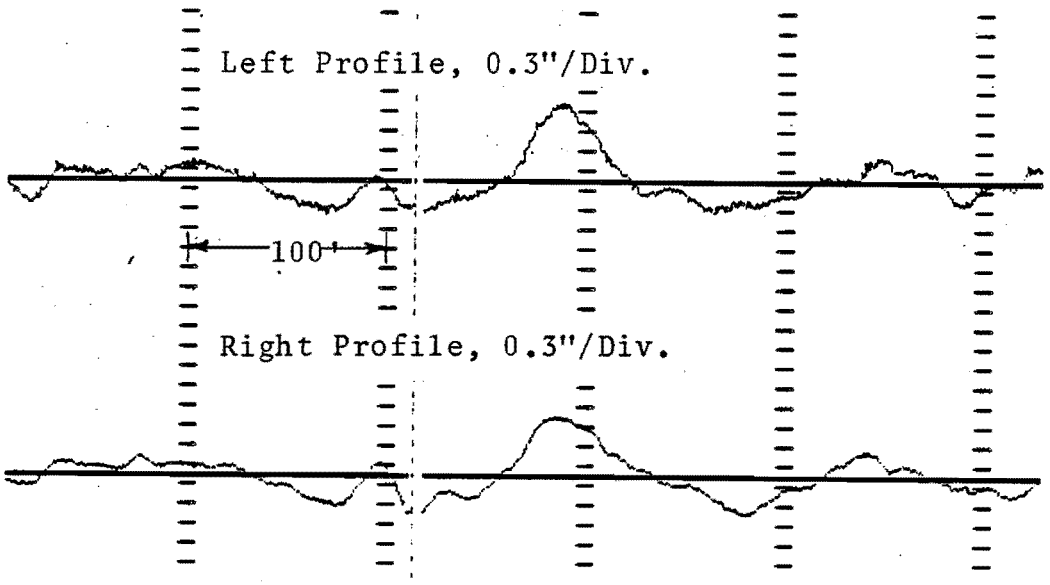

Figure 3-10. A Bump in Mean Profile at a Bridge (Class 5, Tangent, Welded)

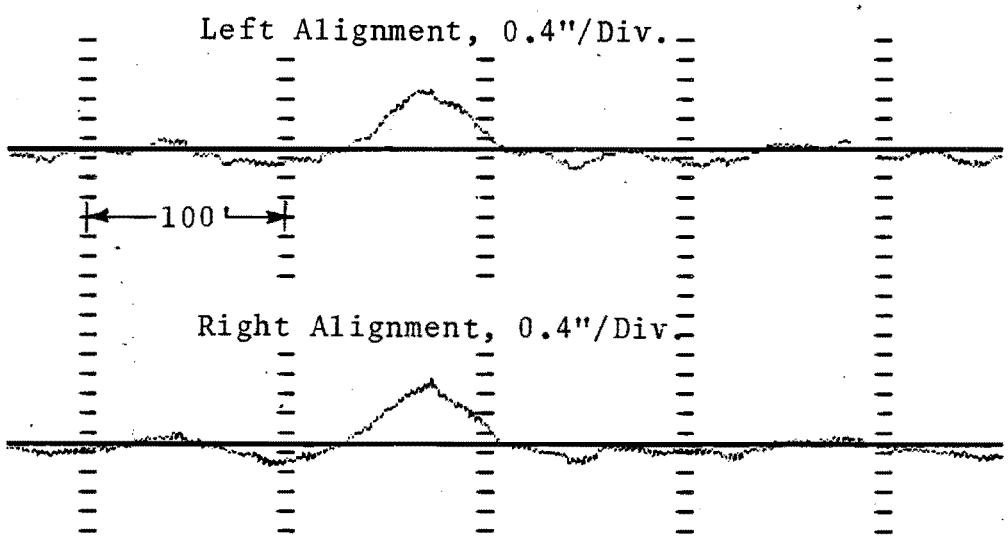

Figure 3-11. A Bump in Mean Alignment in a Curve (Class 6, Curve)

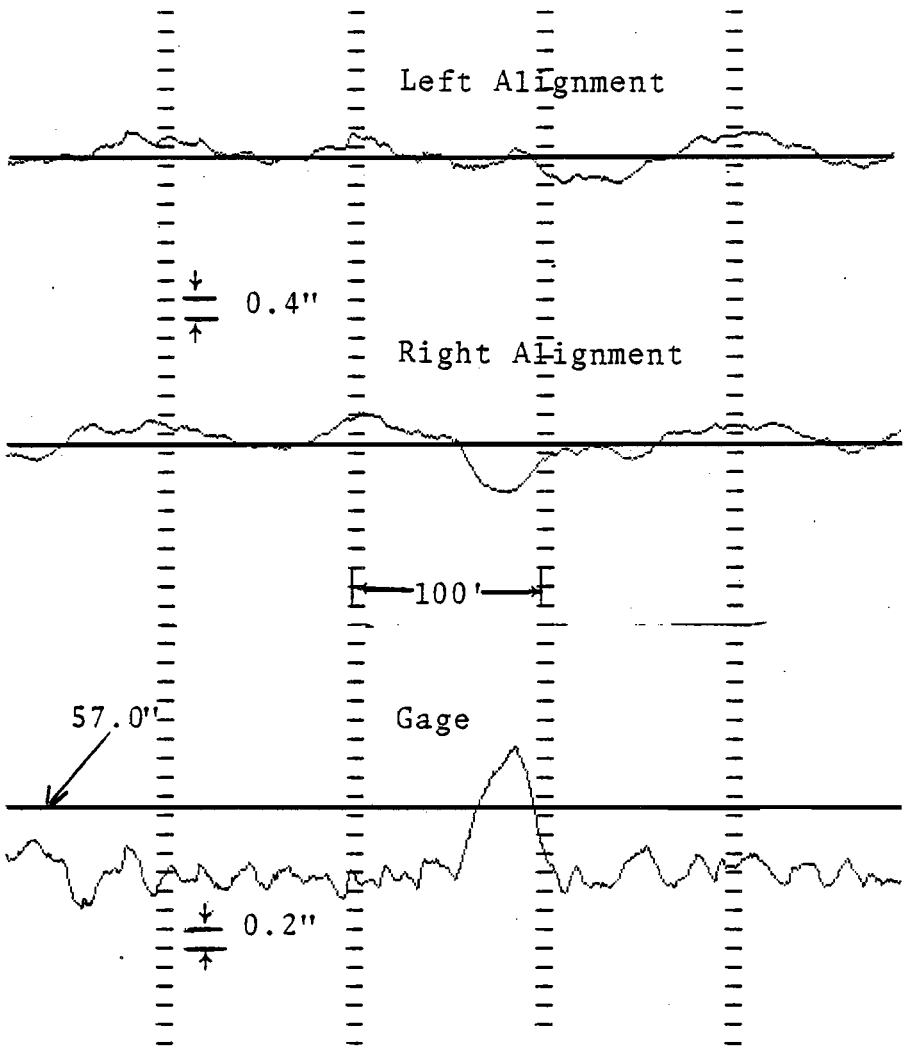

Figure 3-12. A Bump in Gage (Class 3, Tangent)

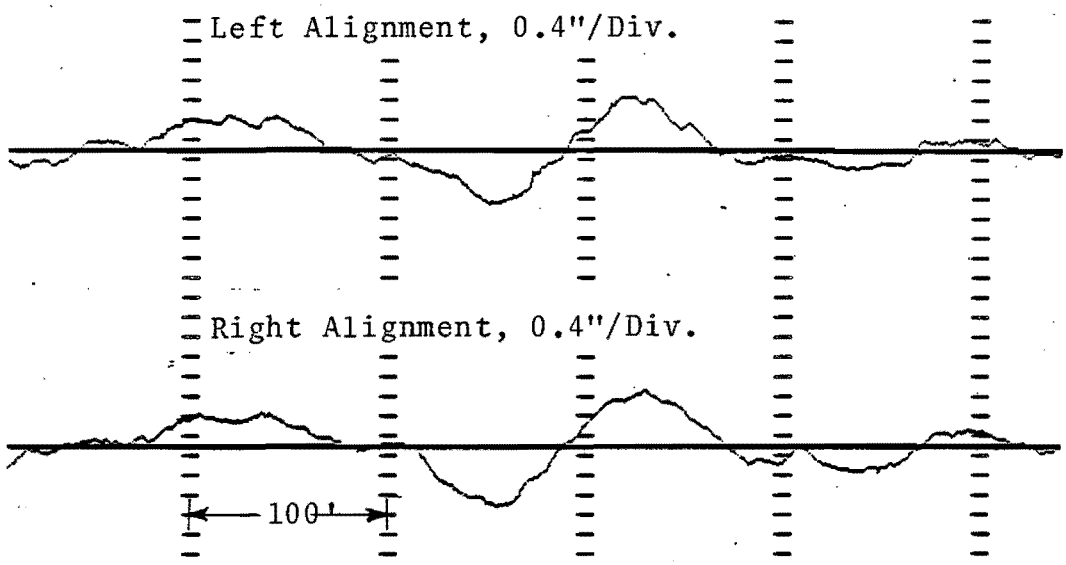

Figure 3-13. A Jog in Mean Alignment on Tangent Track (Class 2, Tangent)

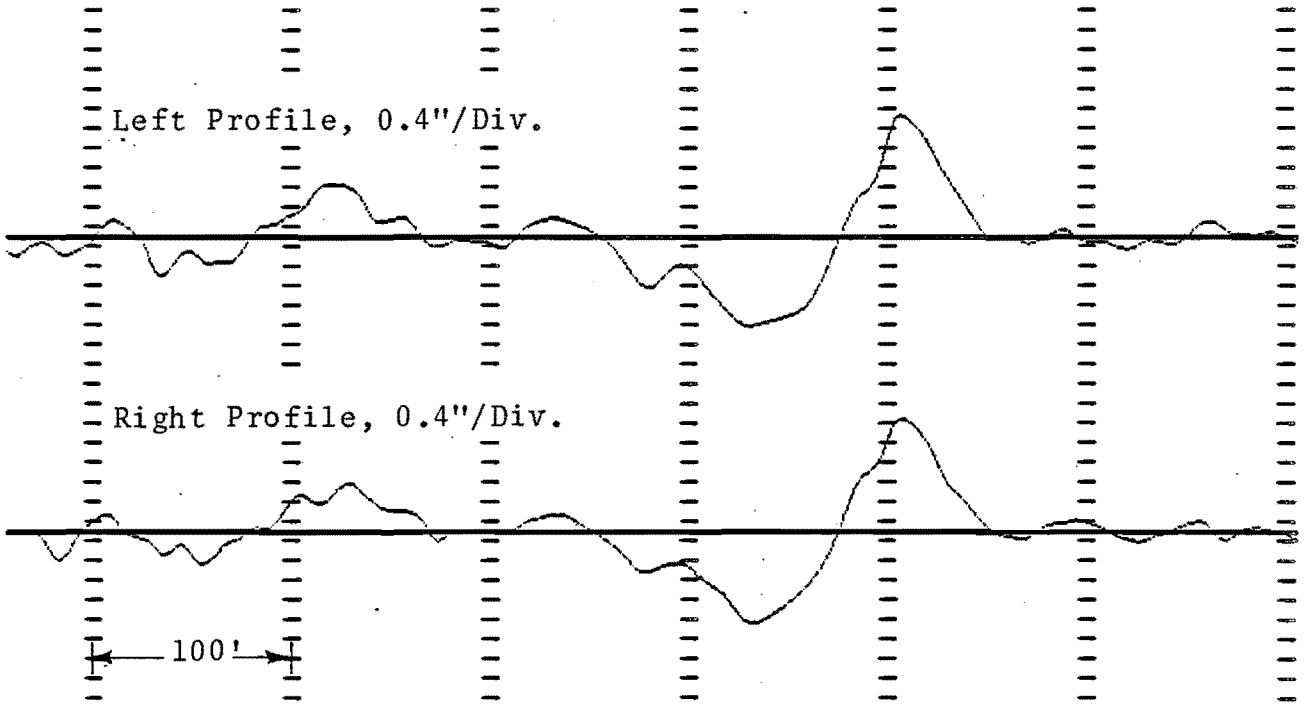

Figure 3-14. A Jog in Mean Profile at an Interlocking (Class 4, Tangent)

believed to be due to change in track stiffness. A plateau can also occur in gage on curves due to rail wear of high rail. Figures 3-15 and 3-16 show the examples of plateau in mean alignment and profile respectively.

A combination of a cusp and a plateau is sometimes observed in spirals and just prior to the spiral. This is usually considered a dangerous situation since the rapid dynamic shift of load can cause a serious vehicle/track interaction.

A trough is usually observed in mean profile and mean alignment in areas of poor drainage and localized soft subgrade. An example of trough in mean alignment is shown in Figure 3-17.

A sinusoidal signature is rarely found as a single cycle; it usually occurs in a periodic fashion. A single sinusoid has been observed in mean profile and mean alignment at bridges and in reverse curves with no tangents. An example of a sinusoid signature in mean alignment is shown in Figure 3-18.

A damped sinusoid signature usually occurs by itself. It is often found in either single rail profile and alignment or mean profile and alignment. This usually occurs at areas of significant change in track stiffness in curves, grade crossing and switches where a vehicle receives transitory input. An example of this signature in mean alignment is shown in Figure 3-19. If traffic flows in both directions, decaying sinusoids would be found on both sides of a transient input.

A sin x/x is a rare signature and also usually occurs as a single event. This signature has been observed in single rail profile at a stiff road crossing having traffic in both directions. An example is given in Figure 3-20.

3.2.2 PERIODIC VARIATIONS

The key signatures occurring in succession are defined as periodic track geometry variations. The periodic variations can cause severe vehicle/track dynamic interaction. Large amplitude vehicle response results when the frequency of these variations coincides with the natural frequency of vehicles.

The periodic variations have been observed in the form of cusp, bump, jog and sinusoid signatures. The periodic behavior was not observed for other signatures in the track geometry data analyzed in this study. There was only one occurrence where one negative plateau was followed by a positive plateau.

Perhaps the most familiar example of periodic phenomenon is the rock and roll behavior on class 2 or 3 track. This usually happens on half staggered bolted track because of poor tie and road bed conditions. The cuspy type depressions develop on joints and half-stagger results in alternating low spots on each rail. Short tangents between curves are usually subjected to dynamic vertical load transfer and are likely to develop pronounced rock and roll condition. In track geometry data, this cuspy periodic behavior is usually evident in crosslevel traces. Figure 3-21 shows an example of this periodic behavior in profile and crosslevel traces.

At long bridges, the design of the bridge may contribute to periodic profile variations. An example is shown in Figure 3-22. Mean profile in this figure shows upward cusps every 90 feet. It should be noted that this bridge is a multiple span deck girder supported on piers on 90-foot centers.

A succession of bumps is sometimes observed in mean profile at mud spots and other locations where drainage is a problem. A combination

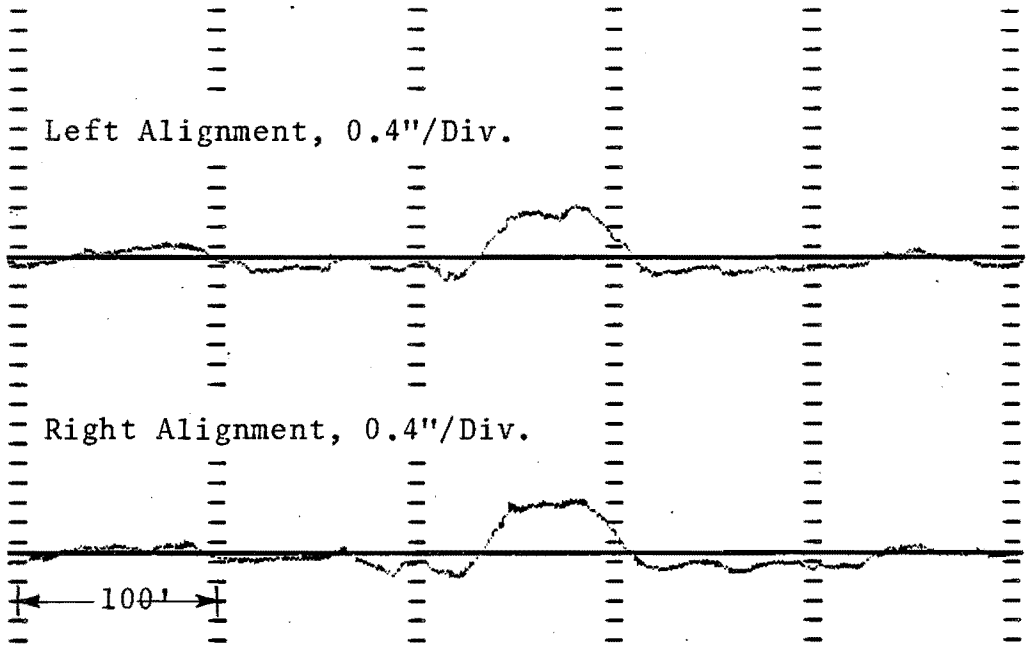

Figure 3-15. A Plateau in Mean Alignment (Class 5, Tangent)

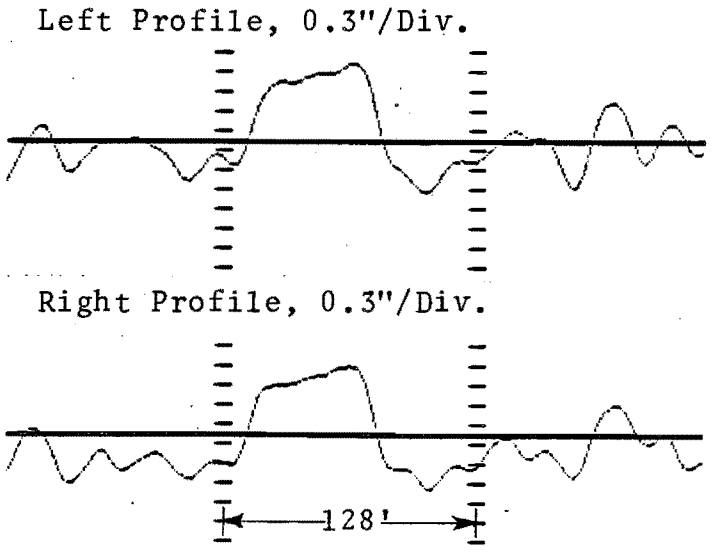

Figure 3-16. Profile Plateau at a Bridge (Class 2, Tangent)

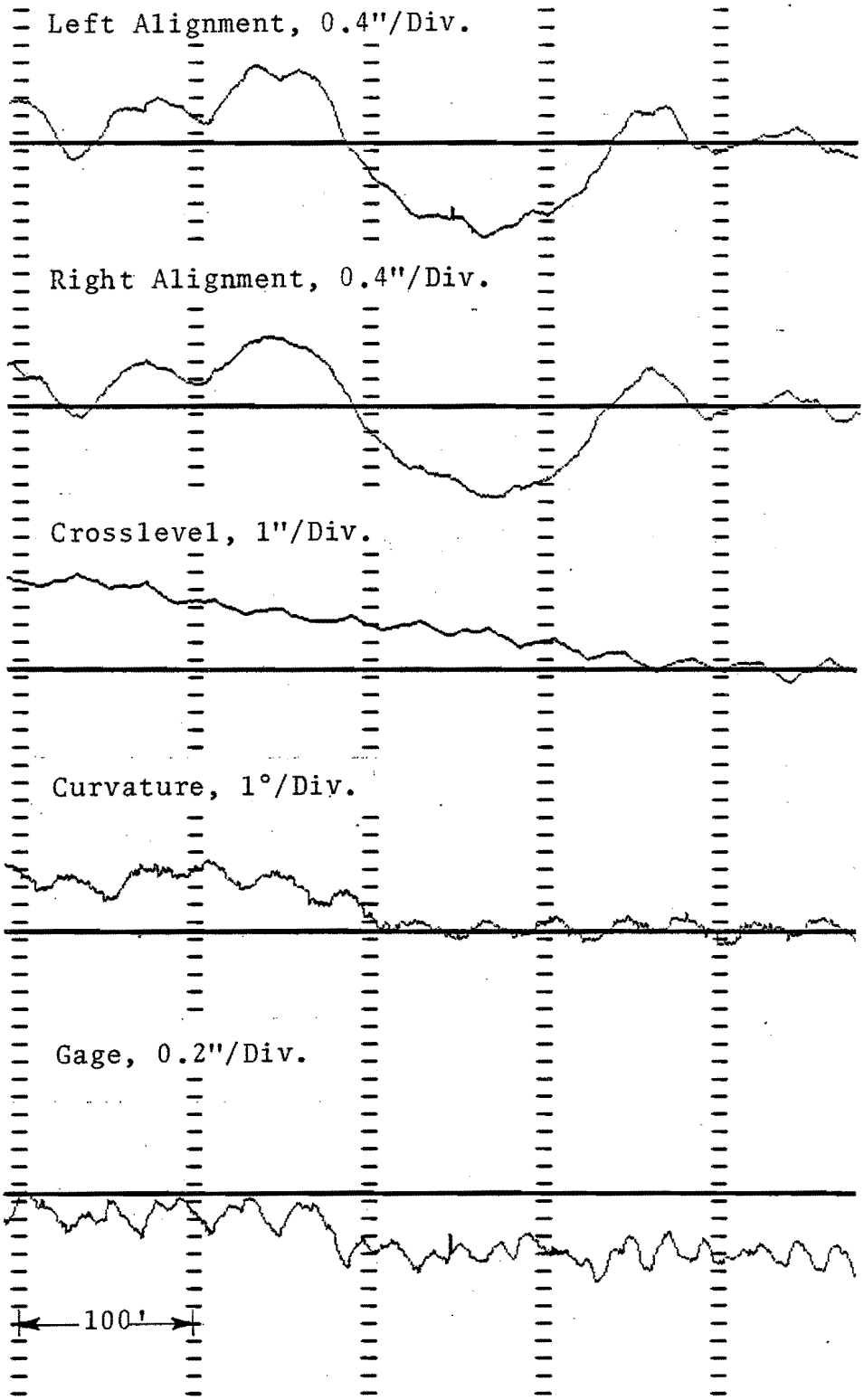

Figure 3-17. Alignment Trough, Note Also Change in Gage (Class 2, Spiral)

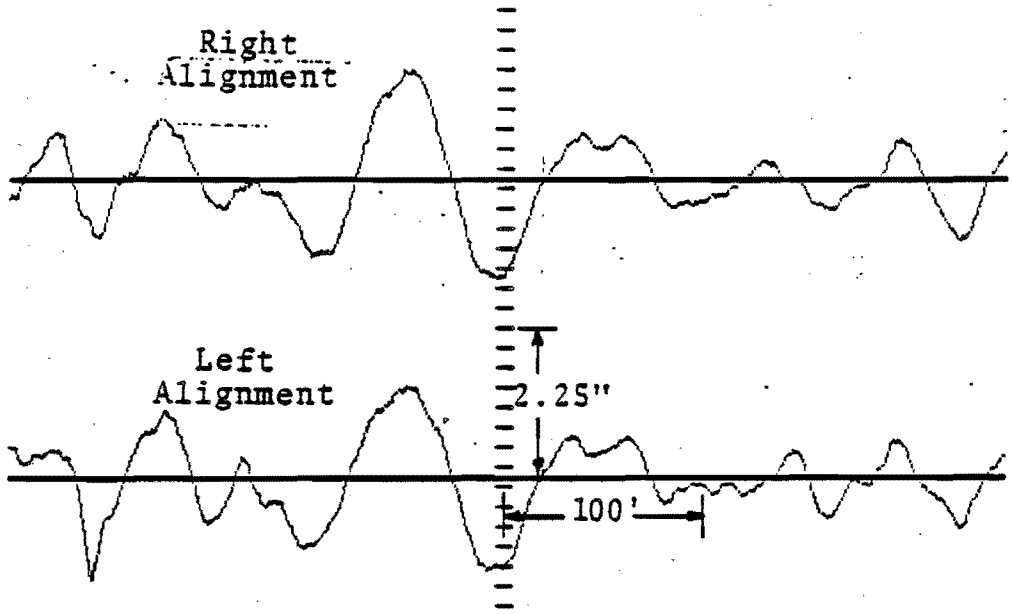

Figure 3-18. A Sinusoid in Mean Alignment Near Bridge

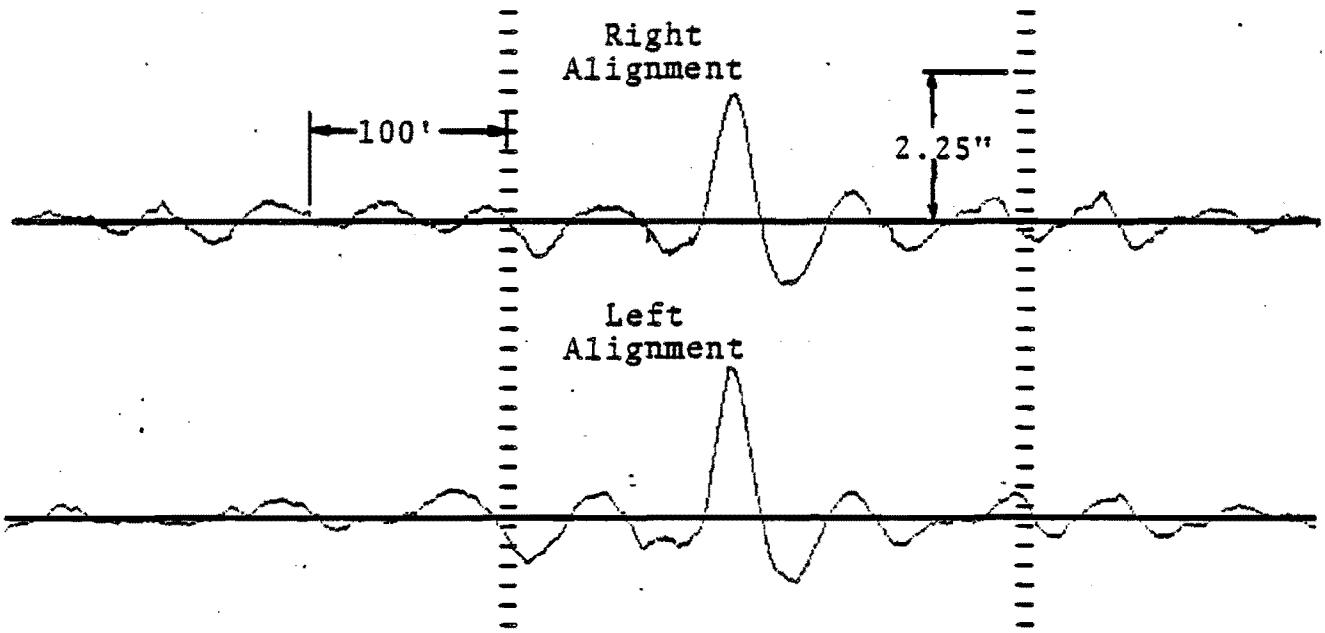

Figure 3-19. A Damped Sinusoid in Mean Alignment

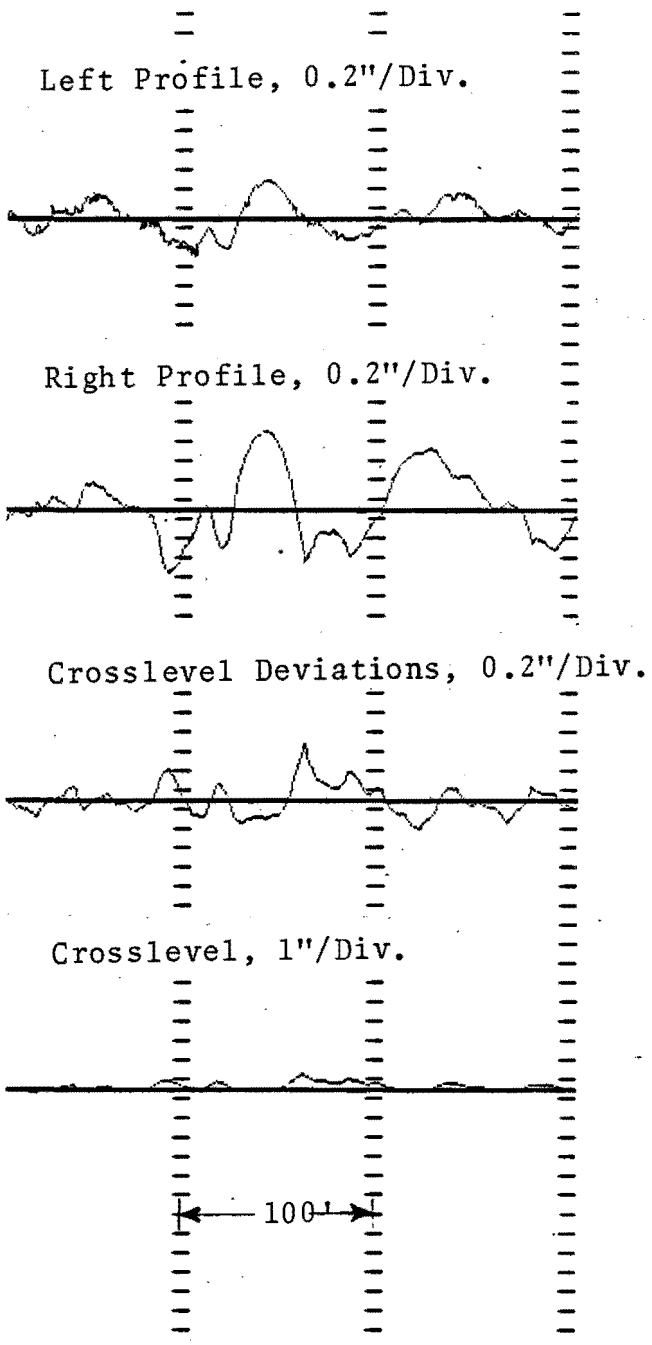

Figure 3-20. Sin x/x Signature in Profile (Class 3, Bolted, Tangent)

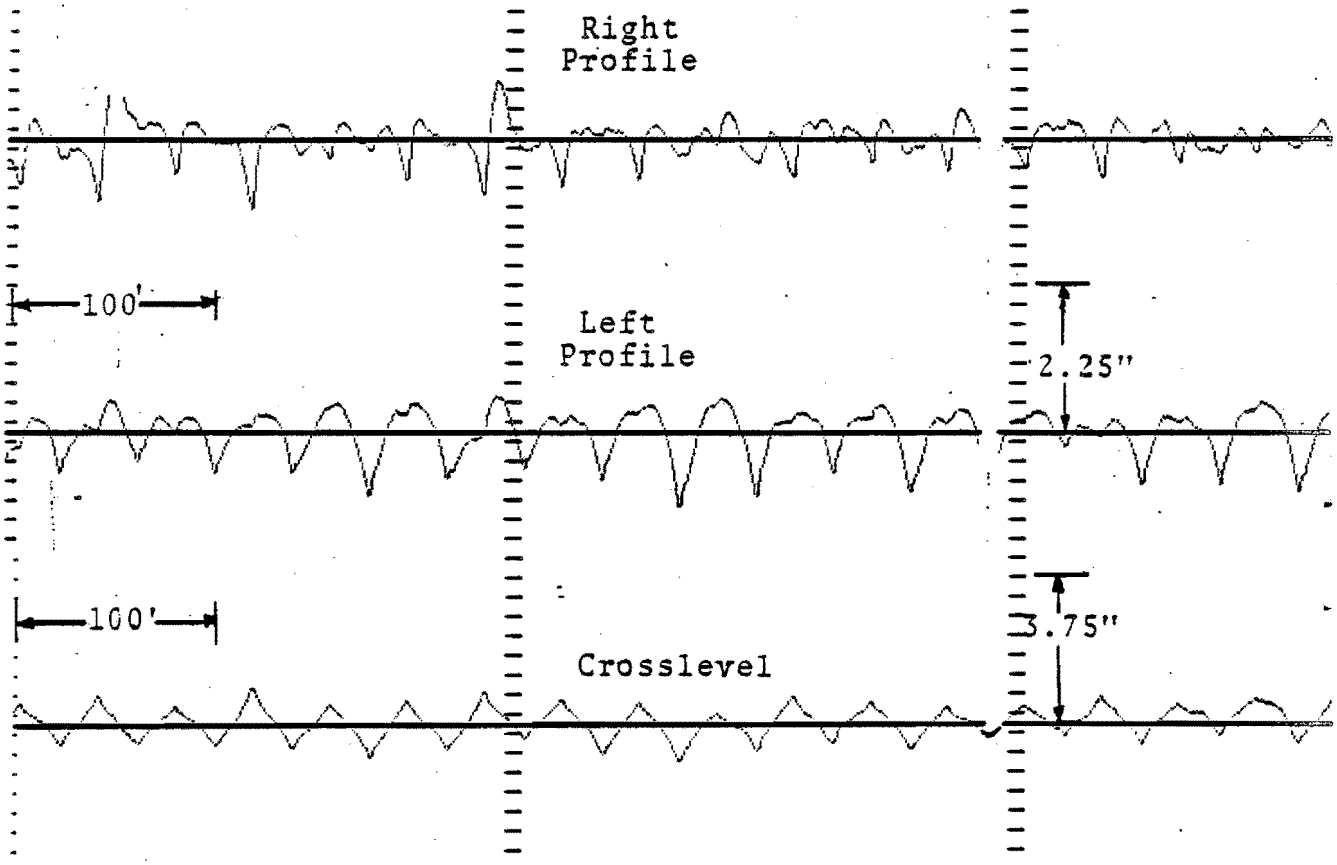

Figure 3-21. Example of Series of Cusps in Profile and Crosslevel (Rock and Roll Track)

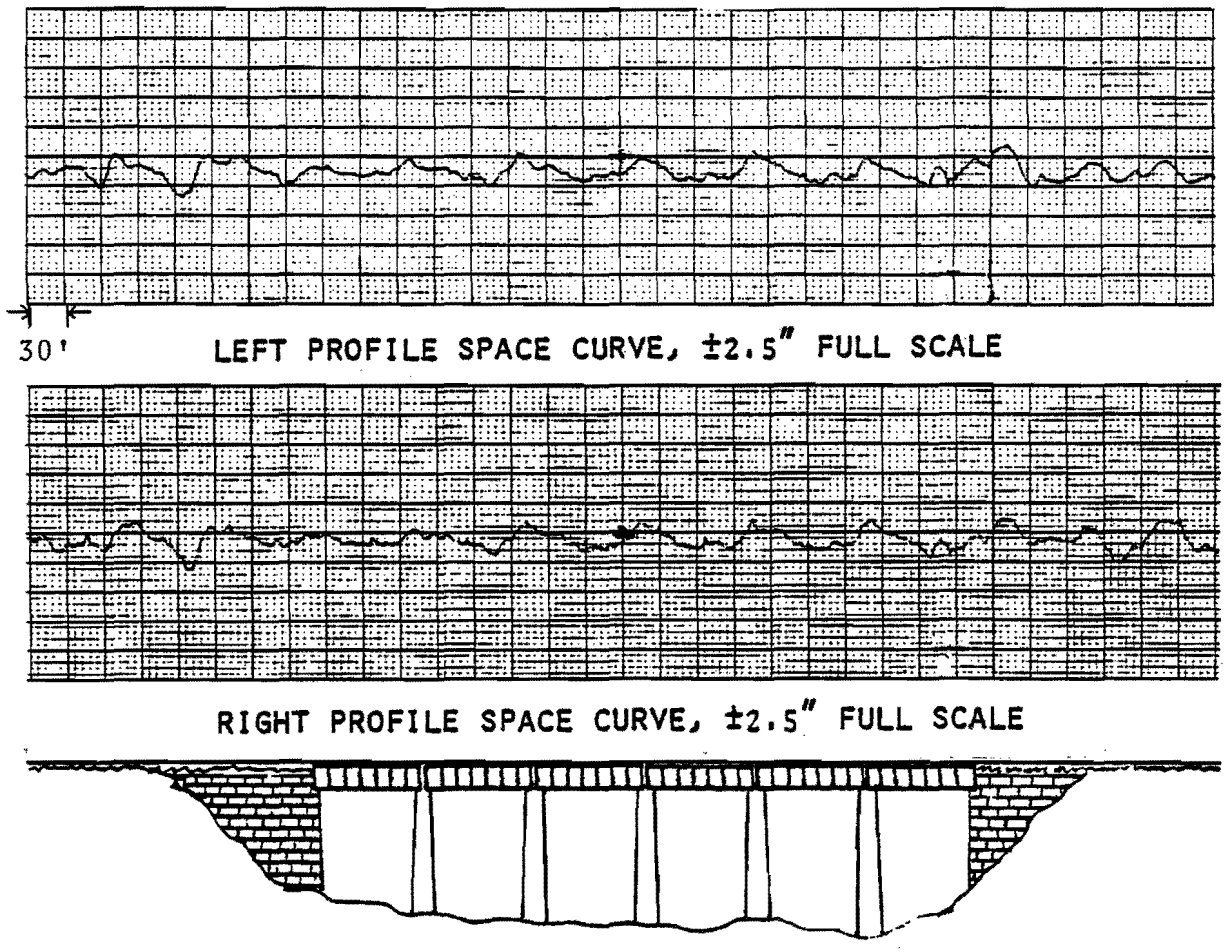

Figure 3-22. Periodic Profile Variations on a Bridge

of bumps and jogs in mean profile can be observed at bridges and grade crossings. Mean profile traces also exhibit succession of jogs in spirals due to dynamic behavior of vehicles.

A periodic cuspy behavior is sometimes observed in gage and single rail alignment. This usually occurs in curves when one rail has more alignment activity than the other. The typical wavelength of this periodic behavior is equal to the rail length. The alternating in/out cusps on one rail may create a 78-foot wavelength. This usually happens in continuous welded rail. An example of periodic cusps in gage and alignment is shown in Figure 3-23.

Alignment traces often reveal 90 to 120 feet periodic variations which have been induced on track due to the dynamic behavior of passing consists. This periodic alignment behavior is believed to be due to the yaw motion of locomotives where the wavelength of perturbation is equal to twice the distance between truck centers. The periodic alignment behavior is most often observed at spirals and bridges where a lateral transient input can excite the yaw mode of a locomotive into several cycles of oscillation.

A section of track with periodic alignment bumps is shown in Figure 3-24. This section includes a reverse curve with a short bridge over a river. The geometry traces exhibit 90-foot wavelength oscillations in alignment at the bridge. These alignment oscillations have been impressed on the track by the dynamic behavior of the vehicles. The marshy characteristics of this region has probably played a roll in the development of these oscillations.

Periodic bumps in mean alignment are also observed in tangents near high speed interlocks. When the train exits high speed interlocks it changes from a curve-type motion to tangent-type motion and as a result bounces back and forth a few times. This produces characteristic 90-foot periodic bumps in mean alignment which are vehicle induced phenomenon and caused by a typical 45-foot distance between truck centers.

A succession of jogs in mean alignment usually occurs in spirals. A pair of jogs has often been observed at grade crossings and bridges. Figure 3-25 shows series of alignment jogs in a spiral.

A sinusoidal periodic alignment behavior is sometimes observed in curves and spirals. Figure 3-26 shows an example of sinusoidal periodic behavior in alignment in a curve.

Main points of the periodic track geometry variations discussed in this section are summarized in Table 3-5.

3.2.3 COMBINED VARIATIONS

For the purpose of this discussion, the combined track geometry variations are defined as the ones which occur simultaneously in more than one track goemetry parameter. Some of the track geometry parameters such as gage and alignment, and crosslevel and profile are closely related with each other. However, large amplitude isolated variations may also exist simultaneously in other pairs of track geometry parameters. Such combined variations may cause a severe vehicle/track dynamic interaction.

An increase or decrease in single rail alignment will result in relatively wide or narrow gage if the other rail does not have a similar alignment activity. This is usually the case in curves where one rail may constantly be subjected to more lateral load than the other. The increased rail wear in curves usually creates a gage maintenance problem in curves.

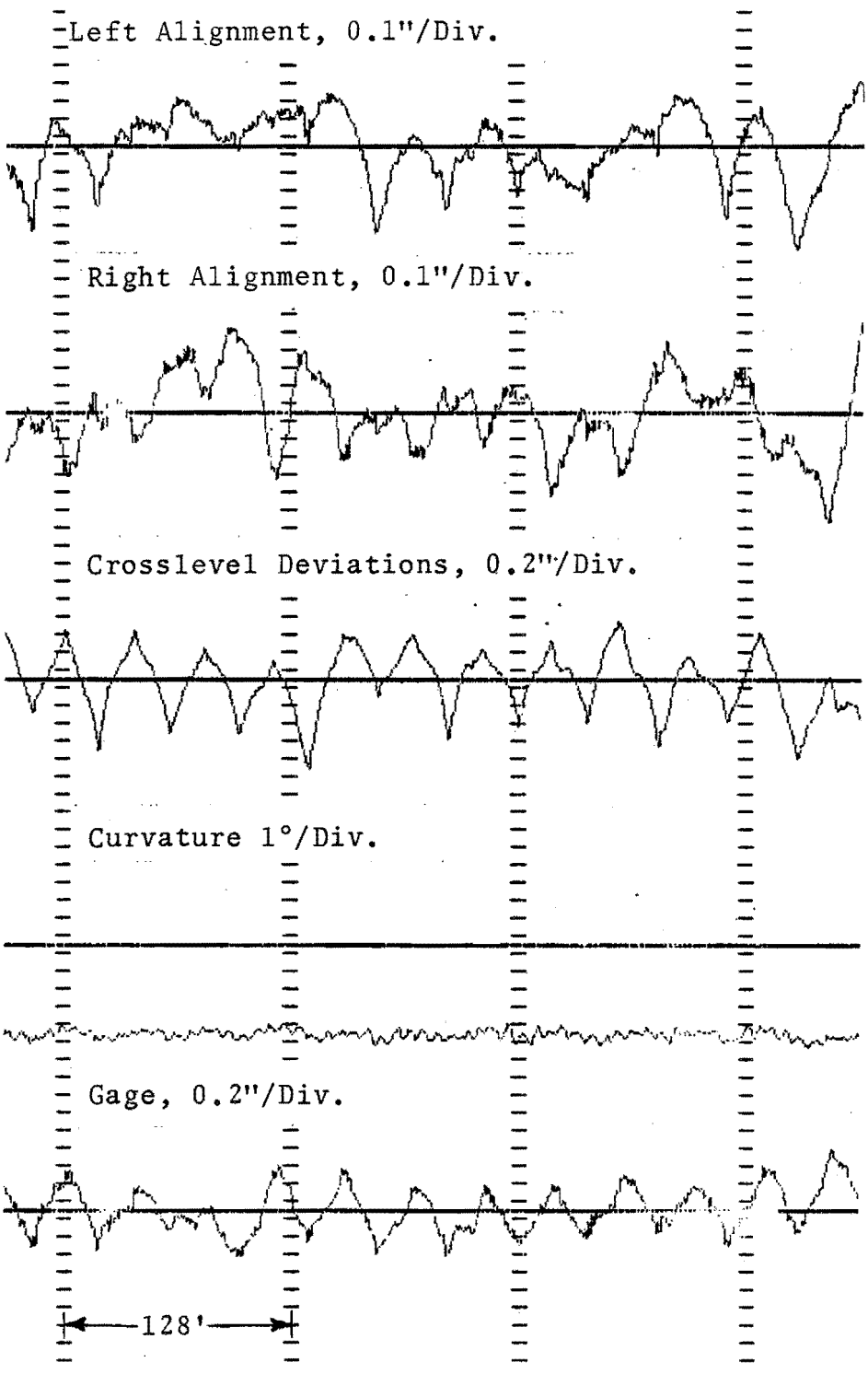

Figure 3-23. Combined Periodic Gage and Alignment (Class 3, Curve)

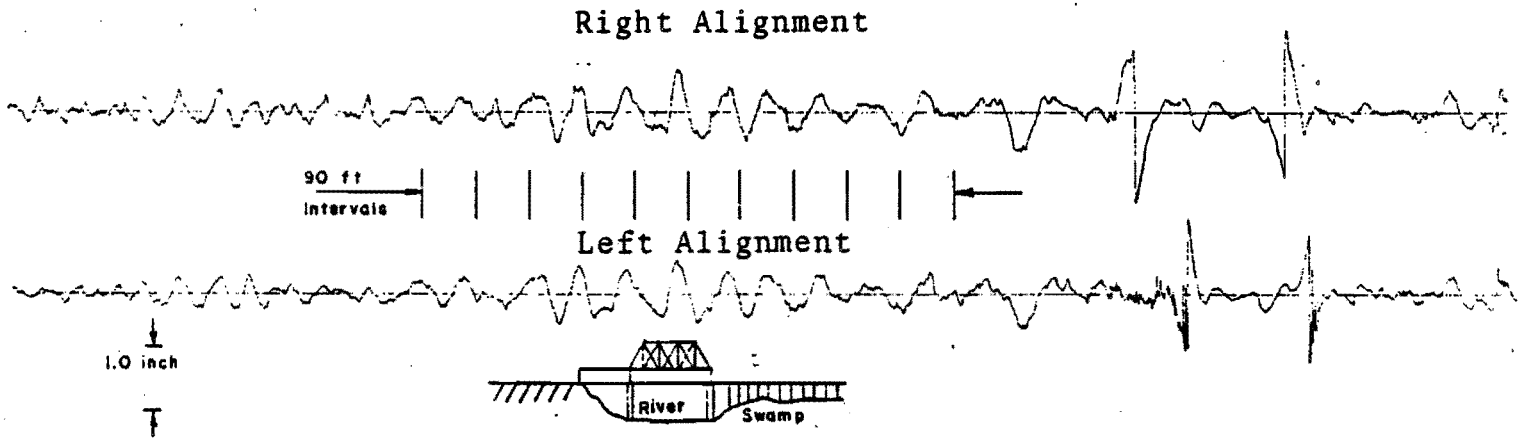

Figure 3-24. Periodic Alignment Bumps

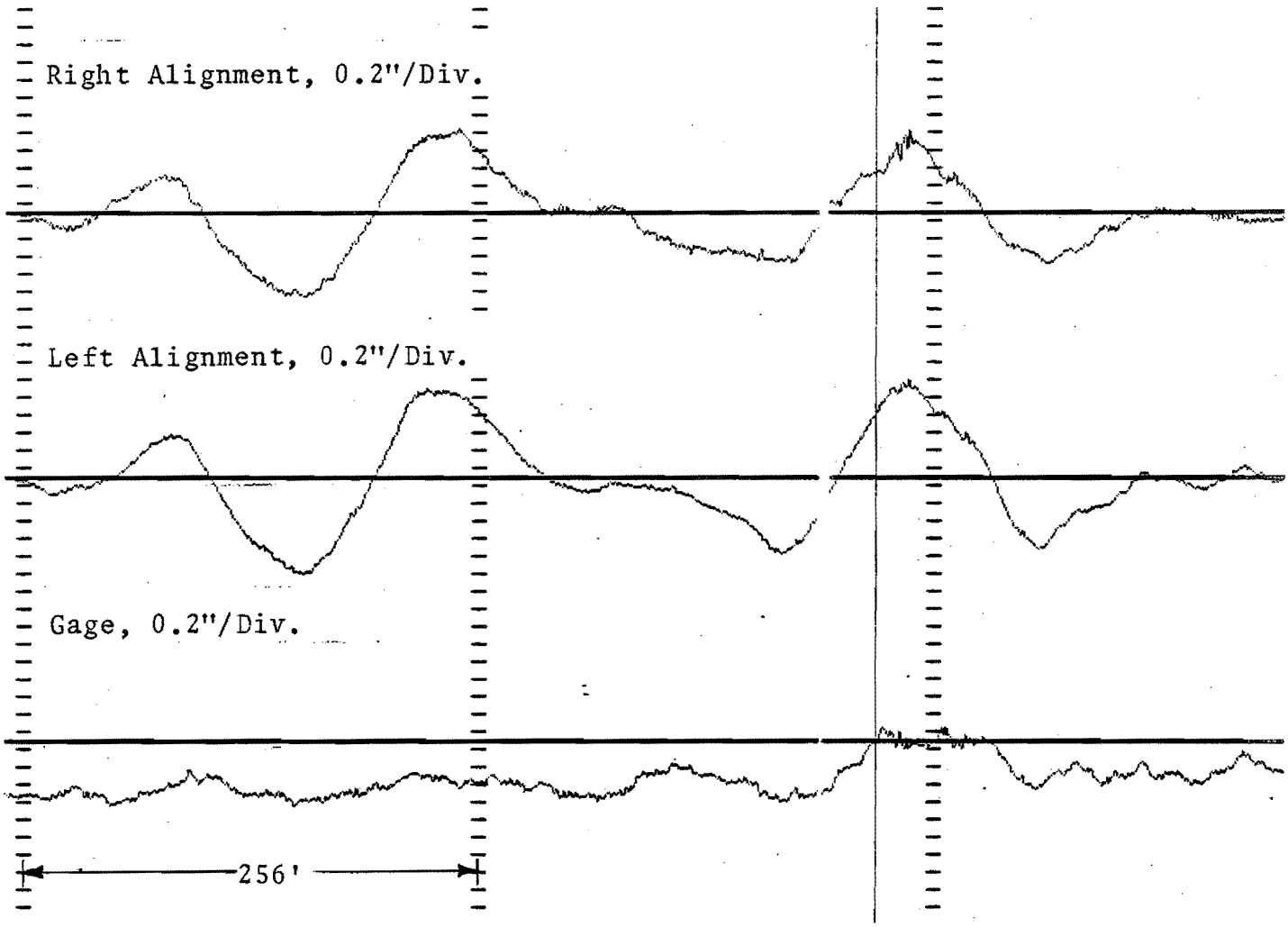

Figure 3-25. Series of Jogs in Mean Alignment (Class 6)

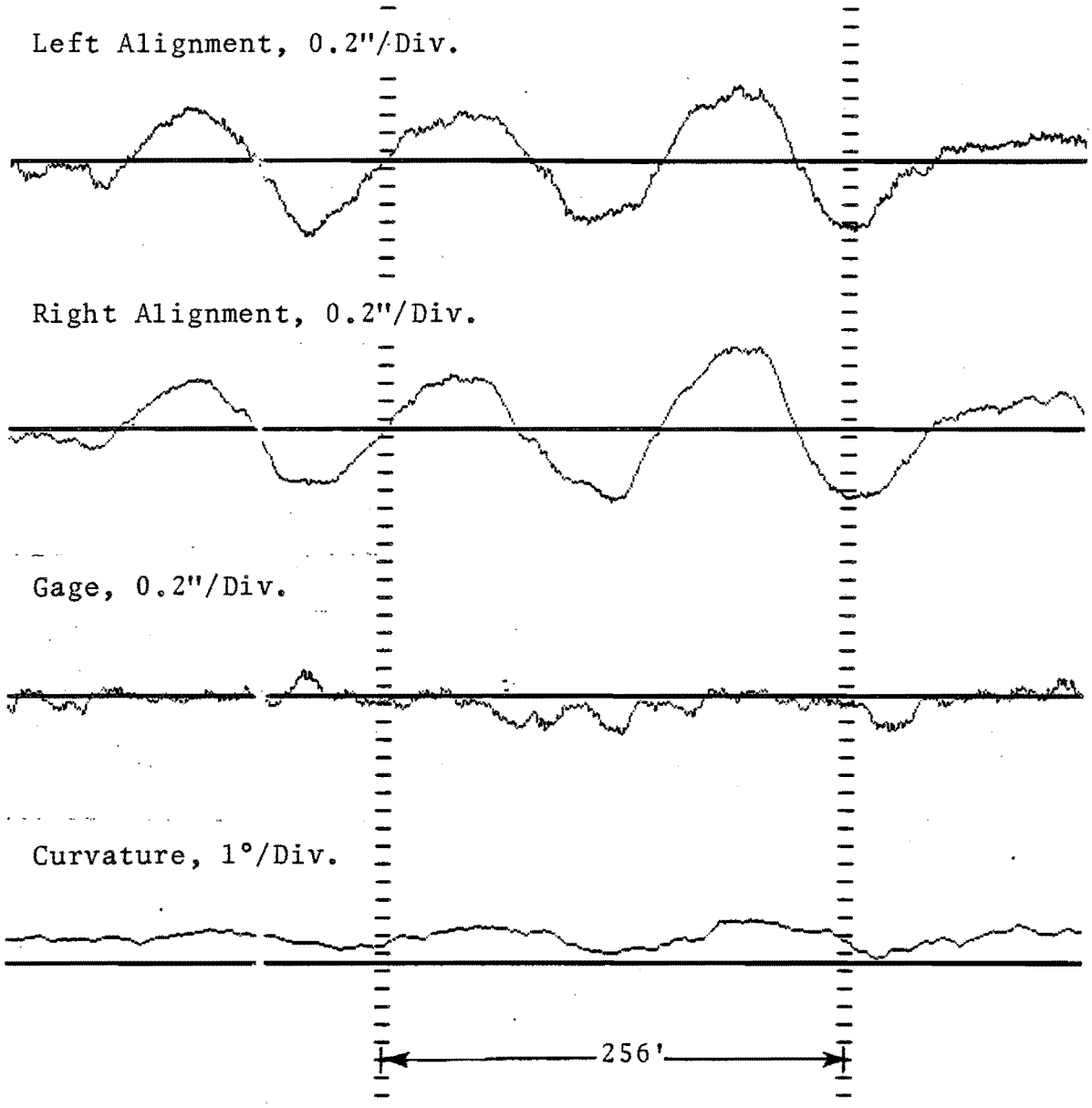

Figure 3-26. Periodic Sinusoidal Variations in Mean Alignment Near an Undergrade Creek Bridge (Class 6)

TABLE 3-5. PERIODIC SIGNATURES

Track Geometry Parameter	Signature	Typical Wavelength (Feet)
Crosslevel	Alternating positive and negative cusp (rock and roll)	39
Single Rail Profile	Cusps at joints	39
Mean Profile	Bumps at mud spots Jogs in Spirals Cusps at a long bridge	50 to 90 100 90
Gage	Cusps in curves	39
Single Rail Alignment	Cusps in curves Alternating positive and negative cusps in curves	39 78
Mean Alignment	Bumps at bridges Jogs in spirals Sinusoids in curves	90 80 to 300 80 to 200

A profile cusp or bump in one rail is usually accompanied by a depression on the opposite rail. However, a low joint is also seen as a cusp in crosslevel since the depression on the opposite rail has smaller amplitude than the low joint.

Accelerated track degradation results in combined deterioration of all the track geometry parameters at joints or welds. Thus relatively poor track geometry develops at every half rail length in half-staggered rail. A further discussion of this phenomenon is provided in Section 4.0.

Examples of isolated combined track geometry variations are provided in Appendix C.3. A few examples are shown in Figures 3-27 through 3-29. Figure 3-27 shows combined variations in all track geometry parameters as single events. The gage and alignment show single events in the form of cusps. At the same location, the crosslevel and profile show jog signatures.

Figure 3-28 also shows single events in all track geometry parameters. However, in this case, gage and crosslevel also show the periodic cuspy behavior. Figure 3-29 shows combined periodic variations in all track geometry parameters.

3.3 FREQUENCY OF OCCURRENCE

As discussed in Section 3.2, the isolated track geometry variations usually occur in spirals, special track work and other track anamolies such as the areas of poor subgrade or drainage. Therefore, isolated track geometry variations will occur more frequently where there are more of these special track features. This depends on territory and type of service. It is, thus, not possible to derive universal conclusions regarding the frequency of occurrence of isolated variations from a limited sample of U.S. track as analyzed in this study.

The high speed track in the Northeast has few curves and road crossings. Most of the isolated variations are found at switches, bridges, overpasses, buffer rail joints, and insulated joints. Isolated variations in some of these areas develop due to changing weather conditions and the fact that track is laid on earth foundation which settles at times. The isolated variations in these areas are mostly in the form of bumps and jogs in profile and alignment.

In mountainous areas with many curves, track condition deteriorates rapidly. Higher longitudinal and lateral forces are exerted on the track due to grade and curvatures. Poor drainage accelerates ballast and foundation deterioration. A cuspy type gage behavior is common in such areas. In addition, jogs in alignment and profile are encountered frequently in spirals. Sinusoidal alignment behavior is also observed in these areas.

The arid regions of the Southwest and Midwest have mainly tangent track with infrequent special track work. The isolated track goemetry variations are rarely found in such regions. However, the flat arid and hot areas may develop a dangerous situation known as "sun kinks." This is observed as isolated variations in the form of bumps in alignment. The rail may even buckle due to very high temperatures.

In northern states where seasonal freezing and thawing of the track bed is an annual event, heaving, and pumping and movement of curves due to cold temperature are some of the causes of geometric deviations. In the west drainage is not a real problem because of the sandy subgrade and little rain fall. In the mideast and midwest, drainage is a problem because the subgrade is quite often a clay or silt and rain fall is more frequent.

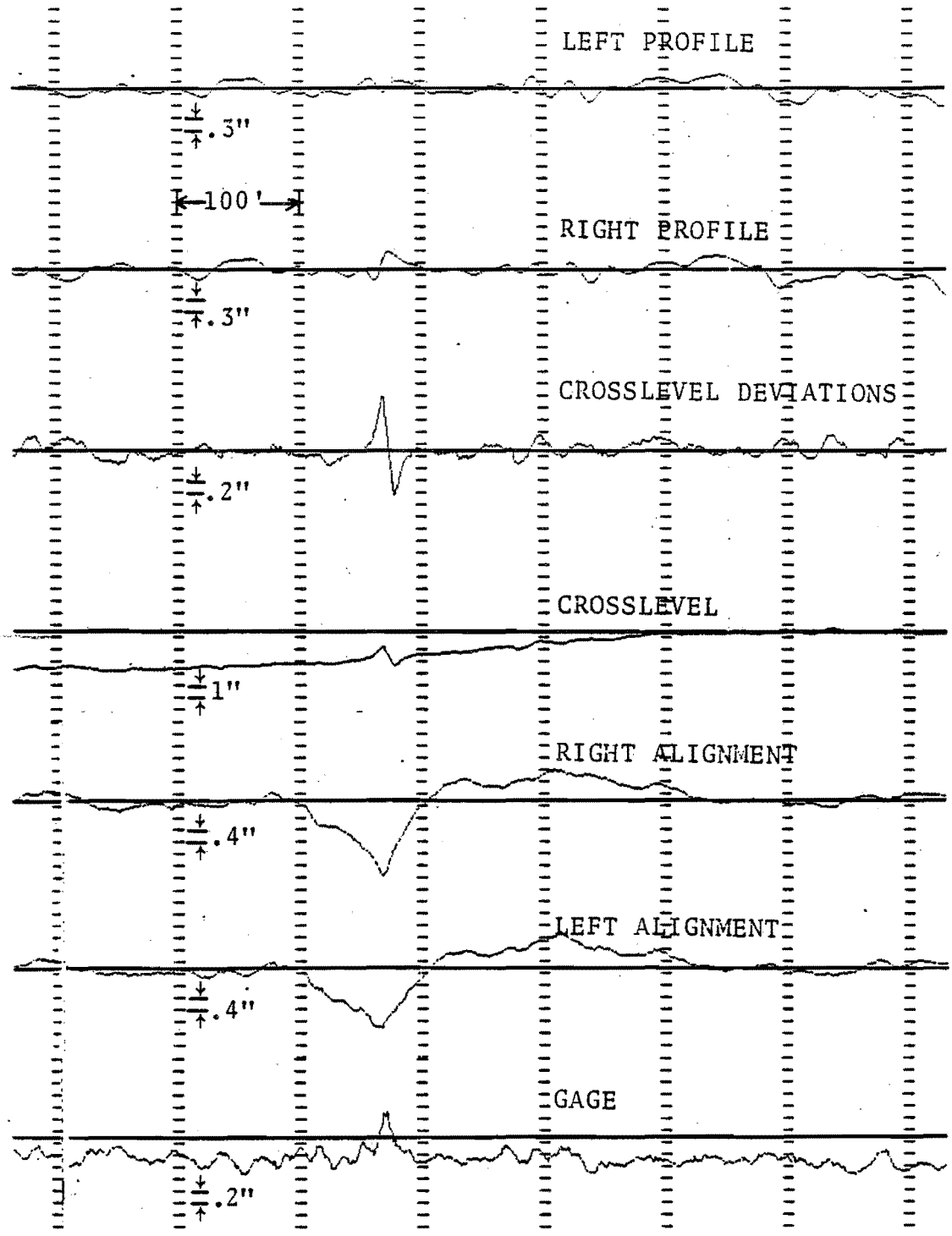

Figure 3-27. Combined Track Geometry Variations in All Parameters (Class 3, Welded, Spiral)

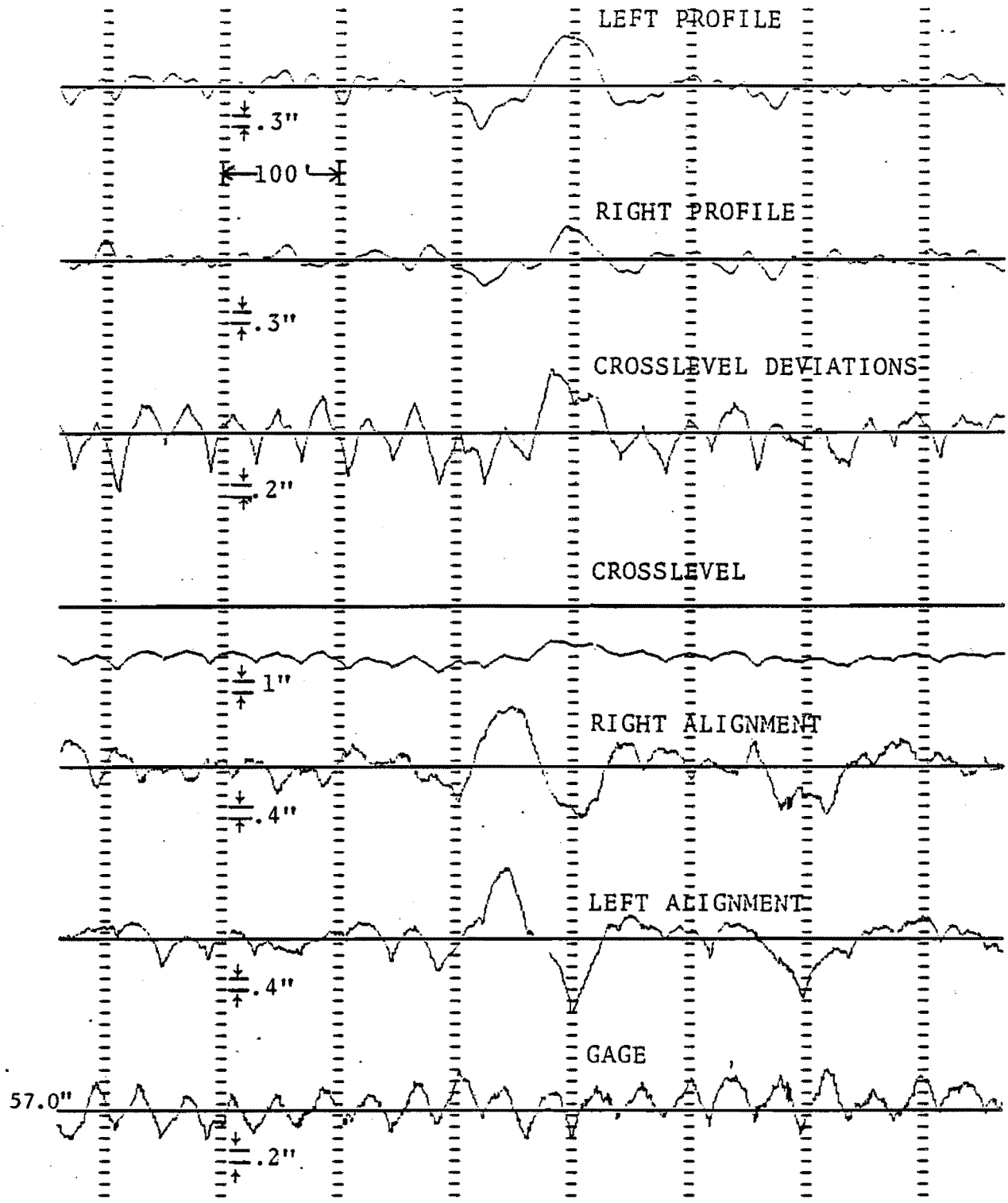

Figure 3-28. Combined Track Geometry Variations, and Periodic Gage and Crosslevel (Class 3)

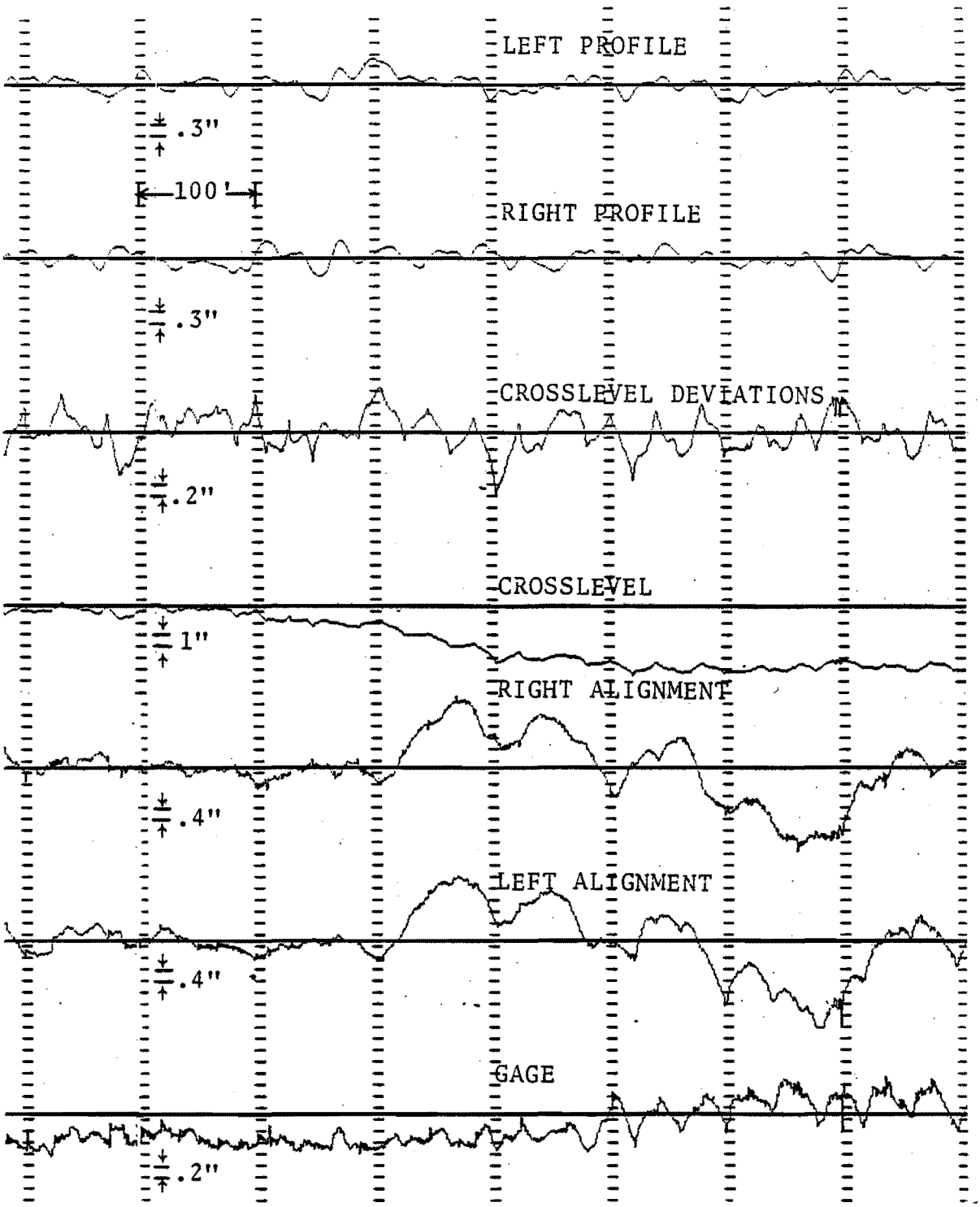

Figure 3-29. Combined Periodic Gage and Crosslevel Cusps (39') and Periodic (100') Alignment (Class 3, Spiral)

3.4 SUMMARY AND CONCLUSIONS

This section addressed isolated track geometry variations. Key signatures are identified and their mathematical form is given. Typical occurrences of these variations are also discussed.

Eight key signatures have been identified in isolated track geometry variations. These are a cusp, bump, jog, plateau, trough, sinusoid, damped sinusoid and sin x/x. These signatures can be described as a function of two parameters; amplitude, A and a duration related parameter, k. The values of A and k depend upon track class, track geometry parameters and the signature itself.

The key signatures can occur as single events, in periodic forms or in combination with each other. Furthermore, isolated track geometry variations can occur simultaneously in more than one track geometry parameter.

Isolated track geometry variations usually occur in spirals, at special track works and other track anomalies such as soft subgrade or poor drainage areas. Isolated variations have been identified at such track features as road crossings, turnouts, interlocking, bridges, etc. Their frequency of occurrence depends upon number of curves and special track features.

The most common periodic forms are found in crosslevel and mean alignment. The most common wavelengths of such periodic forms are 39 feet for crosslevel and 78 feet for alignment. A periodic cuspy type behavior is also commonly observed in gage and single rail alignment in curves. The mean profile can also develop quasi-periodic bumps at mud spots and periodic jogs in spirals.

4.0 RELATIONSHIPS BETWEEN TRACK GEOMETRY PARAMETERS

4.1 INTRODUCTION

Track geometry parameters are traditionally measured and maintained individually. However, a vehicle receives simultaneous input from gage, line and surface irregularities. Combined track geometry defects can cause severe dynamic interaction between vehicle and track. For example, the simultaneous presence of two defects that are individually tolerable may create an unacceptable combined response. The effect of simultaneous alignment and crosslevel defects on carbody roll is a clear example.

In order to provide reasonable experimental and analytic simulations of actual railroad operating conditions, it is therefore necessary to establish analytic representations of the statistical relationships between track geometry parameters. This is also important for the development of track performance standards based on the dynamic interaction of vehicle and track.

Analyses were conducted to develop the relationships between various track geometry parameters. The following sections describe the methodology used and the results of these analyses.

4.2 METHODOLOGY

The methodology involved the establishment of a suitable data base, development of software, data processing and the analysis to determine the relationship between track geometry parameters. Figure 4-1 is the block diagram of the methodology. The following paragraphs describe the data base, software and the data processing techniques. Results of the analyses are presented in the next section.

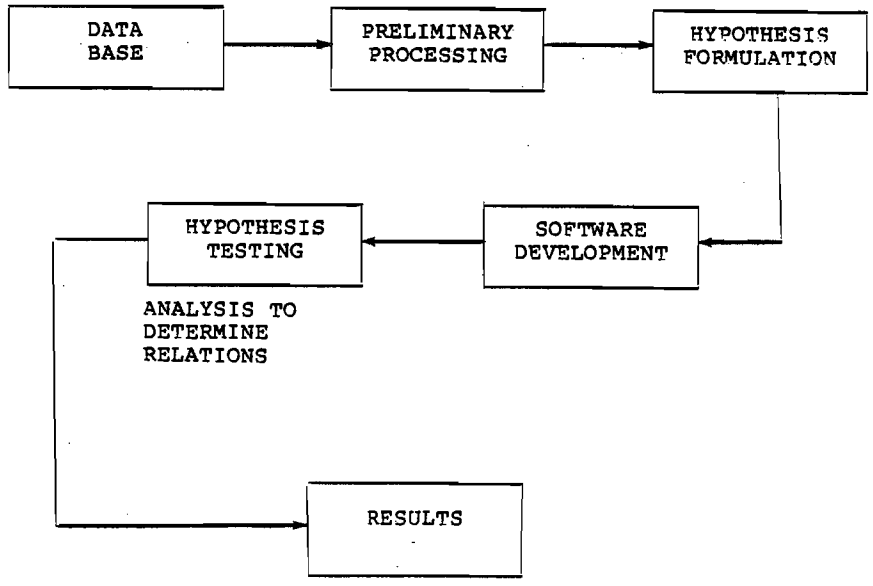

Figure 4.1. Block Diagram of Methodology Used to Develop the Relationships Between Track Geometry Parameters

A comprehensive track geometry data base was established to represent a reasonable sample of the United States track. Appendix C gives a detailed description of this data base. The data base consisted of approximately 300 miles of track geometry data selected from approximately 50,000 miles of data collected by FRA T-6 vehicle. In most cases, five sections of track geometry data were selected in each of the FRA track classes. Each section varied from five to ten miles in length.

Relationships between track geometry parameters were first hypothesized based on review of track geometry data. Track geometry data were then processed to verify the results of analyses.

Raw track geometry data were first processed to generate gage, curvature, crosslevel, crosslevel variations, alignment space curve and profile space curve. The long wavelength cut-off for the filter used to process alignment and profile was 208 feet.(2) Track geometry data were sampled at one-foot intervals and hence the Hyquist wavelength was two feet.

An analysis of the power spectra of track geometry parameters can provide useful information about the relationship between track geometry parameters. A software package, FEDAL, was developd to determine the relationships between gage and alignment variations. A detailed description of FEDAL is given in Appendix D. The meaning of various parameters and algorithms used are also discussed.

FEDAL generates power spectral densities (PSDs), cross power spectral densities, phase spectrum, coherence spectrum and the transfer function. The program FEDAL was used to process data to support the analyses. The segment length used for Fourier transform was 1024 feet to provide maximum frequency resolution. Each segment of data was tapered ten percent on each end to reduce "leakage." Consecutive segments of data were averaged to improve the confidence in spectral estimates.

Appendix E contains the plots of cross spectrum, phase spectrum, coherence spectrum and magnitude of the transfer function. These plots are typical for all FRA track classes. Slight variations exist between different sections of data. The following sections discuss the results of relationships between track geometry parameters.

4.3 GAGE AND ALIGNMENT VARIATIONS

4.3.1 MATHEMATICAL REPRESENTATIONS

Review of track geometry data indicates that the alignment at joints can be expressed by inverted rectified sine, exponential or triangular cusps. Thus, the alignment for a single rail length can be expressed as:

Sinusoidal

$$y(x) = A\left(1 - \left|\sin\left(\frac{\pi x}{L}\right)\right|\right), \qquad -\frac{L}{2} \le x \le \frac{L}{2} \qquad (4\text{-}1)$$

Exponential

$$y(x) = Ae^{-k|x|}, \qquad -\frac{L}{2} \le x \le \frac{L}{2} \qquad (4\text{-}2)$$

Triangular

$$y(x) = A\left(1 - \frac{2|x|}{L}\right), \qquad -\frac{L}{2} \le x \le \frac{L}{2} \qquad (4\text{-}3)$$

where

A = amplitude at joint

L = rail length

x = distance from joint

k = decay factor for the exponential cusp

The amplitude of the exponential joint can be forced to zero at half the rail length from joints by the expression

$$y(x) = A(e^{-k|x|} - e^{-k\,L/2}) \tag{4-4}$$

The amplitude of alignment varies from one joint to another. Therefore, the alignment as a function of distance along the track can be written as:

Sinusoidal

$$y(x,n) = A(n)\left[1 - \left|\sin\left(\frac{\pi x}{L}\right)\right|\right], \quad -\frac{L}{2} \leq x \leq \frac{L}{2}, \quad 0 \leq n < \infty \tag{4-5}$$

Exponential

$$y(x,n) = A(n)\left[e^{-k|x|} - e^{-kL/2}\right], \quad -\frac{L}{2} \leq x \leq \frac{L}{2}, \quad 0 \leq n < \infty \tag{4-6}$$

Triangular

$$y(x,n) = A(n)\left[1 - \frac{2|x|}{L}\right], \quad -\frac{L}{2} \leq x \leq \frac{L}{2}, \quad 0 \leq n < \infty \tag{4-7}$$

The expressions given by Equations (4-1) to (4-7) are applicable to both rails by introducing a proper delay for generating the values for one rail with respect to the other. It should be noted that A(n) can be both positive and negative, and varies from one joint to the other. The gage at any point can be expressed as:

$$G = G_0 + y_\ell - y_r \tag{4-8}$$

where

G_0 = a constant

y_ℓ = left alignment

y_r = right alignment

4.3.2 FORMULATION OF HYPOTHESES

Figure 4-2 presents possible configurations of track alignment at joints. At joints a rail can either go out (towards the field side) or can come in (towards the track centerline). Joints can be either staggered or non-staggered. Furthermore, one rail may have more severe variations than the other.

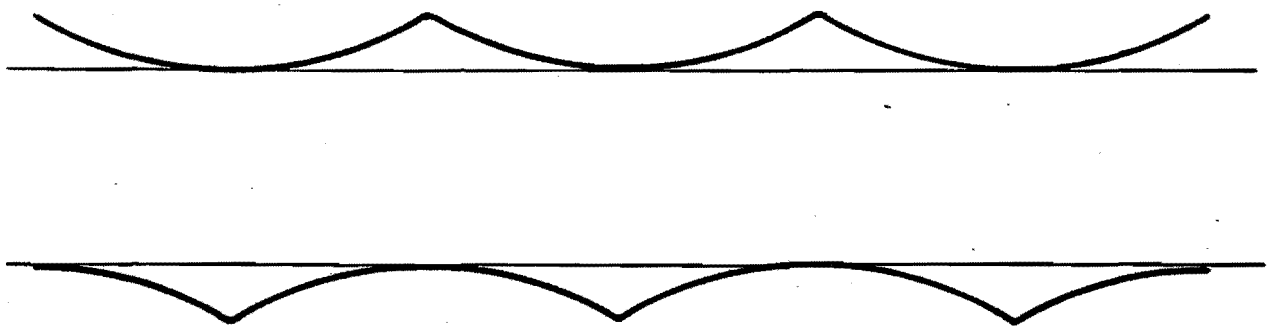

a) Both rails go out at staggered joints

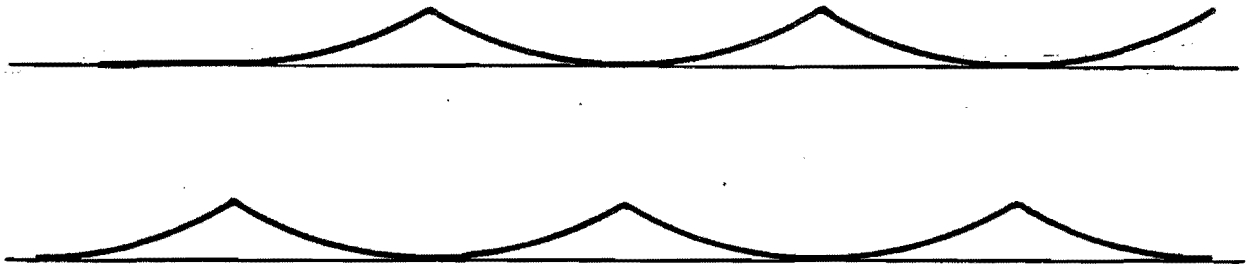

b) One rail comes in and the other goes out at staggered joints

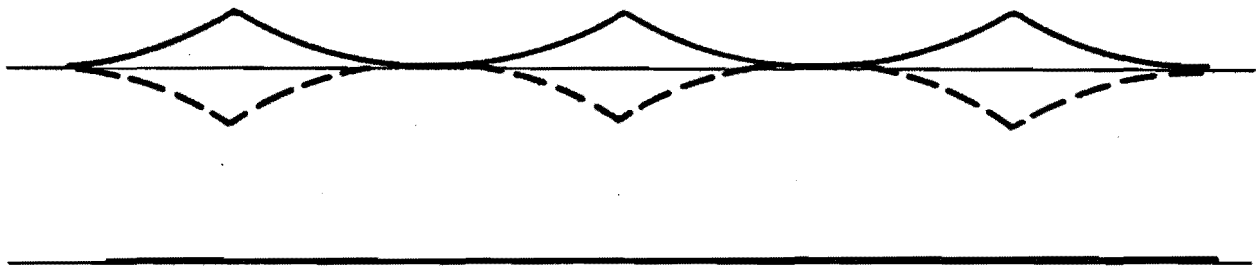

c) Activity on one rail

Figure 4-2. Different Descriptions for Track Alignment at Joints

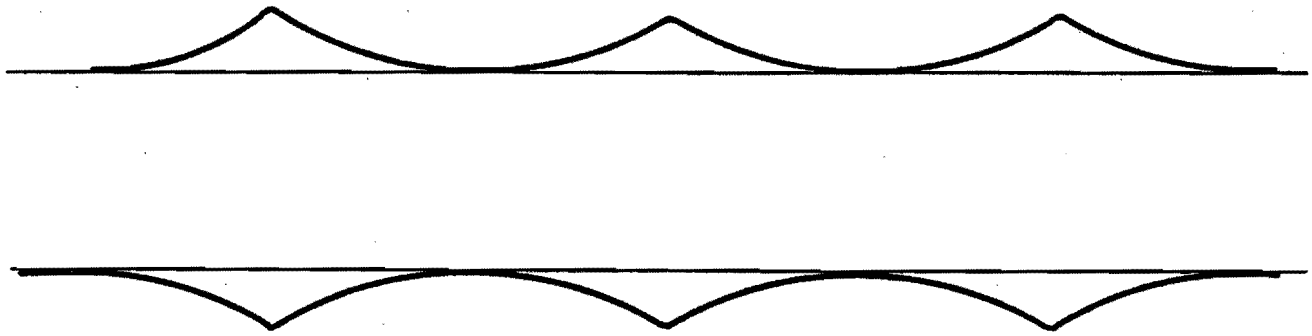

d) Both rails go out at nonstaggered joints

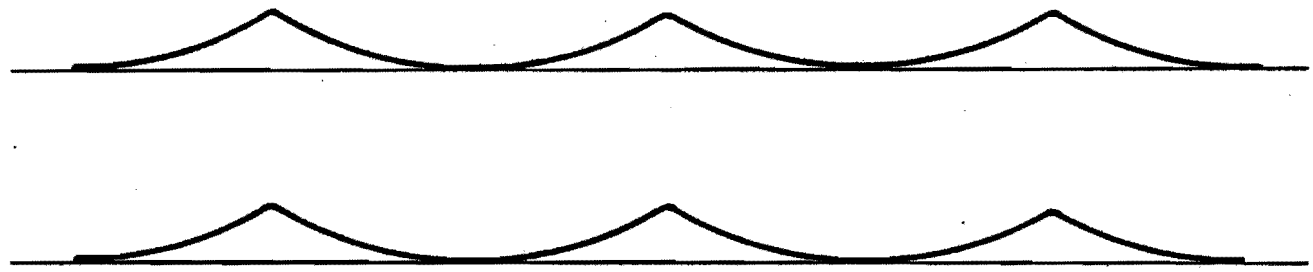

e) One rail comes in and other rail goes out at nonstaggered joints

Figure 4-2 (Cont). Different Descriptions for Track Alignment at Joints

Hypothesis 1: Both Rails have Outward Cusps or Kink at Joints

Figure 4-3 illustrates the condition of track under this hypothesis. Resultant traces for gage (mean removed) and alignment are also shown. According to the sign convention for alignment, an offset to the left corresponds to positive alignment. As shown in Figure 4-3, a positive increase in left alignment is associated with wide gage at joints on the left rail. This will result in a significant positive correlation between gage and left alignment variations. The right alignment has negative cusps at joints which are also accompanied by wide gage. Thus, the right alignment will have significant negative correlation with gage variations. The mean alignment trace shows an equal probability of an increase or decrease, and thus, will result in zero or insignificant correlation between gage and mean alignment. The magnitude of mean alignment follows the gage trace and thus should be highly correlated with gage variations.

Hypothesis 2: Both Rails Have Positive Cusps at Joints, i.e., the Left Rail Goes Out and the Right Rail Comes in at Joints

Figure 4-4 shows the traces for gage and alignment under this hypothesis. In this case, the postive cusps in the left alignment are associated with wide gage and positive cusps in the right alignment are associated with narrow gage. This will tend to give significant positive correlation between gage and left alignment variations and significant negative correlation between gage and right alignment variations. The mean alignment has always positive cusps with either wide or narrow gage which will result in zero or insignificant correlation between gage and mean alignment variations. The same will be true for gage variations and magnitude of mean aligment.

Hypothesis 3: Rails at Joints Have Randomly Varying Positive or Negative Cusps

Consider the illustration in Figure 4-5. For simplicity, in this figure, it is assumed that the track alignment has positive or negative spikes at joints and is zero otherwise. The amplitude of the spikes is assumed to be either A or 2A. The correlation between gage and alignment, ρ_{xy}, is given by (14):

$$\rho_{xy} = \frac{\sigma_{xy}}{\sigma_x \sigma_y} \qquad (4\text{-}9)$$

where

σ_{xy} = covariance of gage and alignment
σ_x = standard deviation of gage
σ_y = standard deviation of alignment

The correlation coefficient between gage and alignment for the illustrative example is given in Table 4-1.

Left alignment shows significant positive correlation with gage and right alignment shows significant negative correlation with gage. There is zero correlation between gage and either left plus right alignment or |left plus right alignment|.

Hypothesis 4: At Joint, the High Rail More Likely Goes Out and the Low Rail More Likely Comes In

Upon repeated loads, rail tends to straighten itself. Therefore, as shown in Figure 4-6 in curves the high rail has a tendency to go out and the low rail has a tendency to come in. Either rail may have more activity than the other depending on the superelevation and balance speed.

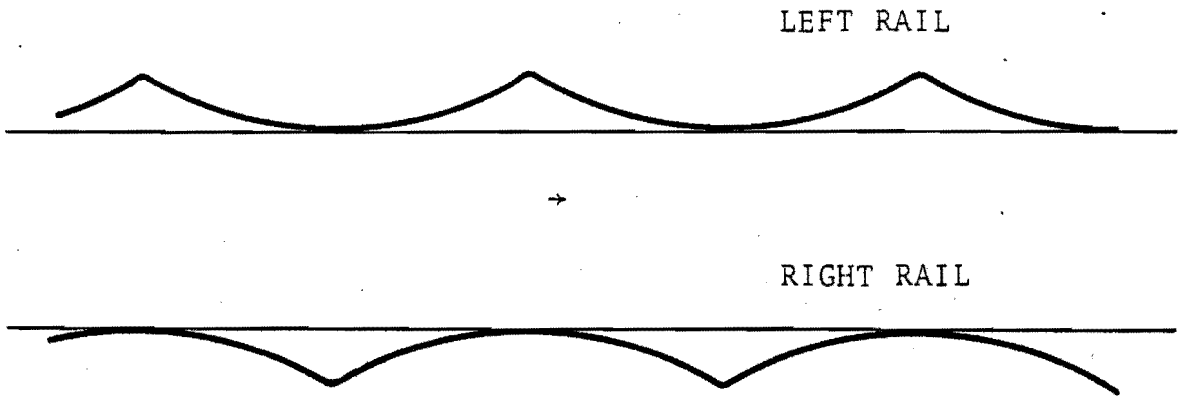

a) Track (left and right alignment)

b) Gage

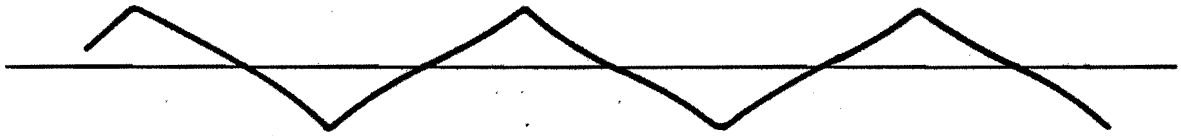

c) Left + right alignment

d) |Left + right alignment|

Figure 4-3. Gage and Alignment When Both Rails Go Out at Joint

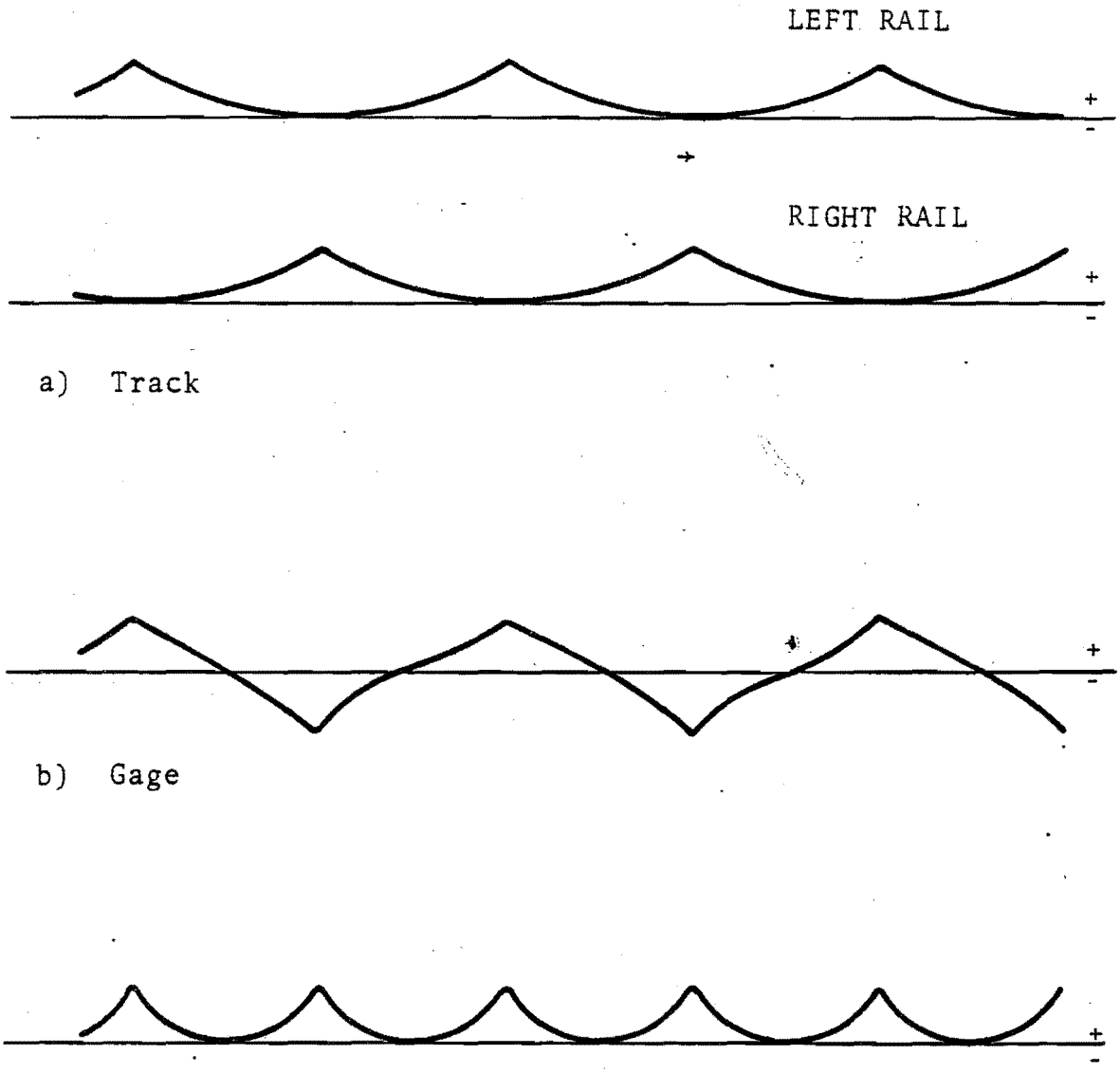

Figure 4-4. Gage and Alignment When Both Rails Have Positive Cusps at Joints.

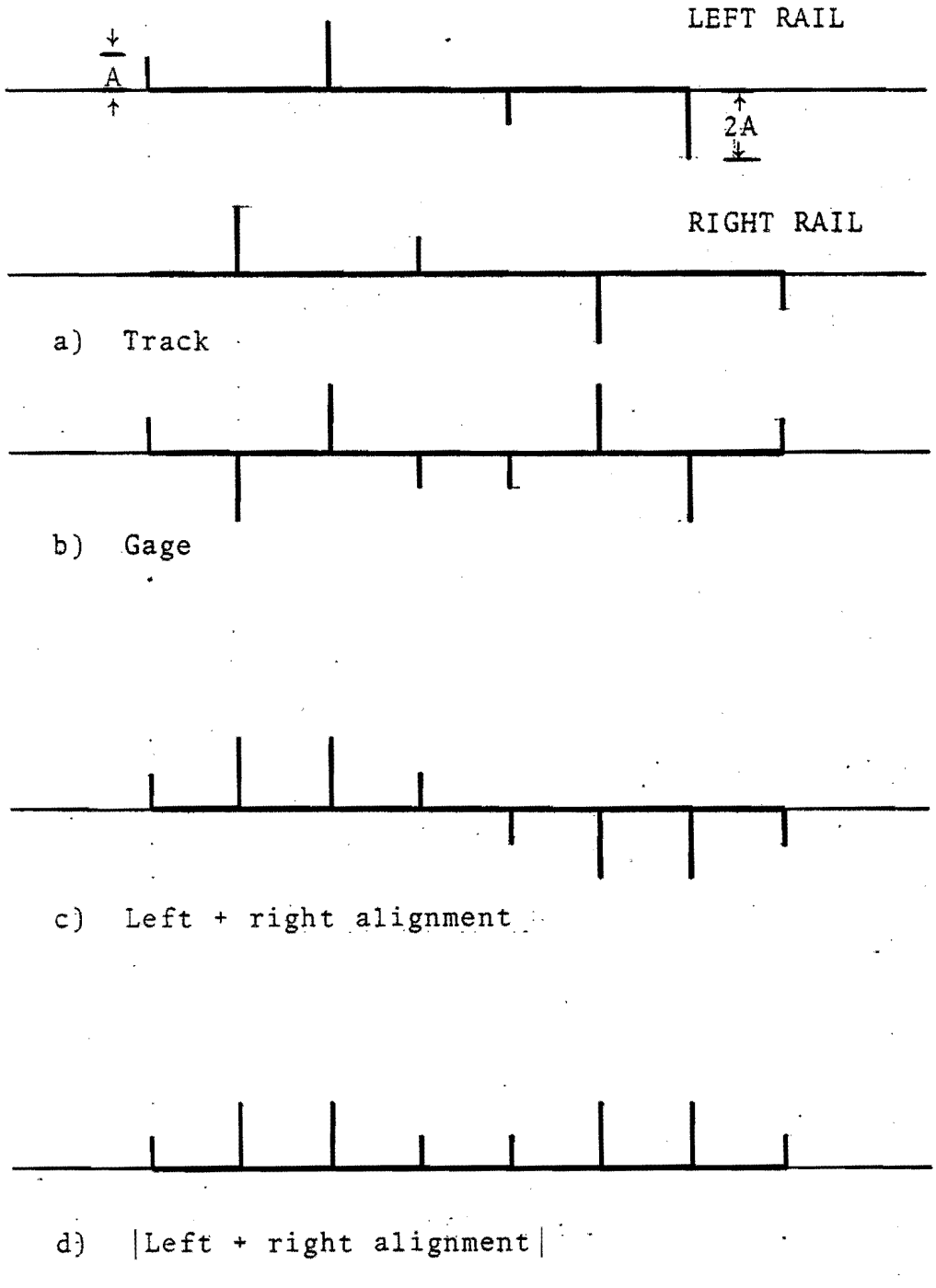

Figure 4-5. Illustration of Positive and Negative Cusps at Joints

TABLE 4-1

THE CORRELATION COEFFICIENT BETWEEN GAGE AND ALIGNMENT FOR THE ILLUSTRATIVE EXAMPLE

Parameter	Correlation Coefficient
Gage Versus Left Alignment	0.707
Gage Versus Right Alignment	-0.707
Gage Versus Left Plus Right Alignment	0.000
Gage Versus |Left Plus Right Alignment|	0.000

4.3.3 HYPOTHESIS TESTING

Review of track geometry data shows that one is unlikely to encounter a majority of track described by either hypothesis 1 or 2. Some tangent track sections may show the behavior depicted by hypothesis 1. On the other hand, some curved sections may show behavior described by hypothesis 2. On a statistical basis most track sections are described by hypotheses 3 and 4. The relationship between gage and alignment at joints can thus be described as follows:

- The alignment cusps at joints can be either positive or negative.
- The amplitude of these cusps varies randomly from one joint to the other.
- Gage can be relatively narrow or wide at joints depending on the sign of alignment cusps.

Figures 4-7 and 4-8 are examples of the measured gage and alignment on Class 2 track. Gage and alignment were high-pass filtered to enhance the joint signatures. Figure 4-7 shows an example of high rail going out at joints whereas Figure 4-8 shows an example of low rail going in at joints. Note that the positive and negative gage values are relative to the local mean and do not necessarily indicate wide or narrow gage as defined in the Federal Track Safety Standards.(10)

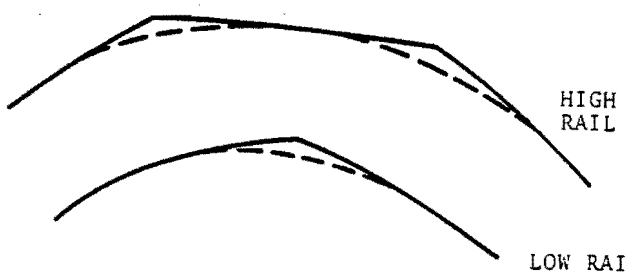

Figure 4-6. Tendency of High Rail to Go Out at Joints and Low Rail to Come In at Joints

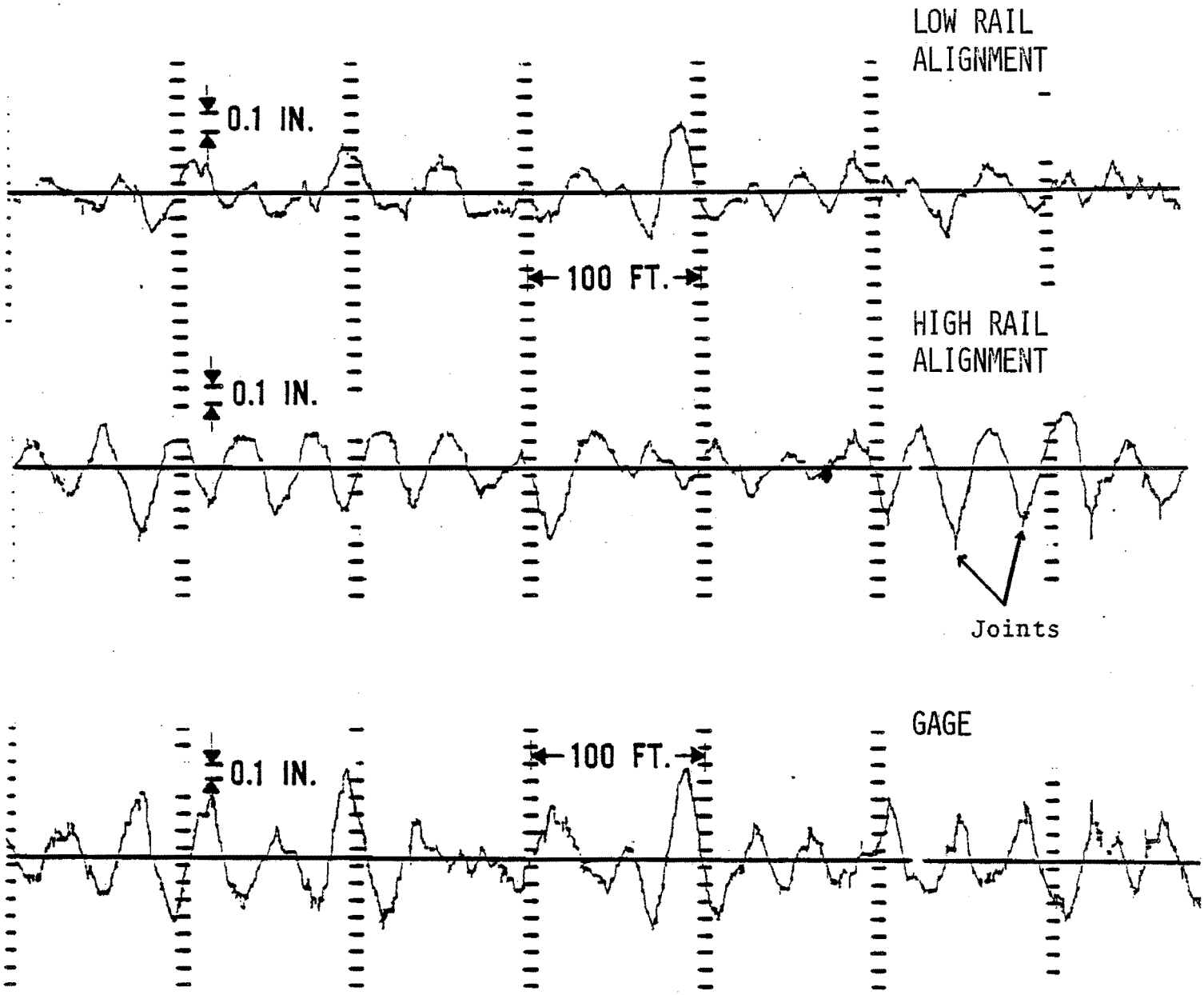

Figure 4-7. Example of High Rail Going Out at Joints

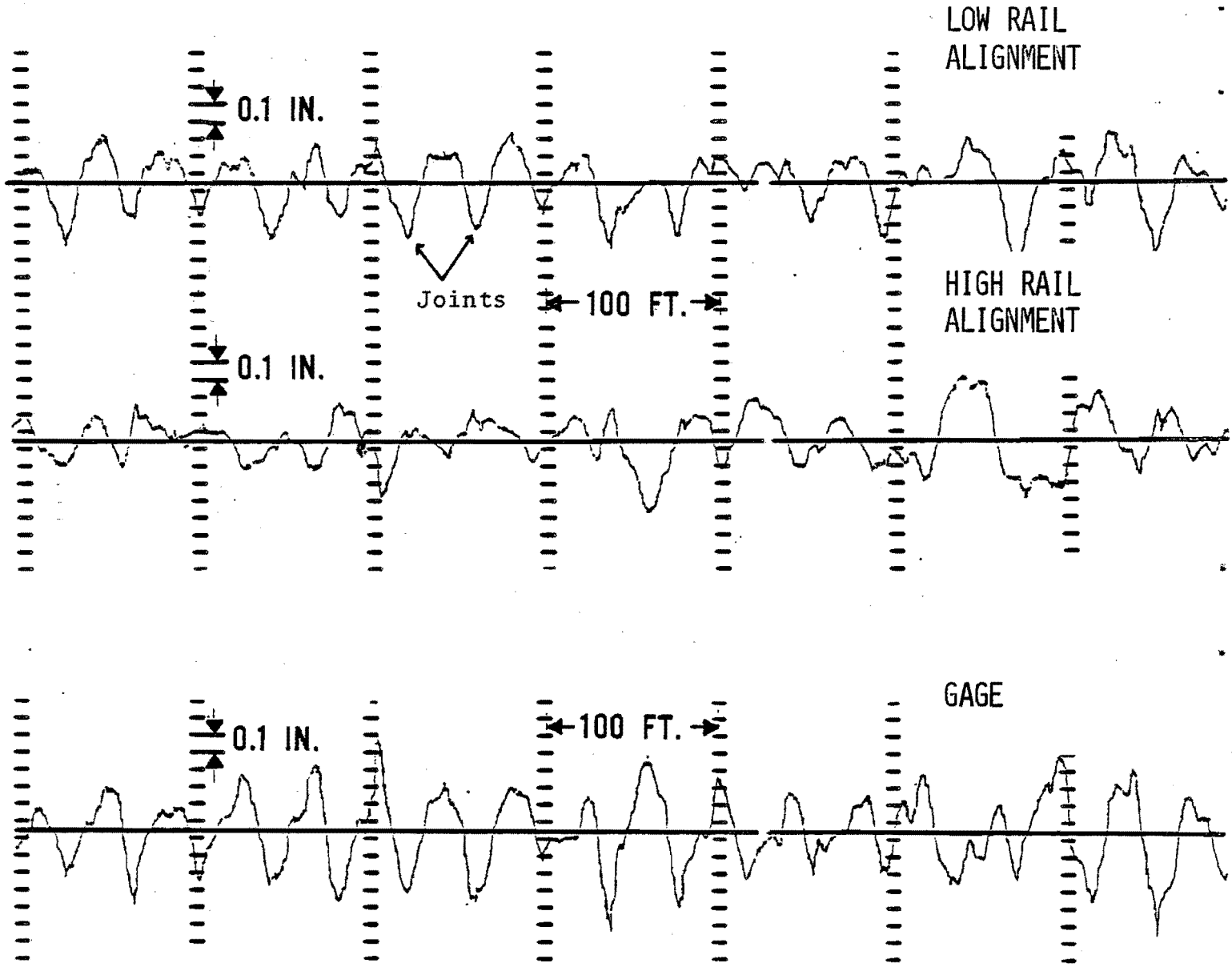

Figure 4-8. Example of Low Rail Going in At Joints

4.3.4. RESULTS OF DATA PROCESSING

Different data processing techniques were investigated to verify the relationship between gage and alignment as depicted by hypothesis 3 and 4 given in Section 4.3.2. Analyses were conducted for gage and alignment variations defined as mean removed gage or alignment.

Analyses were also conducted for magnitude of gage and alignment defined as the measured gage and the absolute value of alignment. Further analyses were conducted to characterize the relationships between left and right alignment and between gage and left minus right alignment to enhance the confidence in the methodology used. In all, nine different combinations were analyzed. Table 4-2 provides a summary of various combinations. Typical results in terms of the cross spectrum, squared coherence, phase spectrum and the magnitude of the transfer function are given in Appendix E.1.

It should be noted that the computed coherence function, $\hat{\gamma}^2_{xy}(f)$ here is defined as (13):

$$\hat{\gamma}^2_{xy}(f) = \frac{|\bar{G}_{xy}(f)|^2}{\bar{G}_x(f)\bar{G}_y(f)} \qquad (4\text{-}10)$$

where

$\bar{G}_{xy}(f)$ = Average cross spectral density
$\bar{G}_x(f)$ = Average auto-spectral density of first parameter
$\bar{G}_y(f)$ = Average auto-spectral density of second parameter

The values of $\hat{\gamma}^2_{xy}(f)$ lie between zero and one. A value of zero indicates no linear relationships between the input/output parameters. On the other hand, a value of unity indicates a perfect linear relationship. The intermediate values are interpreted as the percentage variations of the output explained by the linear relationship betwen input and output. For example, a $\hat{\gamma}^2_{xy}(f)$ value of 0.75 means that 75 percent of the variations in the output parameter are explained by the linear relationship between the input and output. The coherence function as defined here is referred to as squared coherence by some authors and the ordinary coherence is defined as the square root of this function. However, since the coherence function as defined above has direct interpretation, it will be simply referred to as "coherence" in this report.

Figure 4-9 shows typical coherence between the left and right alignment variations. The squared coherence for wavelengths longer than 100 feet is close to unity for most cases. The wavelengths shorter than 100 feet show a decrease in coherence. This would indicate that variations of both left and right alignment are alike for wavelengths longer than 100 feet. However, the alignment variations of the two rails become more or less independent as the wavelength decreases.

Figure 4-10 is an example of coherence between gage and single rail alignment. This figure shows strong coherence between gage and the single rail alignment for wavelengths shorter than 100 feet. This was true for most sections of data processed in this study. In particular, wavelengths shorter than 70 feet exhibited a coherence varying from 0.5 to 1.0 with a nominal average of 0.7. In some cases, low coherence was observed for one rail. However, this was accompanied by high coherence values for the other rail. Mixed results were obtained for wavelengths between 70 and 100 feet. In few cases this region showed poor coherence between gage and the single rail alignment. In such cases both rails had strong 78-foot alignment perturbations. This would result in strong coherence between left and right rail

TABLE 4-2

VARIOUS COMBINATIONS FOR CHARACTERIZING THE RELATIONSHIPS BETWEEN GAGE AND ALIGNMENT

Parameter	$\lvert x_1 \rvert$	$\lvert x_2 \rvert$	$\left\lvert \frac{x_1+x_2}{2} \right\rvert$	$\tilde{x}_1$	$\tilde{x}_2$	$\frac{\tilde{x}_1+\tilde{x}_2}{2}$	x_1-x_2
G	X	X	X				
$\lvert x_1 \rvert$		X					
g				X	X	X	
$\tilde{x}_1$					X		

G = Gage - 54 inches (magnitude of gage)

g = Gage variations (mean removed gage)

x_1 = Left Alignment Space Curve

x_2 = Right alignment space curve

$\tilde{x}_1$ = Left alignment variations (mean removed alignment)

$\tilde{x}_2$ = Right alignment variations

An X mark in the entry indicates that analyses were performed on the pair of parameters.

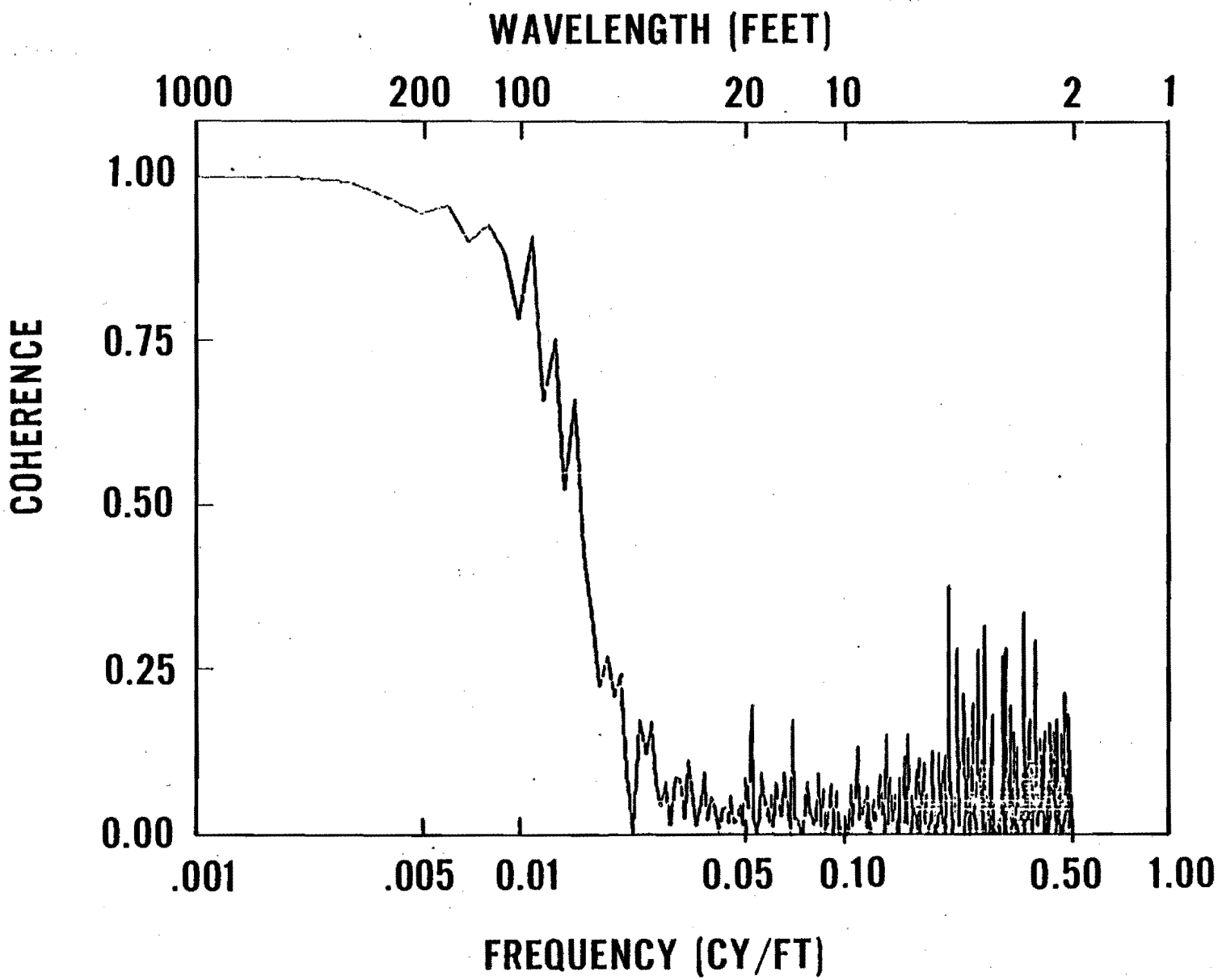

Figure 4-9. Coherence Between Left and Right Alignment

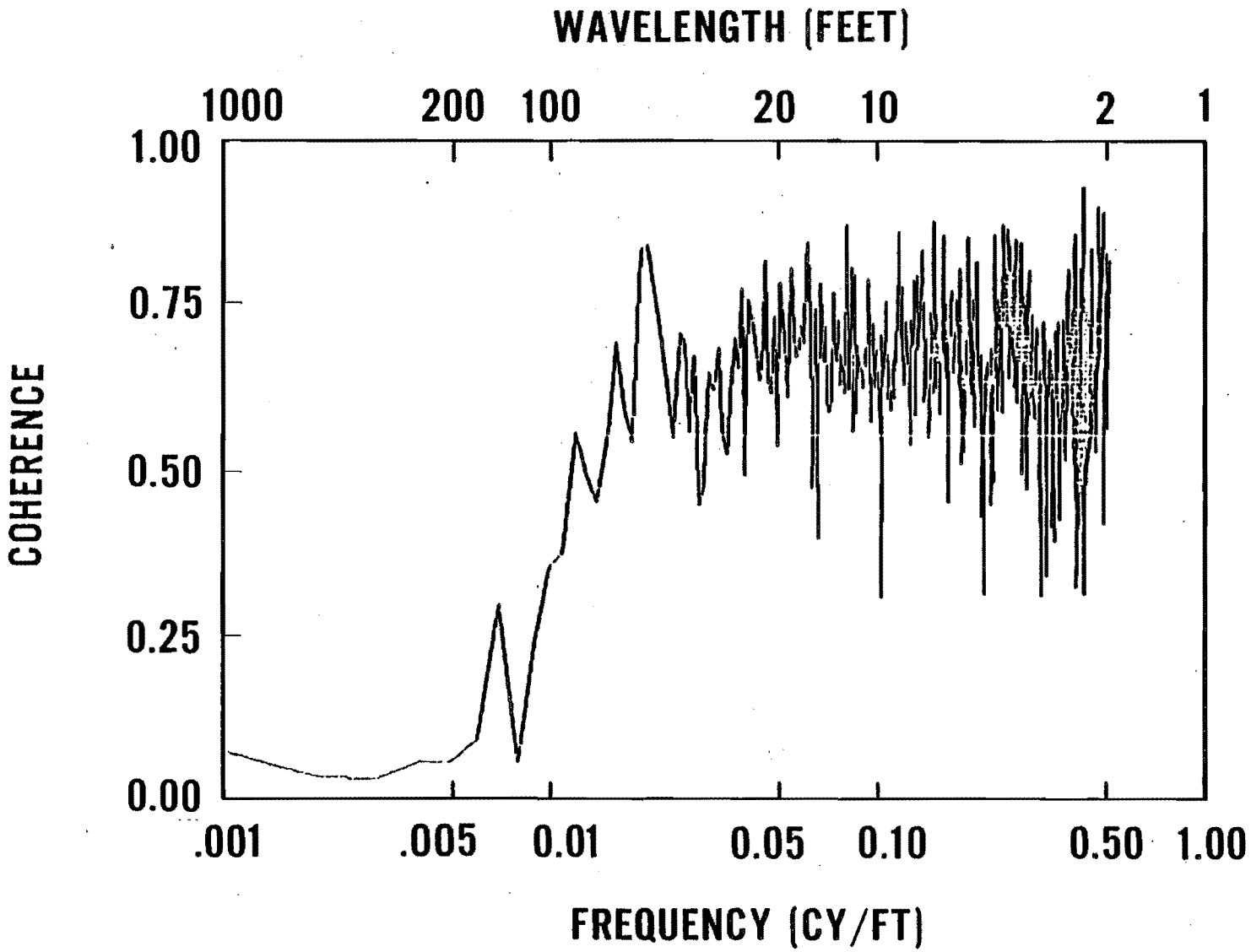

Figure 4-10. Coherence Between Gage and Single Rail Alignment

alignment and a poor coherence between gage and the single rail alignment.

The results in the previous paragraphs indicate that there is a strong linear relationshp between gage and single rail alignment variations for wavelengths up to 100 feet for most cases. However, sometimes this is offset by a strong alignment activity in both the left and right rails for wavelengths between 70 and 100 feet.

Data were also processed to analyze coherence between gage and mean alignment variations.* The observed coherence was mainly below 0.25 with a nominal value between 0 and 0.1. There were occasional peaks at wavelengths corresponding to the rail length and its harmonics. These results indicate that gage and mean alignment variations are not linearly correlated with each other.

Relationships were also investigated between the magnitude of gage (G) and the magnitude of alignment. The coherence for all track classes was insignificant. This means that an increase in gage does not necessarily imply an increase in the magnitude of alignment.

4.3.5 TANGENT AND CURVED TRACK

In the previous section, it has been shown that there is a significant linear relationship between gage and single rail alignment variations for short wavelengths. In some cases gage variations showed stronger relationships with one rail than with the other. Further analyses were conducted to determine the cause of this difference. Analyses were performed separately for the tangent track, track with left hand curves and the track with right hand curves.**

In all cases, the coherence between gage and either single rail alignment was similar for purely tangent track. Figures 4-11 and 4-12 show an example of coherence between gage and single rail alignment variations. The coherence for both the left and right rail is of the same order of magnitude.

For the lower class track (e.g., Class 2) gage variations showed a slightly stronger relationship with the single rail alignment for the curved track than that of the tangent track. The relationship appeared to be slightly better with the low rail for both the left and right curves. However, the difference was not significant.

For the higher class track, i.e., Class 4 or above, gage variations showed higher coherence with the high rail alignment than with the low rail. Figures 4-13 and 4-14 are the examples of the gage coherence with the high and low rail alignment. The coherence with the high rail is significantly higher than that with the low rail.

On the tangent track, both the left and right rails are, in general, subjected to the similar lateral loads. Therefore, the alignment variations in the two rails are more or less of the same order of magnitude. In this case, the coherence between gage and single rail alignment is found to be of the same order of magnitude for both the left and right rails. For lower class track, the posted speed may be lower than the balance speed in larger curves. Therefore, the train has a tendency to ride the low rail and the low rail tends to have more alignment activity than the high rail. In this case, gage tends to have stronger relationships with the low rail alignment. On the

---

*Average of left and right alignment.

**Left hand curve means the left rail is the low rail; the right hand curve means that the right rail is the low rail.

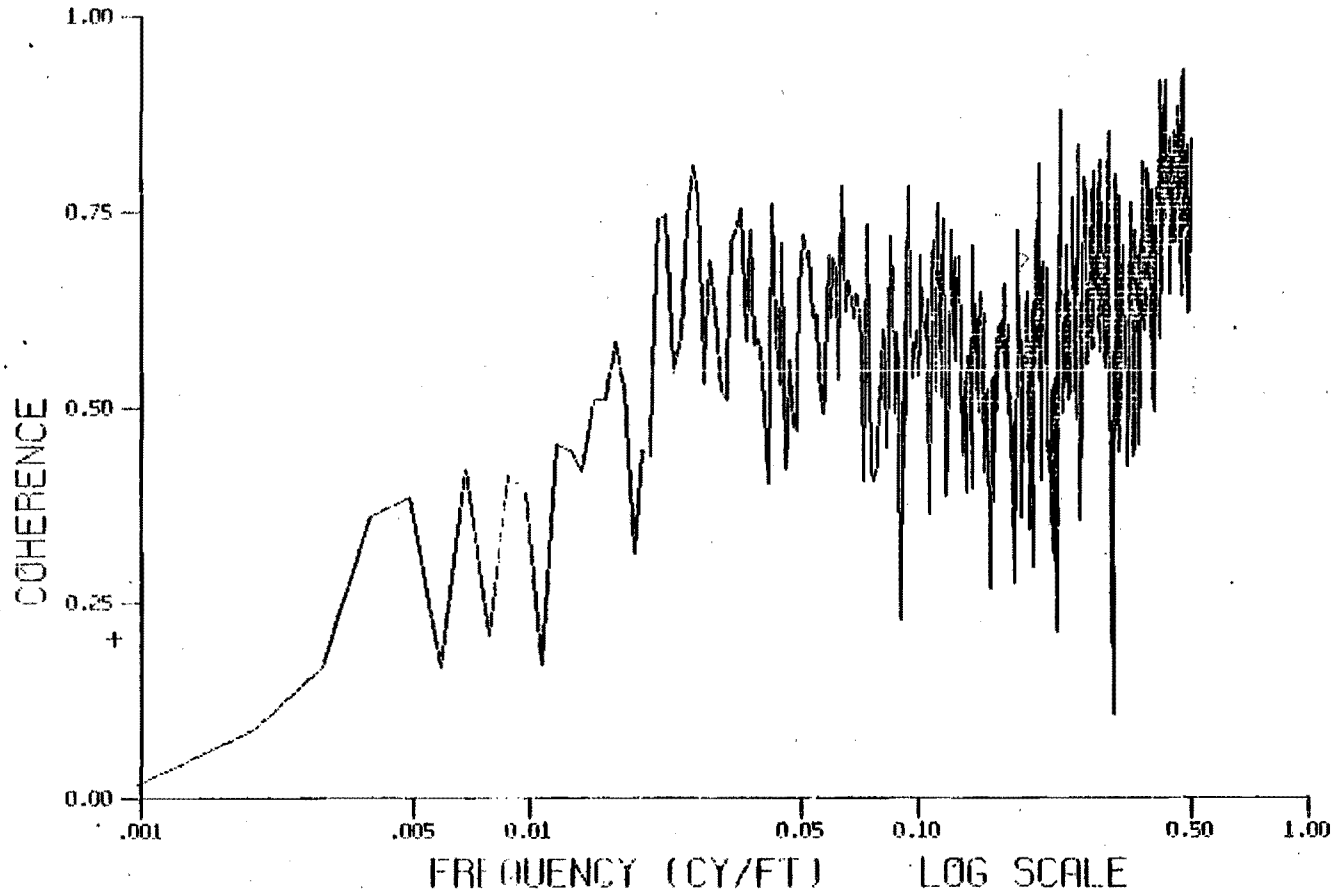

Figure 4-11. Coherence Between Gage and Left Rail Alignment Variations for Tangent Track

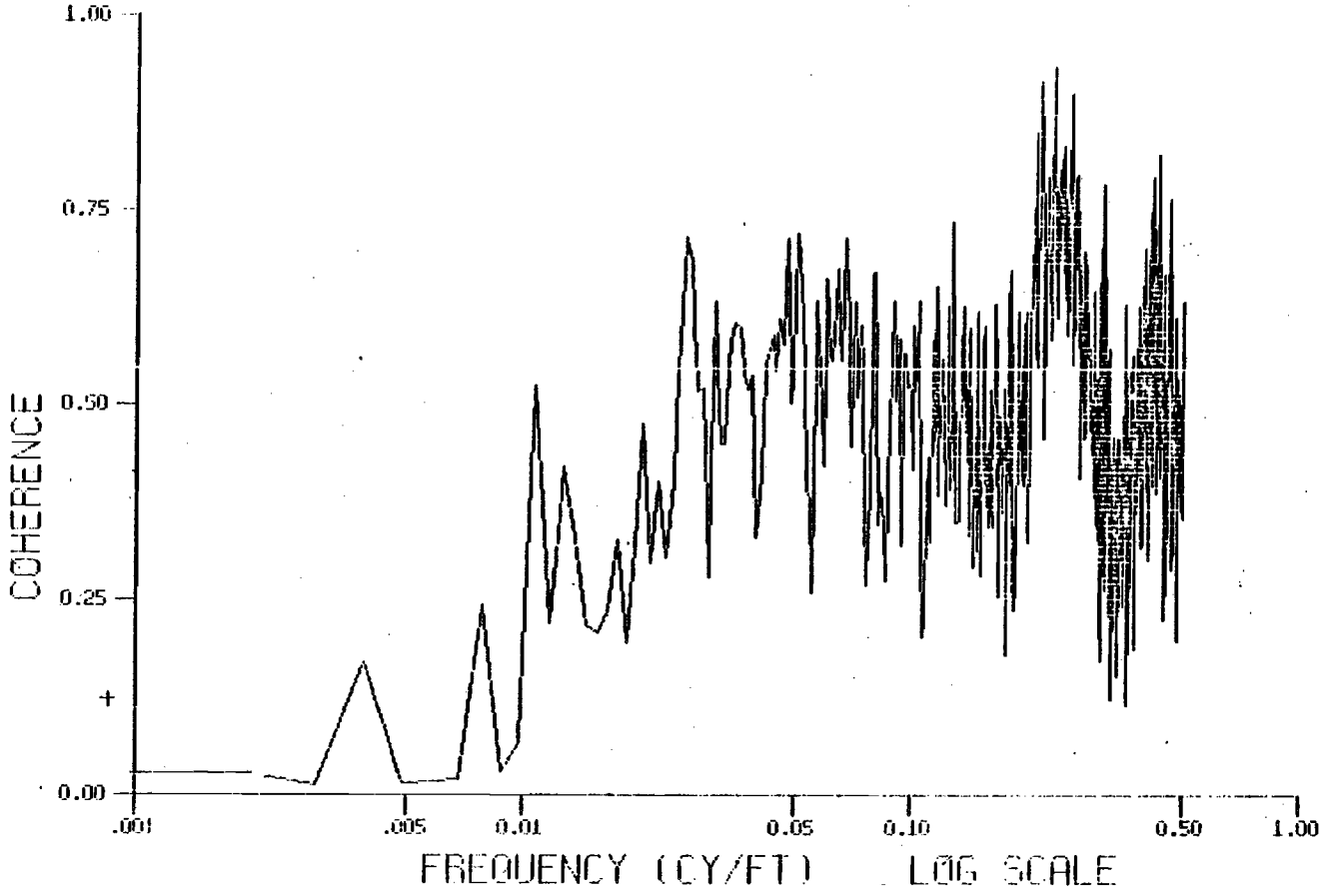

Figure 4-12. Coherence Between Gage and Right Rail Alignment Variations for Tangent Track

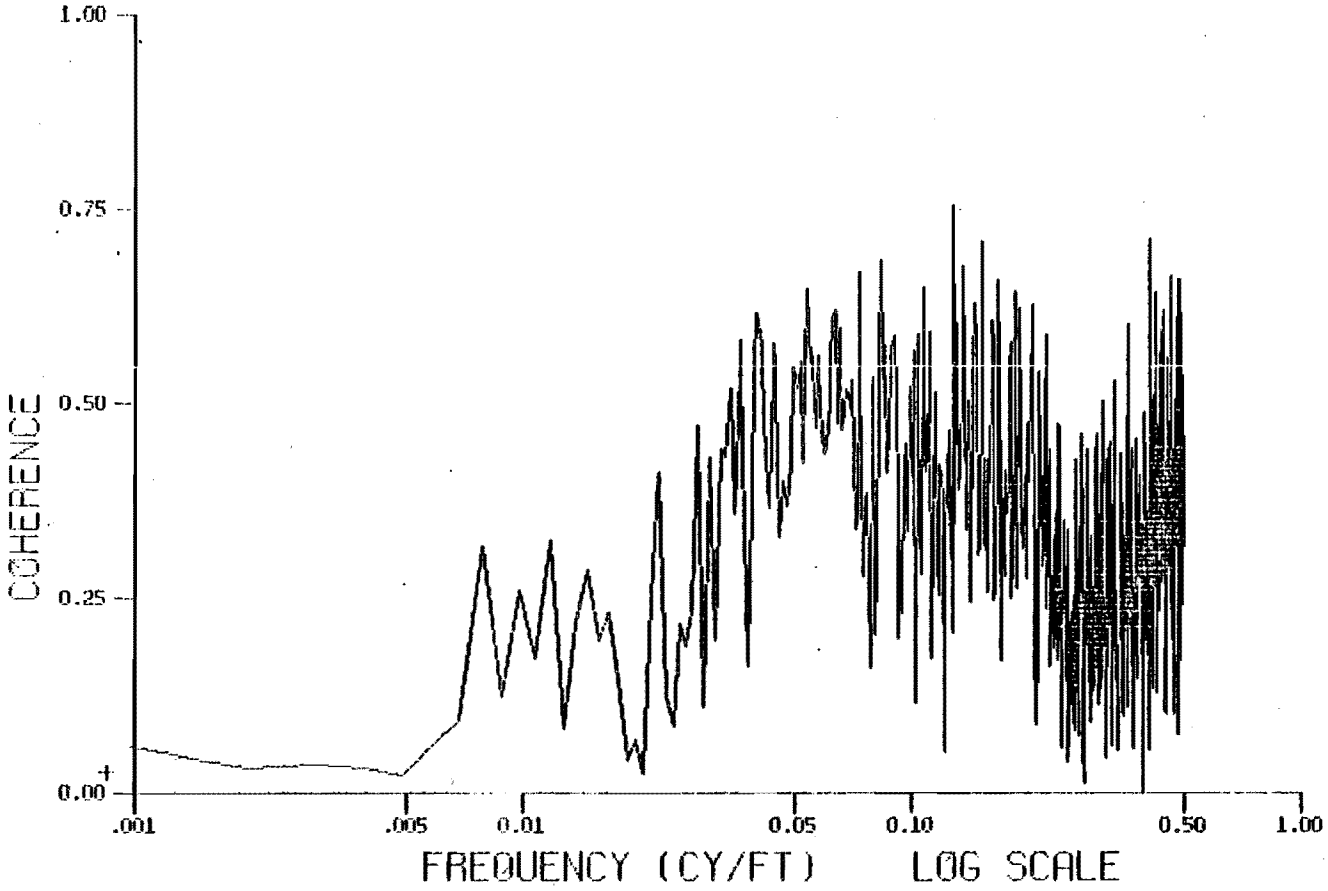

Figure 4-13. Coherence Between Gage and Low Rail Alignment Variations for Curved Track (Class 4)

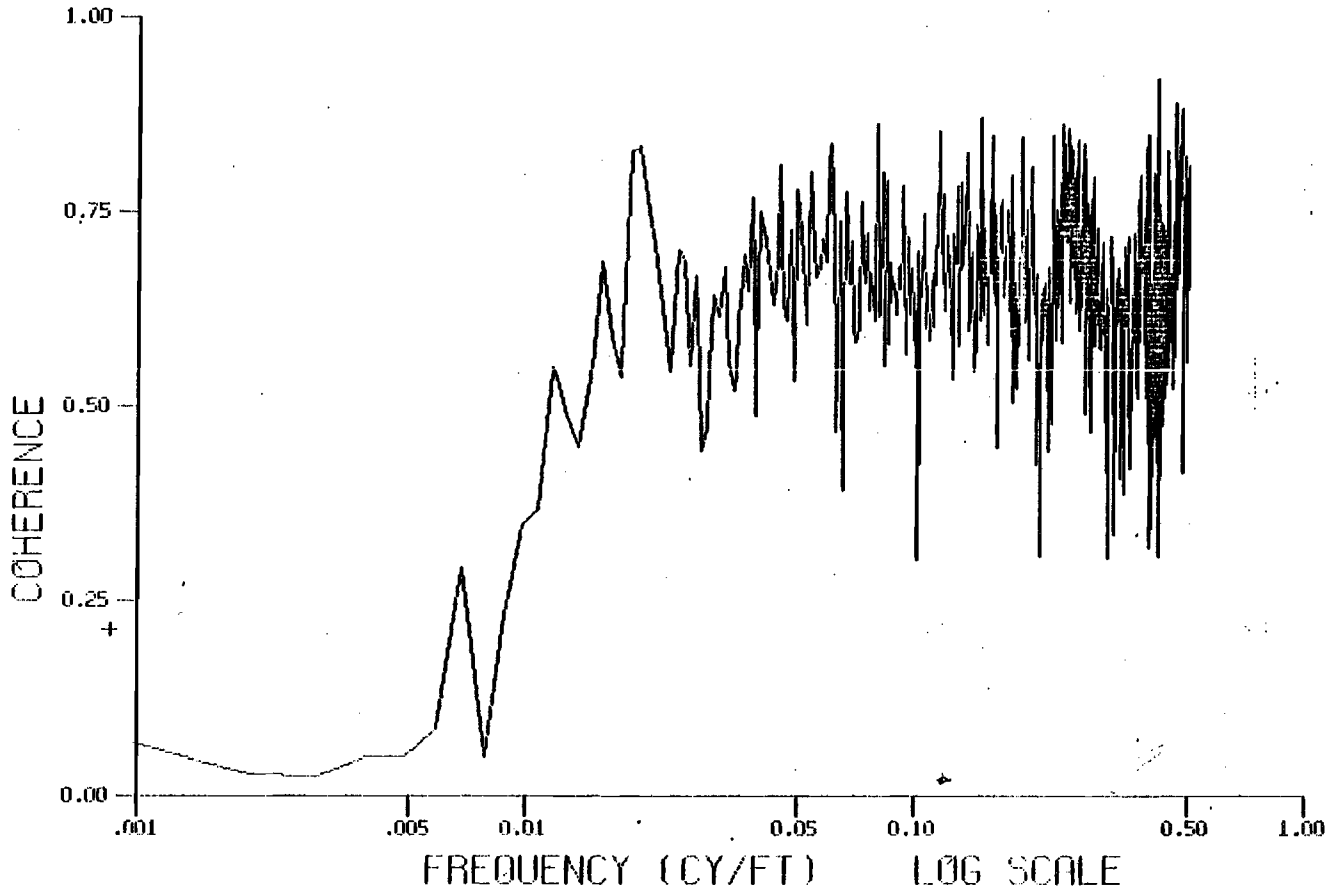

Figure 4-14. Coherence Between Gage and High Rail Alignment Variations for Curved Track (Class 4)

other hand, on the higher class track, i.e., Class 4 or above, the balance speed may be less than the maximum allowable class speed and the traffic tends to go over balance speed. Therefore, the high rail is subjected to more lateral load than the low rail. Consequently, the alignment variations in the high rail are more severe than those of the low rail. In this case gage has a stronger relationship with high rail alignment than with the low rail alignment.

4.3.6 MATHEMATICAL FORMULATION

Data processing results in Sections 4.3.4 and 4.3.5 verify the track descriptions hypothesized in Section 4.3.3. Thus, we can conclude that alignment at joints has randomly varying positive or negative cusps at joints. This means that each rail can deform either towards track centerline or towards field side. At joints gage will be relatively narrow or wide depending on the direction of alignment cusps. This gives a strong linear relationship between gage and alignment variations.

The relationship between gage and single rail alignment can be described by a transfer function. This transfer function can be characterized by the gain factor and phase angle as a function of frequency.

The transfer function, H(f), for gage and single rail alignment variations can be defined as:

$$H(f) = \frac{G_{xy}(f)}{G_x(f)} \qquad (4\text{-}11)$$

where

$G_{xy}(f)$ = cross spectral density between gage and alignment

$G_x(f)$ = auto-spectral density of gage

$H(f)$ = transfer function

The transfer function relates the input and output variables by:

$$Y(f) = H(f)X(f) \qquad (4\text{-}12)$$

where

$Y(f)$ = Fourier transform of alignment variations

$X(f)$ = Fourier transform of gage variations

The transfer function can be expressed as:

$$H(f) = |H(f)|e^{-i\phi(f)} \qquad (4\text{-}13)$$

where

$|H(f)|$ = gain factor

$\phi(f)$ = phase angle

TABLE 4-3
GAIN FACTOR BETWEEN GAGE AND
SINGLE ALIGNMENT VARIATIONS

Track Class	Gain Factor*
1	0.51
2	0.50
3	0.49
4	0.48
5	0.49
6	0.45

*Average for left and right alignment

The average value of phase angle for gage and left alignment is zero at short wavelengths. The corresponding value for the right alignment is 180 degrees. This is due to the sign convention used for alignment. A positive offset in the left alignment means an offset away from the track centerline which results in wide gage. For the right alignment, a positive offset means an offset to the track centerline which results in relatively narrow gage.

Table 4-3 gives the average gain factor between gage and alignment variations at short wavelengths. This table indicates that there is no significant difference between different track classes and that the average gain factor is approximately 0.5. This could imply that, on the average, one-half of the gage variations accounted by the linear relationships are due to the alignment variations of one rail and the other half due to the alignment variations of the other rail.

4.4 CROSSLEVEL AND PROFILE

4.4.1 TRACK DESCRIPTIONS

Observation of track geometry data reveals that profile exhibits depressions or negative cusps at joints. Bolted track is usually half staggered, therefore, depressions on opposite rails occur every half rail length. Depressions on joints eventually die away within 1/4 to 1/2 the rail length on either side.

The profile and crosslevel representation for the half-staggered bolted track is shown in Figure 4-15. The crosslevel is the difference between left and right profile. According to the sign convention used, positive crosslevel corresponds to a dip on the right rail and negative crosslevel corresponds to a dip on the left rail.

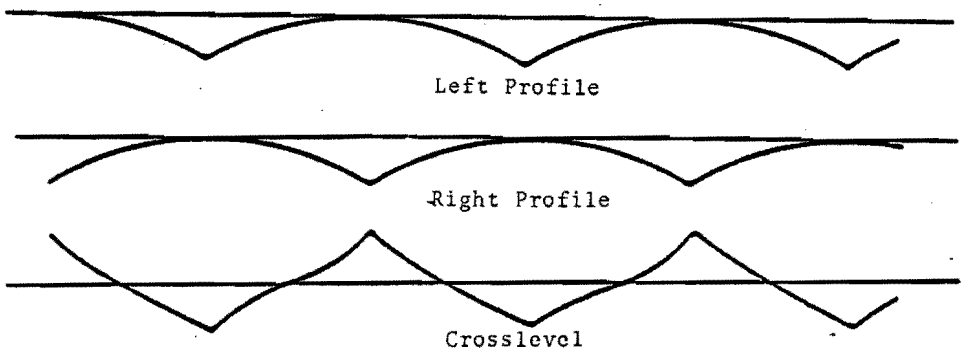

Figure 4-15. Profile and Crosslevel Representations for Half-Staggered Bolted Track

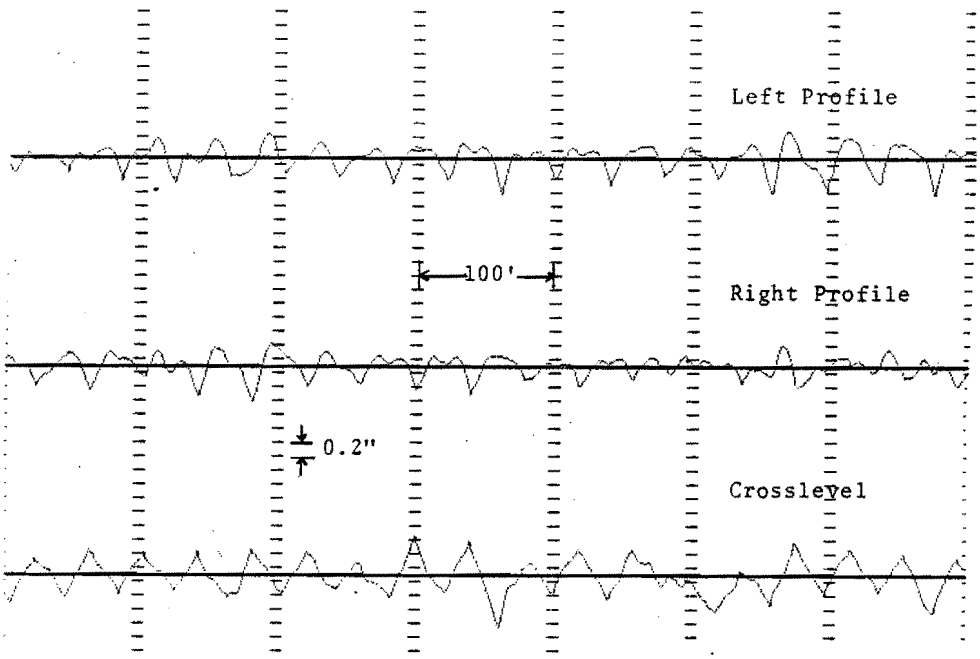

Figure 4-16. Crosslevel and Profile Showing Joint Signatures

As shown in Figure 4-15, a negative offset in single rail profile is usually accompanied by an equal probabilty of positive or negative crosslevel. In this case, the crosslevel will have insignificant correlation with the single rail profile. However, at joints, a depression in left profile is always accompanied by a negative cusp in the crosslevel. This will result in a significant positive correlation between the crosslevel and the left profile at a wavelength equal to the rail length. Similarly a depression in the right profile is always accompanied by a positive cusp in the crosslevel. This will result in a significant negative correlation between the crosslevel and the right profile.

Figure 4-15 also indicates that a negative cusp in the mean profile is always accompanied by a positive or negative cusp in the crosslevel. Therefore, the crosslevel variations will have an insignificant correlation with mean profile variations.

Figure 4-16 is an example of measured crosslevel and profile data for the bolted track. Both the profile and crosslevel have been high-pass filtered to enhance the joint signatures. Note that the measured data agree with the representation hypothesized in Figure 4-15.

Mathematical representations for the rail profile were developed under a previous contract and were given in reference (1). A modified form including the superelevated term is given in reference (15). A simplified representation of the profile for a single rail is given by:

$$z(x) = ce^{-\alpha|x|}, \qquad -\frac{L}{2} \leq x \leq \frac{L}{2} \tag{4-14}$$

where

$z(x)$ = profile
c = joint amplitude
α = decay factor
x = distance from the joint
L = rail length

The joint influence can be forced to zero at one-half the rail length from the joint by the expression:

$$z(x) = c(e^{-\alpha|x|} - e^{-\alpha L/2}) \tag{4-15}$$

The joint amplitude varies from one joint to the other. Therefore, the profile as a function of distance along the track can be expressed as:

$$z(x,n) = c(n) \quad e^{-\alpha|x|} - e^{-\alpha L/2} , \quad -\frac{L}{2} \leq x \leq \frac{L}{2} \tag{4-16}$$

$$0 \leq n \leq \infty$$

The expressions given by Equations (4-14) through (4-16) are applicable to both rails by introducing a proper delay, depending on the joint stagger, for generating the values of one rail with respect to the other. The crosslevel variations at any point can be expressed as

$$\zeta = z_{\ell} - z_{r} \tag{4-17}$$

where

ζ = crosslevel variation

z_{ℓ} = left profile

z_{r} = right profile

4.4.2 RESULTS OF DATA PROCESSING

Various combinations of data processing used to verify the relationships between crosslevel and profile variations are given in Table 4-4. Plots of the cross spectral density, coherence, phase angle and the magnitude of the transfer function are given in Appendix E.2. The following paragraphs summarize the results obtained.

TABLE 4-4

COMBINATIONS OF DATA PROCESSING FOR CROSSLEVEL AND PROFILE VARIATIONS

Parameter	p_{ℓ}	p_r	$\bar{p}$	$p_{\ell}-p_r$
ζ	X	X	X	X
p_{ℓ}		X		

ζ = crosslevel variations (high-pass filtered crosslevel)

p_{ℓ} = left profile space curve

p_r = right profile space curve

$\bar{p}$ = mean profile space curve

Figure 4-17 is an example of coherence between the left and the right rail profile. A significant coherence is shown for wavelengths longer than 20 feet. Analysis of different track sections showed coherence values between 0.75 and 1.0 for longer wavelengths except at some wavelengths such as the ones corresponding to the rail length. For Class 2 and 3 bolted track, the coherence was almost zero at 39 feet wavelength. However, there was a significant coherence peak at 20 feet wavelength. This is attributed to the regularly spaced half-staggered joints.

Figure 4-18 shows typical coherence values between crosslevel and the single rail profile. The coherence is not very significant for most wavelengths. However, significant peaks are found at wavelengths of 39 and 13 feet. Most track sections showed coherence values of 0.1 and 0.4 except at wavelengths corresponding to the rail length and its harmonics. Typical values at such wavelengths were between 0.3 and 0.5. Coherence peaks of 0.6 and 0.8 were observed at 39 feet wavelength for Class 2 and 3 bolted track. This is attributed to the fact that the crosslevel variations at joints are predominantly due to surface depressions at joint.

Figure 4-19 is an example of the coherence between crosslevel and the mean profile. Crosslevel shows almost zero coherence with the mean profile. Similar results were obtained for most track sections.

Results in this section verify the track descriptions hypothesized in Section 3.4.1. Thus, one is likely to encounter a majority of track as represented in Figure 4-15 for profile.

4.5 CROSSLEVEL AND ALIGNMENT

Investigations were performed to determine the relationships between the crosslevel variations and alignment variations. This was done for both the single rail alignment and the mean alignment. Typical plots showing the frequency domain relationships are given in Appendix E.3.

Figure 4-20 is an example of the coherence between crosslevel and alignment variations. This is typical of both the single rail alignment and mean alignment. The coherence is almost zero at all wavelengths. Specifically, analyses of other track sections showed similar results. In general, the coherence between the crosslevel and alignment was less than 0.1. However, at certain wavelengths such as 39, 19, 13, 9 and 5 feet, coherence peaked from 0.3 to 0.5. It should be noted that these wavelengths correspond to the rail length and its harmonics. This would imply that relatively more severe crosslevel and alignment variations exist at joints which give relatively higher coherence, at frequencies that are related to the joint spacing.

In some cases, strong coherence was found between crosslevel and alignment variations at certain long wavelengths. An example is shown in Figure 4-21 where a coherence peak at 54 feet wavelength is pronounced. This was especially true for some welded track sections of Class 4 or better track. In many cases, the most pronounced wavelength was 78 feet where the coherence in some cases peaked from 0.7 to 1.0. The exact cause for this is not known at this time. This can possibly be attributed to combined crosslevel and alignment variations due to certain structural, traffic or maintenance practices in certain territories.

4.6 OTHER TRACK GEOMETRY PARAMETERS

Data were also processed to determine the relationship between gage and crosslevel, gage and profile, and profile and alignment. Typical results are given in Appendix E.4.

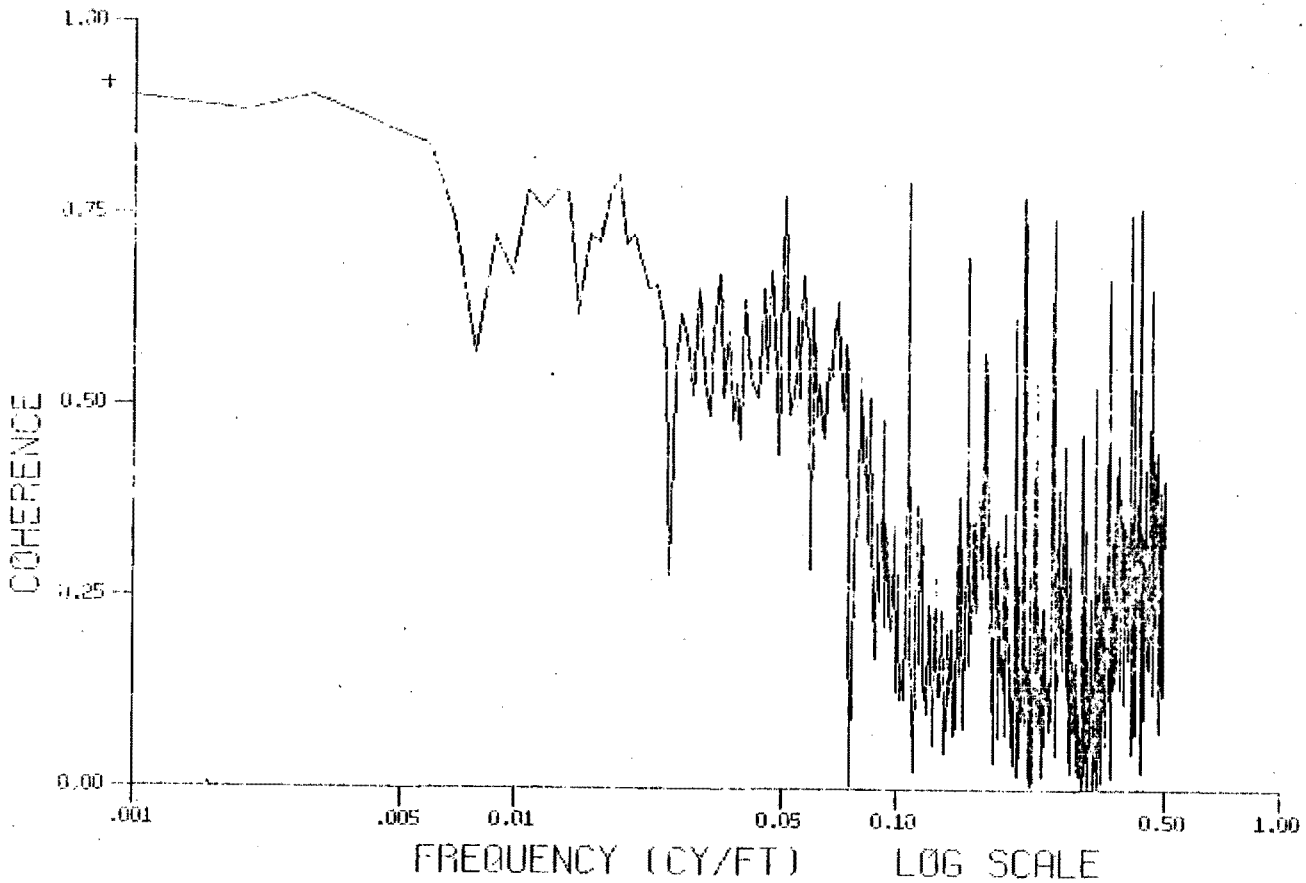

Figure 4-17. Coherence Between Left Profile and Right Profile

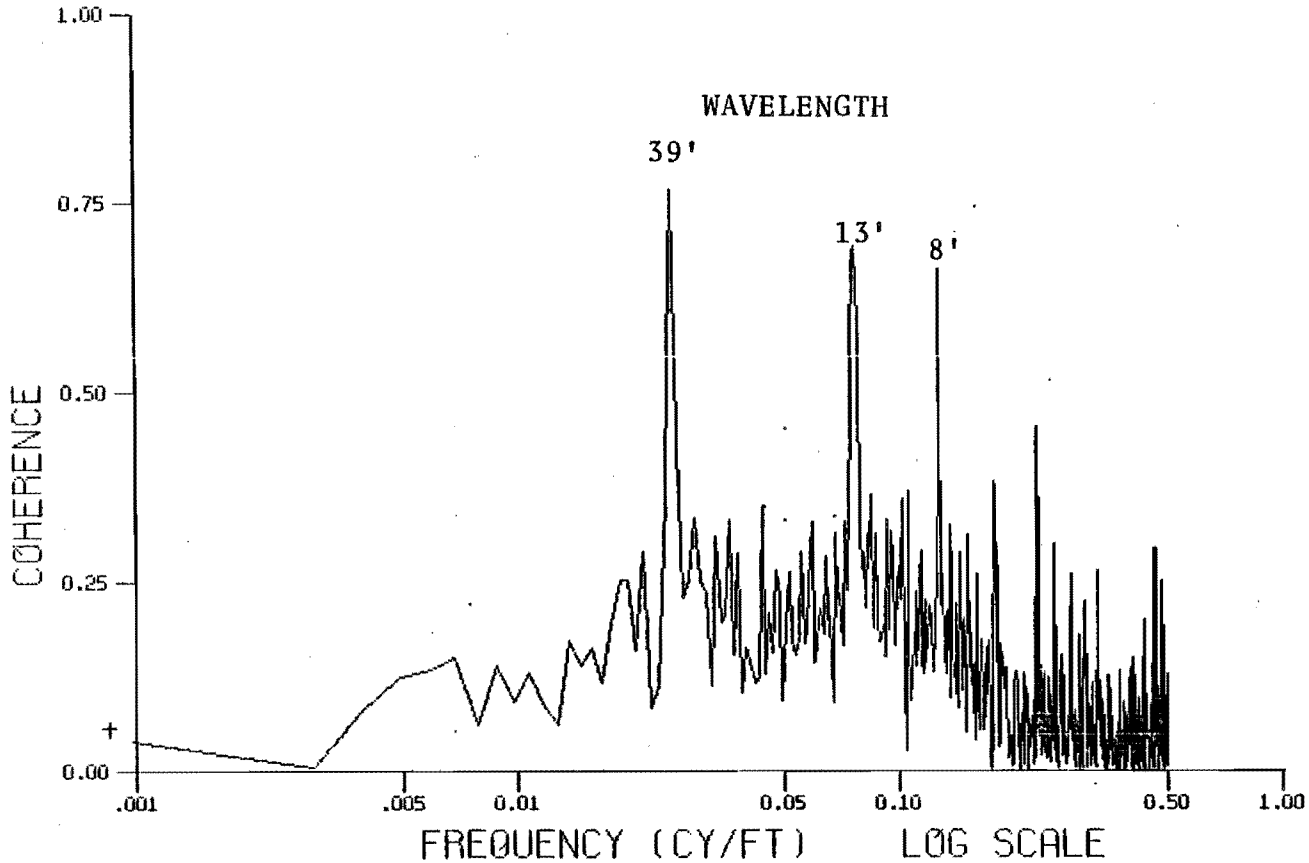

Figure 4-18. Coherence Between Crosslevel and Left Profile

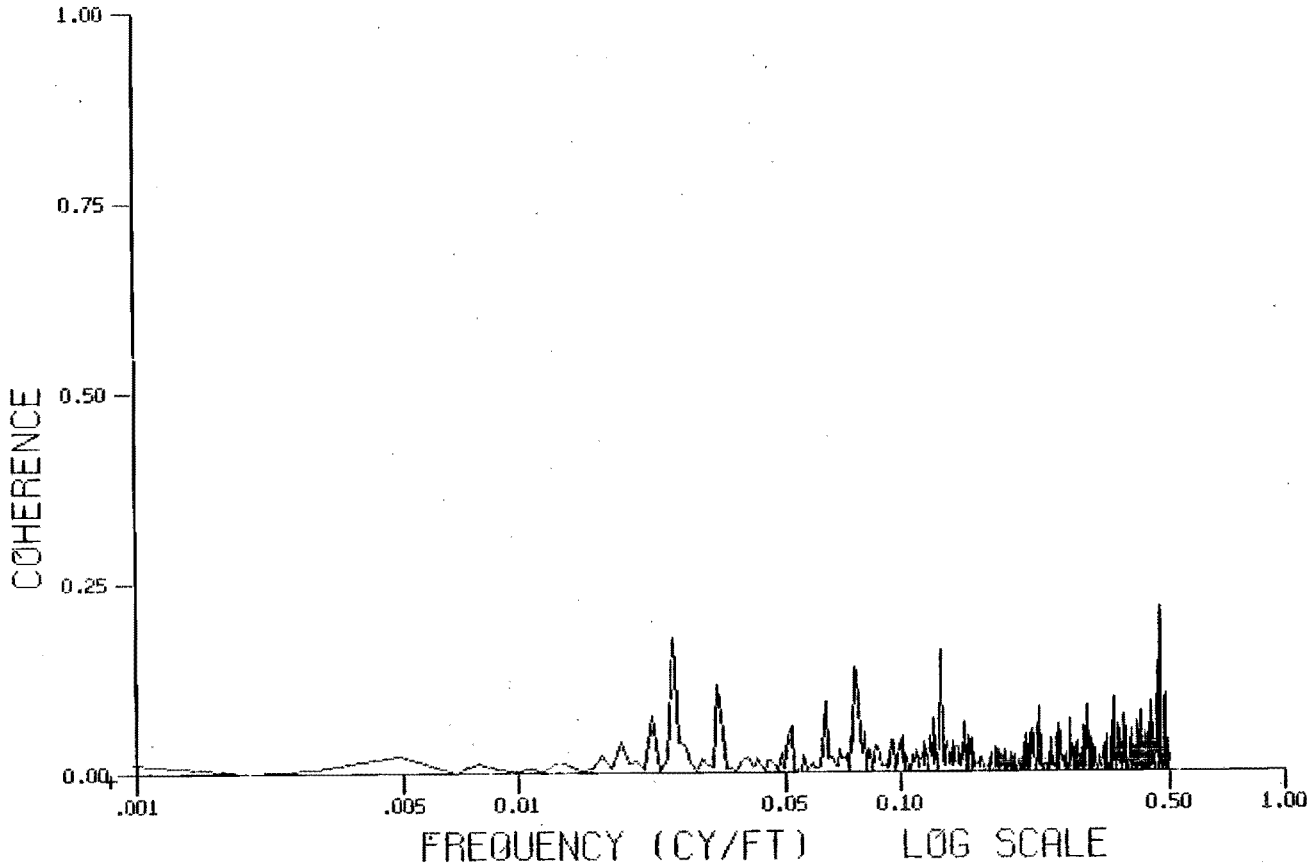

Figure 4-19. Coherence Between Crosslevel and Mean Profile

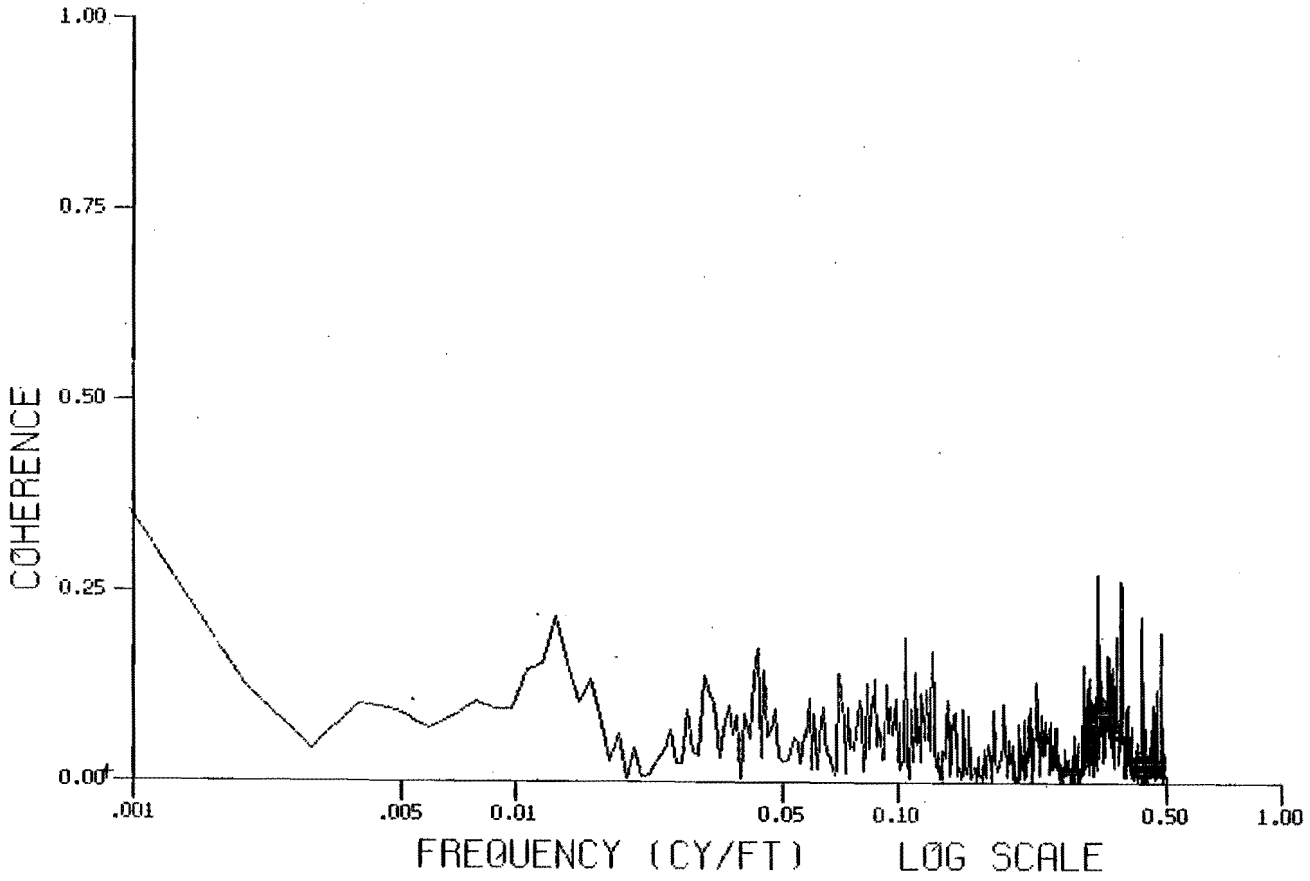

Figure 4-20. Coherence Between Crosslevel and Right Alignment

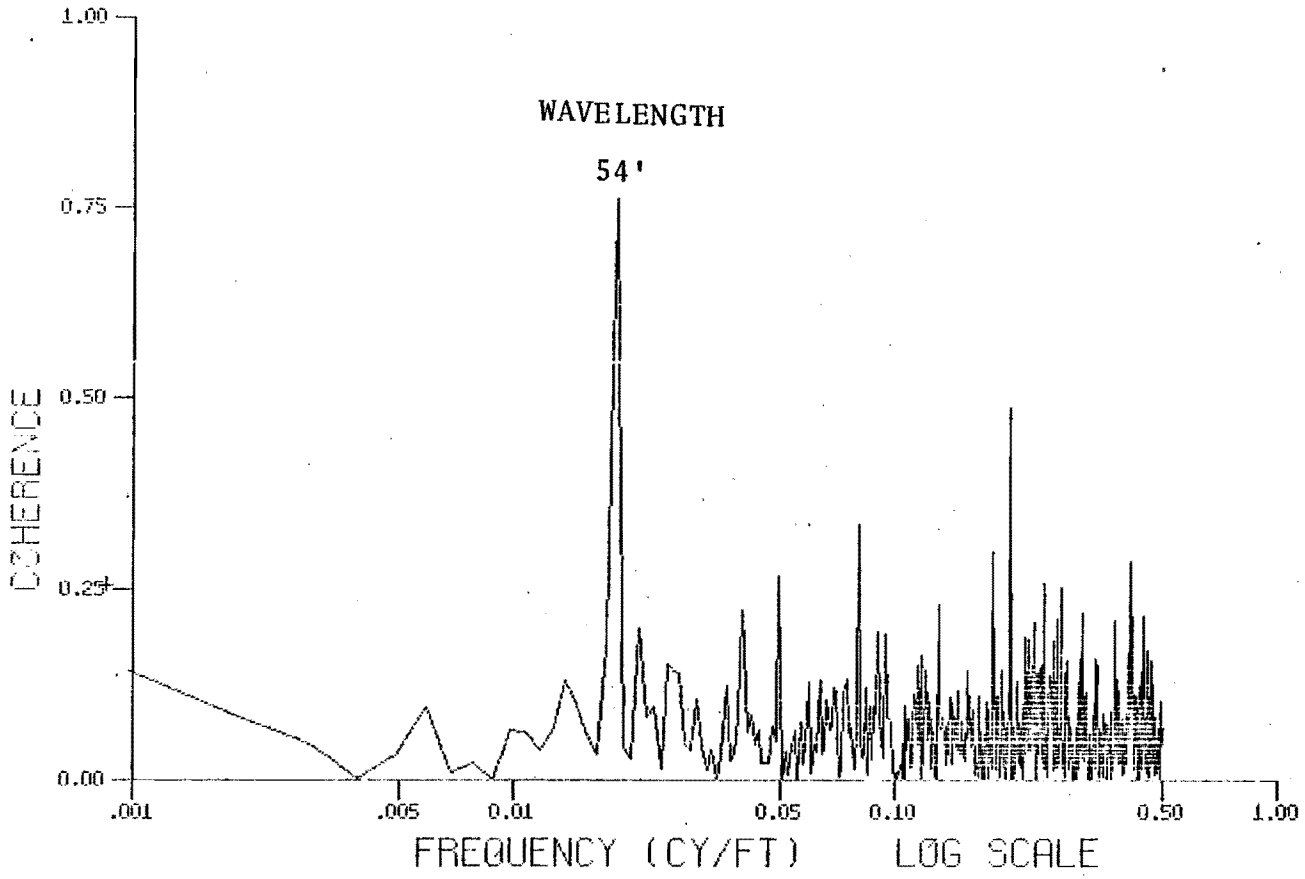

Figure 4-21. An Exceptional Coherence Between Crosslevel and Right Alignment

Figure 4-22 is an example of coherence between gage and crosslevel variations. The coherence is almost zero for all wavelengths. Similar results were obtained for both the bolted and welded track in most cases. However, in some cases coherence peaks up to 0.3 were observed at certain wavelengths such 78, 39, 19.5, 13 and 9 feet.

Similar results were also obtained for relationships between the gage and profile, and between profile and alignment variations for most wavelengths. In particular, almost zero coherence was observed for welded track sections at all wavelengths. However, the bolted track showed a significant coherence peak at a wavelength equal to one-half the rail length. Furthermore, the coherence was non-zero between wavelengths of 13 and 39 feet. Examples are shown in Figures 4-23 and 4-24. Note a significant coherence peak at a wavelength of 19.5 feet. This is believed to be due to the simultaneous degradation of gage, profile and alignment at joints. The degradation corresponding to a joint is encountered at every half the rail length on the half staggered bolted track. This results in a significant linear relationship between gage and profile, and profile and alignment variations at a wavelength equal to one-half the rail length.

4.7 SUMMARY AND CONCLUSIONS

Track geometry data typical of U.S. track were analyzed to determine the linear relationships between track geometry parameters. These analyses were conducted in the frequency domain by generating autospectal densities, cross spectral densities, coherence functions and transfer functions.

These analyses have shown that certain track geometry parameters are correlated. Table 4-5 gives a summary of correlation among track geometry parameters. Numbers in columns indicate the wavelengths at which the two parameters are significantly correlated. Columns left blank or excluded from the table indicate insignificant correlation. These correlations should be taken into consideration in developing performance oriented track specifications or performing vehicle dynamic analyses.

Based on the results of this study, it can be concluded that variations in the left and right alignment are the same for wavelengths longer than 100 feet. For wavelengths, typically shorter than 70 feet, there is a strong linear relationship between gage and single rail alignment variations. Left and right rail alignments are more or less independent for these wavelengths.

There is no correlation between gage and mean alignment variations. Furthermore, an increase in gage does not necessarily imply an increase in the magnitude of alignment.

TABLE 4-5

CORRELATED PARAMETERS

Single Rail Parameter	Single Rail Alignment	Single Rail Profile	Crosslevel
Gauge	<70	19.5	
Single Rail Alignment	>100	19.5	50-90
Single Rail Profile	19.5	>20	39

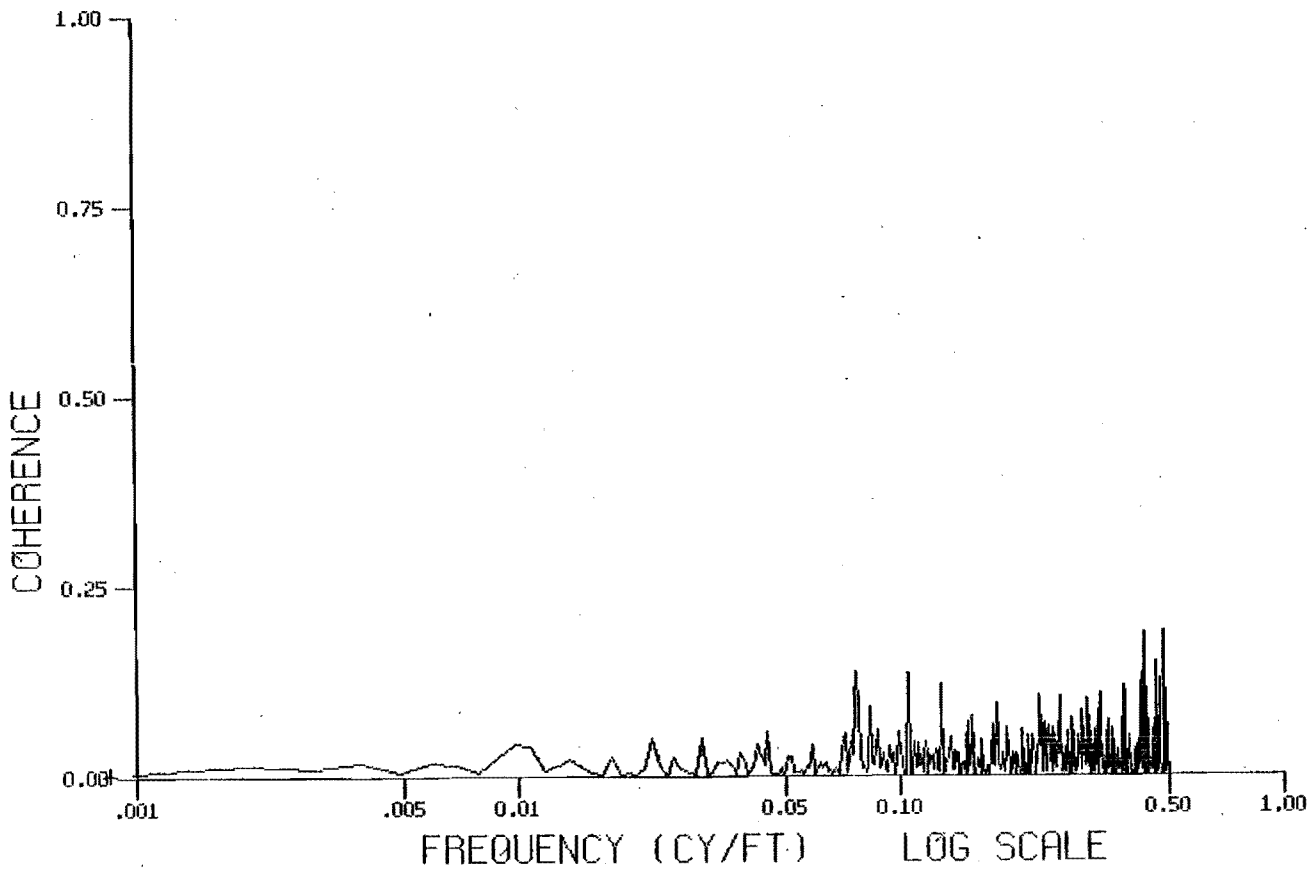

Figure 4-22. Coherence Between Crosslevel and Gage

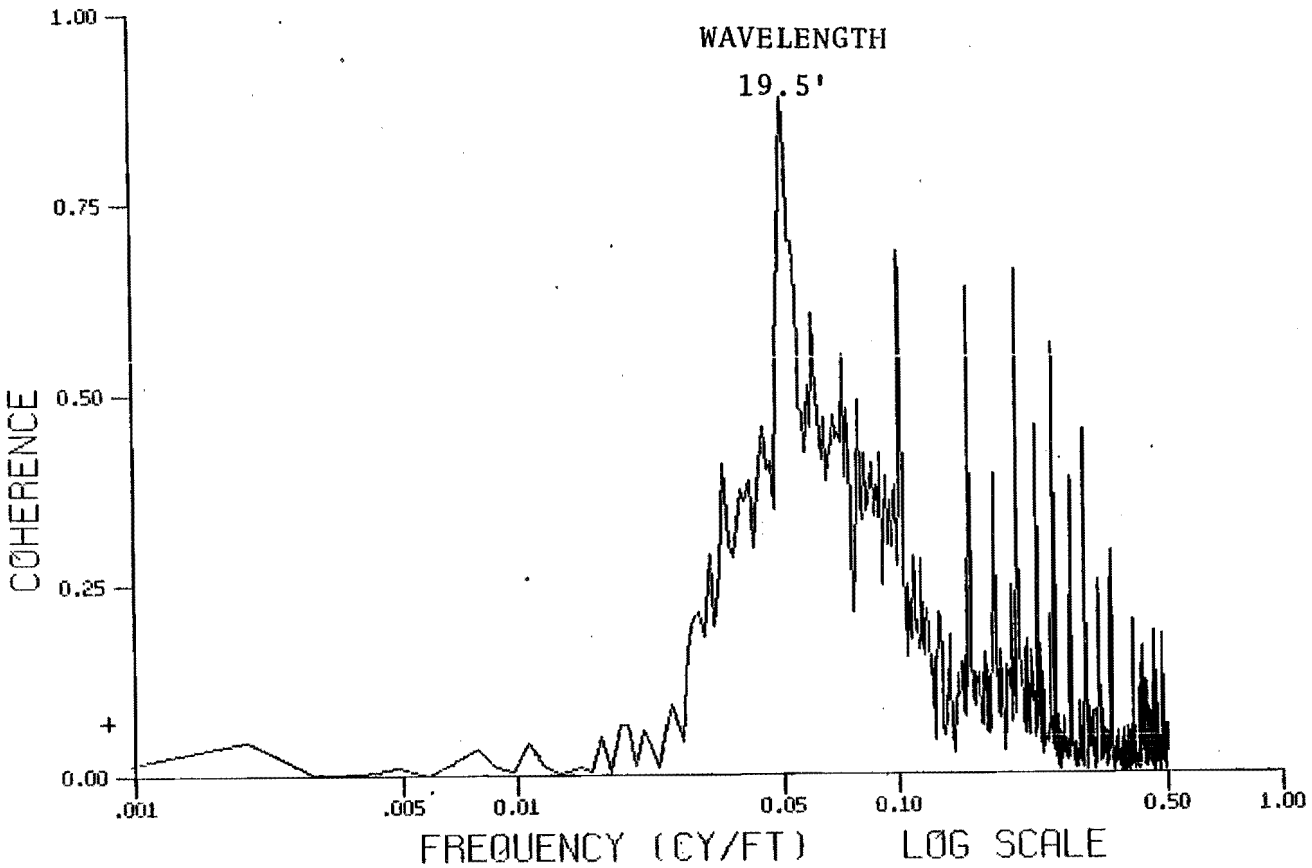

Figure 4-23. Coherence Between Gage and Mean Profile

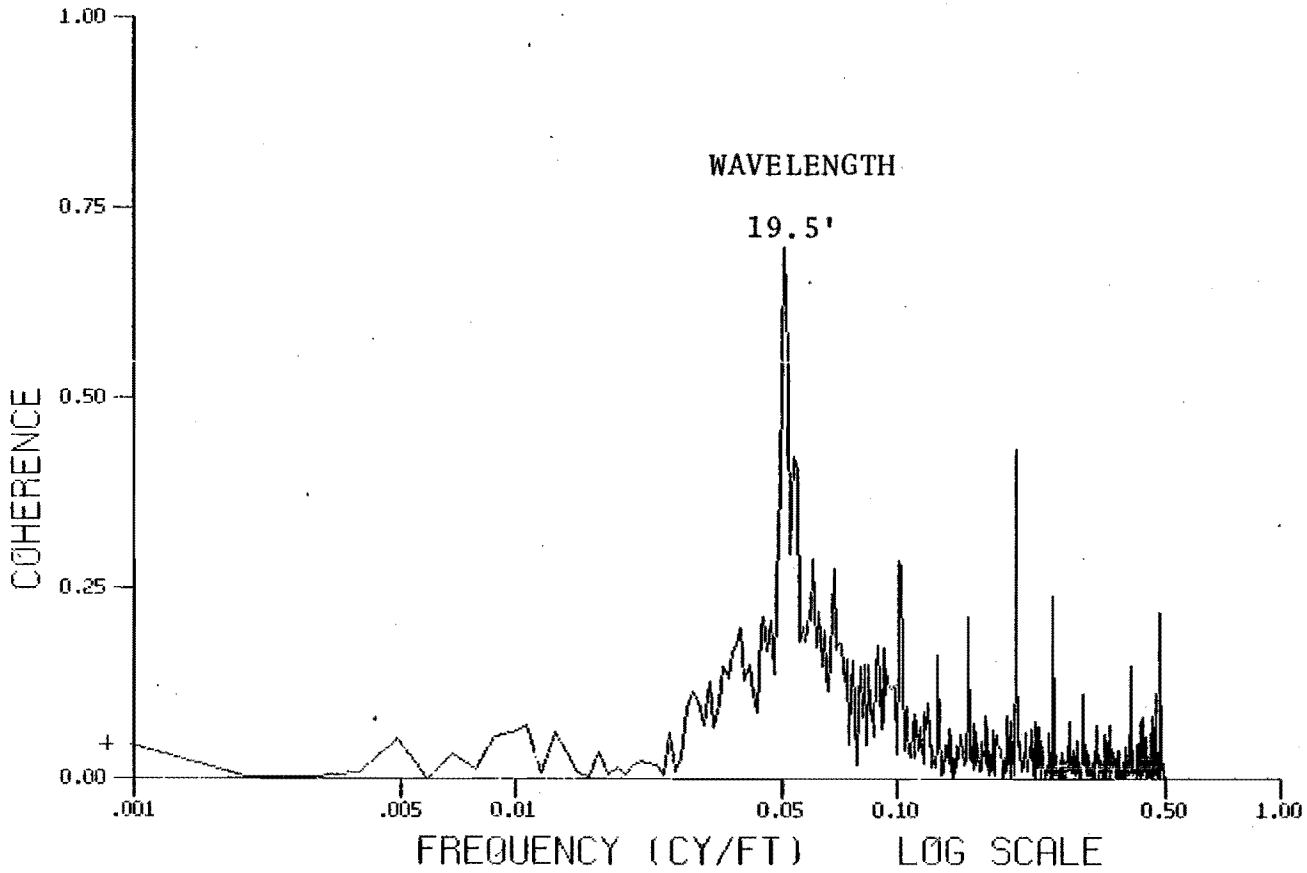

Figure 4-24. Coherence Between Left Profile and Left Alignment

In some cases, gage showed stronger relationship with one rail than the other. Further analyses showed that, in general, the coherence between gage and single rail aligment variations was of the same order of magnitude for both rails when the alignment variations in the two rails were of similar magnitude. However, in some cases one rail showed more alignment variations than the other. In such cases, gage had stronger relationships with the rail having more alignment activity. For example, in curves where the track has been subjected to traffic at speeds higher than the balance speed provided by the superelevation, the high rail will exhibit more alignment variations than the low rail. In this case, gage variations will have stronger correlation with alignment variations of the high rail than those of the low rail.

The transfer function between gage and single rail alignment variations can be characterized by the gain factor (alignment/ gage) and phase angle. For shorter wavelengths, the phase angle betwen gage and left alignment is typically zero, whereas, the value for right alignment is 180 degrees. This is due to the sign conventions used in gage and alignment measurements, i.e., a positive value of left alignment corresponds to increasing gage and a positive value of right alignment corresponds to decreasing gage. The gain factor has an average value of 0.5. No significant variations were found among different track classes. A common gain value of 0.5 for left and right alingment means that one-half of the gage variations are associated with the alignment variations of one rail and the other half are associated with the alignment variations of the other rail. Note that this applies only to the short wavelength gage variations which are linearly related with alignment variations.

Based on the relations between gage and alignment variations, it is concluded that a rail can either go in (towards track centerline) or out (towards the field side) at joints with the amplitude of alignment varying randomly from one joint to the other. It was found that the low rail is more likely to go in and the high rail is more likely to go out at joints. This may be due to the tendency of the rail to straighten itself in curves. As discussed earlier, if one rail is consistently subjected to more lateral load than the other, it will exhibit more alignment activity.

The alignment at joints can be modeled by exponential, rectified inverted sinusoidal, or triangular cusps. The amplitude of these cusps varies randomly from one joint to the other.

Surface variations of the two rails have strong linear relationship for wavelengths longer than 20 feet. However, the half staggered joints result in insignificant coherence between the surface variations of the left and right rail at 39 feet wavelength for the bolted track.

Crosslevel variations have no linear relationship with the mean rail profile and generally have insignificant linear relationship with the single rail profile also. The crosslevel at a joint is predominantly due to a low joint on one rail. This gives a strong coherence between crosslevel and the single rail profile at 39 feet wavelength for bolted track.

The profile exhibits negative cusps at joints. This can be characterized by an exponential model as a function of joint amplitude and a decay factor. The joint amplitude varies randomly from one joint to the other.

In general, there is an insignificant correlation between crosslevel and alignment variations. However, relatively large amplitude variations on joints increase the coherence at 39 feet wavelength. Large long wavelength variations can also occur simultaneously in crosslevel and alignment in some track zones. In such cases, crosslevel shows

strong coherence with alignment variations at some discrete wavelengths typically between 50 and 90 feet.

Typically, there is no correlation between gage and crosslevel variations. This, in general, is also true for gage and profile variations as well as profile and alignment variations. However, simultaneous degradation of track geometry parameters may result in significant coherence at certain wavelengths. The bolted track sections analyzed in this study exhibited strong coherence between the gage and profile and betwen the profile and alignment at a wavelength equal to one-half the rail length.

5.0 RMS VARIATIONS

During the investigations of relationship between gage and alignment, gage occasionally showed better relationship with the alignment of one rail than that of the other. In such cases, the rail having better relationship with gage was found to have more alignment activity than the other. It was hypothesized that the rail with more alignment activity may have been consistently subjected to more lateral load than the other.

Track geometry data were analyzed to determine if statistically there was a difference between the alignment variations of the two rails as a function of degree of curvature and superelevation. This section describes the effect as revealed by the analyses. During these analyses, an rms processor* was used as a descriptor of alignment variations. Results on this processor are also described in this section. Analyses were also conducted to determine the difference between the surface variations of the low and high rail. Results of these analyses appear in Section 5.2.

5.1 GAGE AND ALIGNMENT

Two methods were used to determine the effect of curvature and superelevation on gage and alignment variations. In the first method, sections of track geometry data were separated according to the degree of curvature. RMS variations of gage and alignment were computed separately for each section. Only the data in the body of curves were used and spirals were excluded during this processing. Results are tabulated in Appendix F.

In the second method, a moving point rms window was used to compute the gage and alignment roughness continuously as a function of distance along the track. Plots of gage and alignment variations as a function of distance along the track were generated to analyze these variations. Average values of gage and alignment variations both for typical and isolated variations are tabulated in Appendix F. A summary and discussion of these results is provided in the following sections. Note that the alignment here is defined as the lateral rail deviation from uniformity and typically has a mean of zero.

5.1.1 EFFECT OF CURVATURE

Figure 5-1 shows rms values of gage as a function of curvature for Class 3 bolted track. The data shows a slight increasing trend with the degree of curvature. However, there is enough scatter in the data and the gage rms can be considered more or less constant over the entire curvature range shown in Figure 5-1. Thus no significant effect of curvature is evident in the data analyzed here.

Figure 5-2 shows the alignment variations as a function of curvature for Class 3 bolted track. The curvature does not seem to have any consistent effect on the magnitude of either rail alignment. In general, for curves less than 5 degrees, the high rail shows slightly larger rms values than the low rail. On the other hand, for curves greater than 5 degrees, the low rail shows slightly larger variations than the high rail. However, in both cases, the differences are not very significant.

Table 5-1 shows the average gage and alignment variations in curves for Class 2, 3 and 5 track. Note that for each track class, the rms value of the low rail alignment is almost equal to the rms value of

*root mean square processor (2).

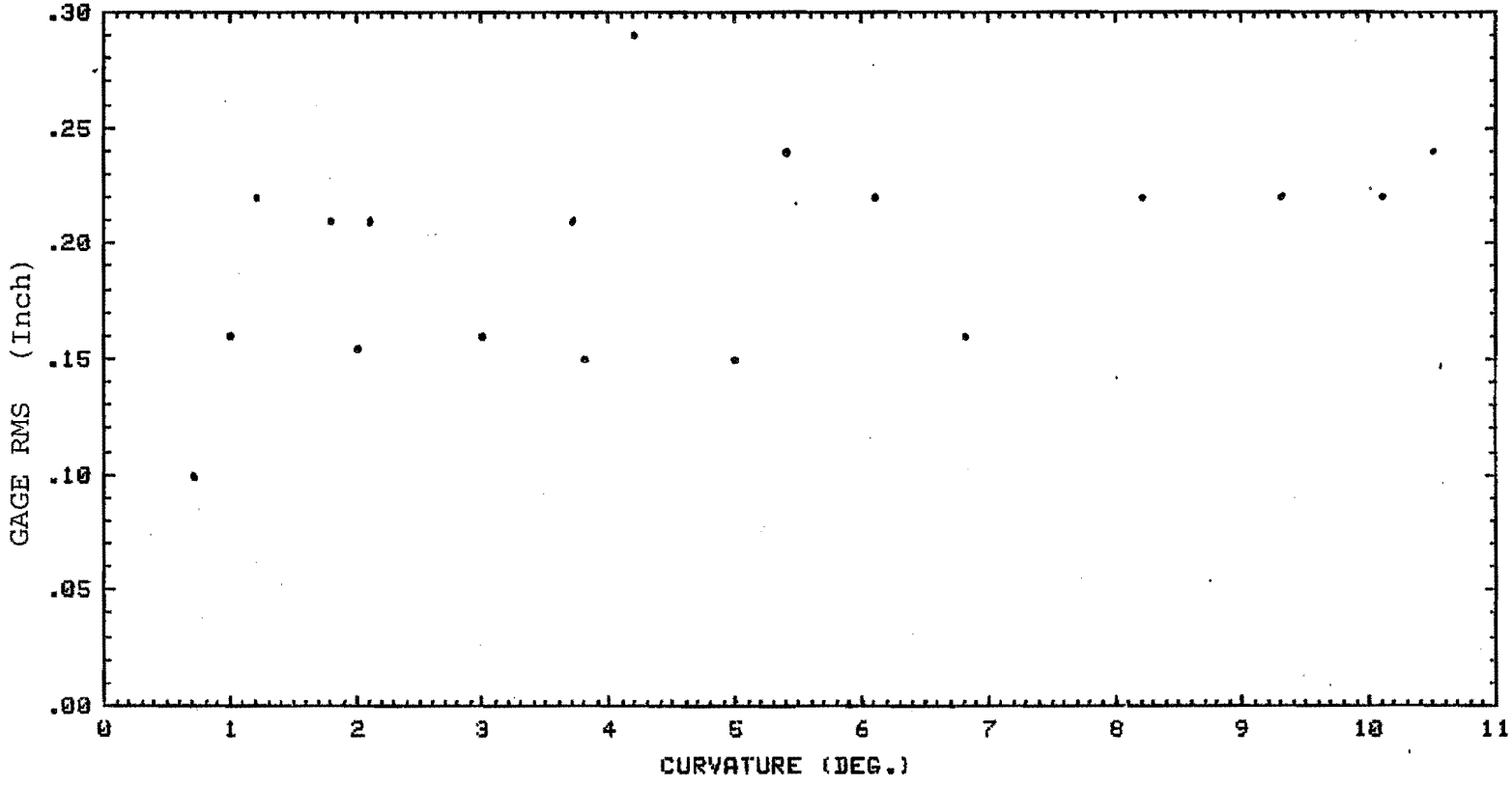

Figure 5-1. Gage Variations as a Function of Curvature

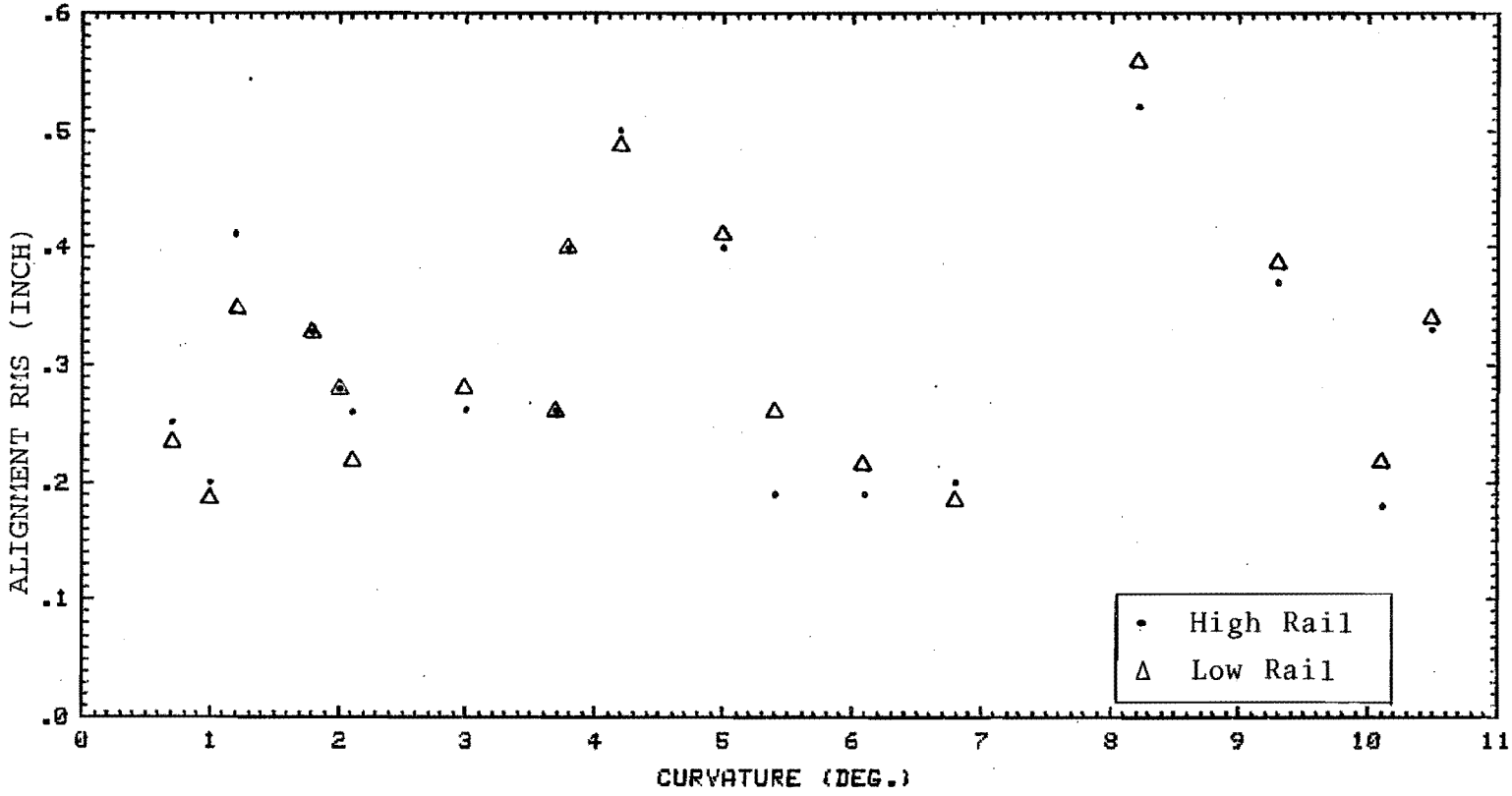

Figure 5-2. Alignment Variations as a Function of Curvature

TABLE 5-1

AVERAGE RMS VALUES OF GAGE AND ALIGNMENT IN CURVES

Track Class	Bolted or Welded Rail	RMS Value (inch) Gage	Low Rail Alignment	High Rail Alignment
2	Bolted	0.41	0.43	0.43
3	Bolted	0.19	0.29	0.29
4	Bolted	0.10	0.16	0.15
5	Welded	0.10	0.15	0.14

the high rail alignment. Therefore, it can be concluded that on the average, the alignment variations of the two rails are of the same order of magnitude.

5.1.2 EFFECT OF SUPERELEVATION

Figure 5-3 shows the effect of superelevation on gage variations for Class 2 and 3 bolted track. Here the gage rms is plotted versus (E - e)*

where:

E = measured superelevation (inch)

e = balanced superelevation for specific values of C and V

$= 0.00066\ CV^2$

C = curvature (degrees)

and V = posted speed (mph).

As expected, values of the gage rms of Class 2 track are higher than those of Class 3 track. The gage rms shows an increasing trend as E - e goes away from zero which is also to be expected. However, no conclusive results can be drawn because of the scatter in the data.

Figure 5-4 shows the effect of superelevation on alignment variations. Here the rms values of the low and high rail alignment are plotted versus E - e. As expected, the rms value of either rail alignment shows an increasing trend as the magnitude of E - e increases. However, no consistent difference is found between the alignment variations of the low and high rail.

One would expect that for positive values of E - e, the low rail should have more alignment activity than the high rail. On the other hand, for negative values of E - e, the high rail should have more alignment activity than the low rail. This behavior is not apparent from Figure 5-4. The following possible reasons can be given for this discrepancy:

*Note that (E - e) 0 means that traffic is below balance speed and (E - e) > 0 means that traffic is above balance speed.

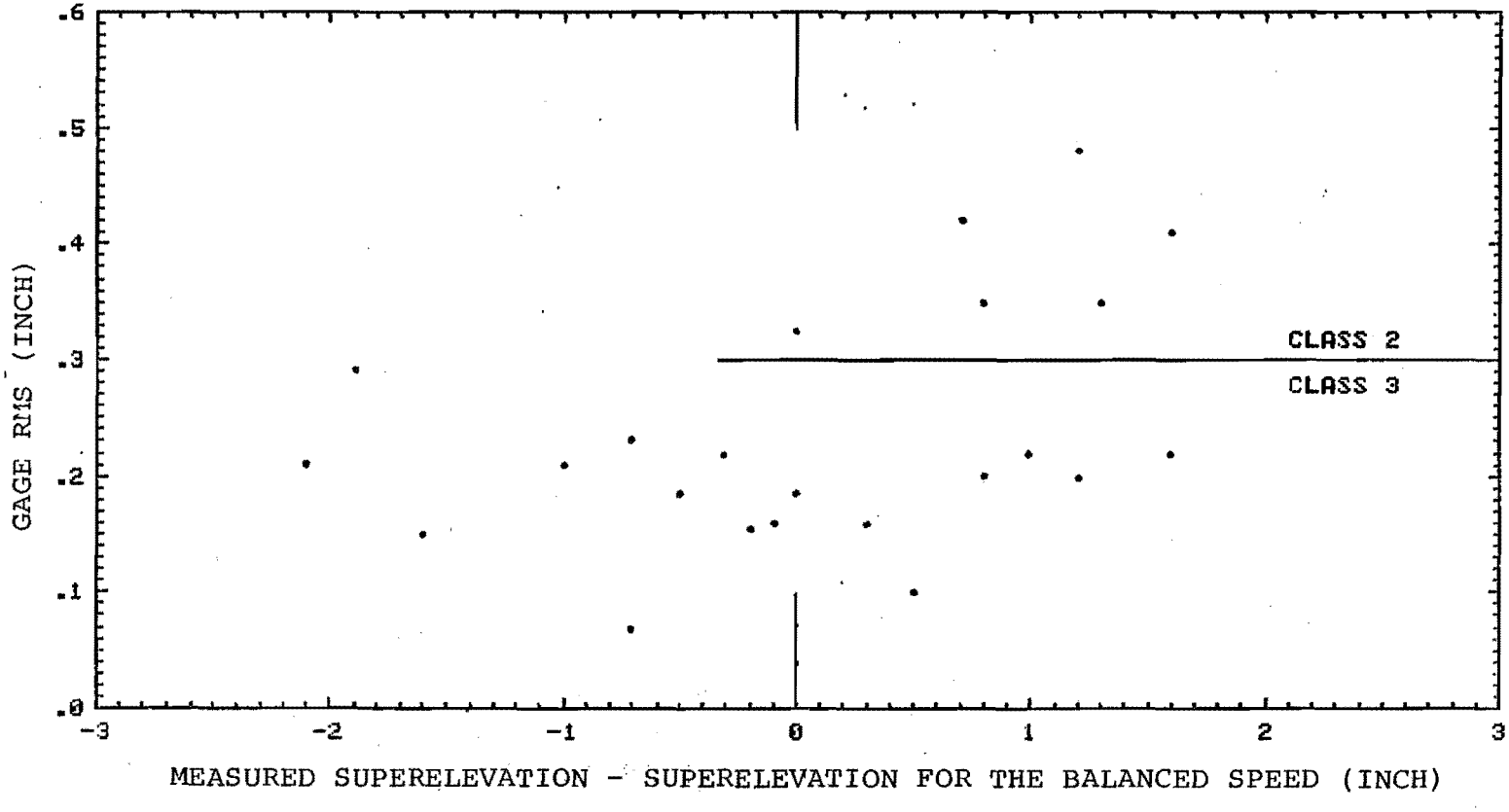

Figure 5-3. Effect of Superelevation on Gage Variations

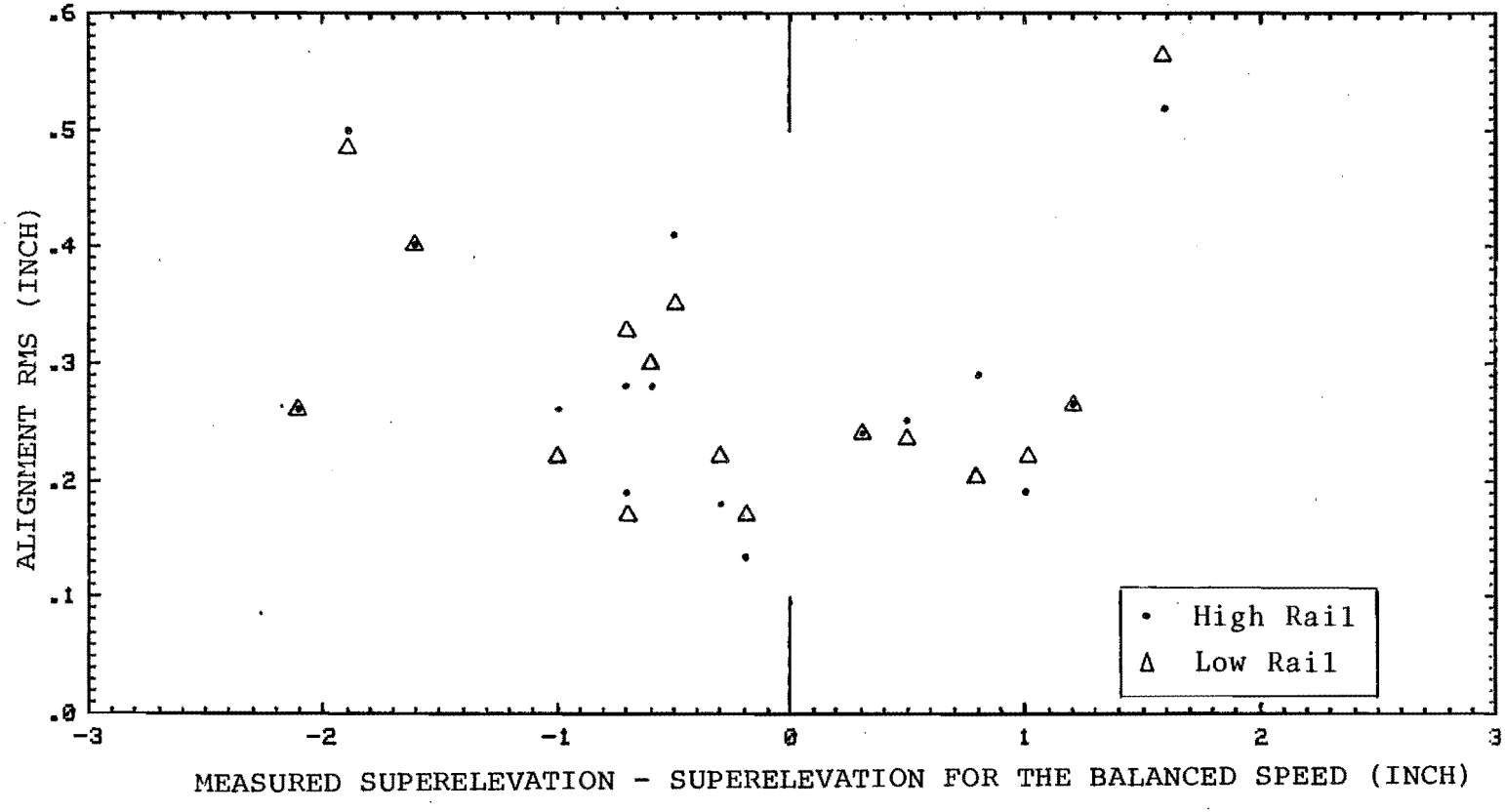

Figure 5-4. Effect of Superelevation on Alignment Variations

- The range of E - e for the existing data is not large enough to isolate the difference between the alignment variations of the high and low rail as a function of E - e.

- The balance superelevation is calculated from the present posted speed. The posted speed varies over the life of the track. Further, the traffic may not always move at the posted speed.

Therefore, no definite conclusions can be made on a statistical basis regarding the difference between the low and high rail alignment variations as a function of superelevation from the existing data. Although, as noted in Section 4, in isolated cases, one rail may have more alignment variations than the other which can be associated with operation at unbalanced speeds.

5.1.3 MOVING POINT RMS

An rms descriptor was used to analyze the typical and isolated variations of gage and alignment. RMS values of mean-removed gage and alignment space curve were computed continuously using a 200 foot moving point window. The following parameters were computed and plotted as a function of distance along the track:

a_r = rms of right alignment (inch)

a_ℓ = rms values of left alignment (inch)

a_m = rms value of mean alignment (inch)

a_g = rms vlaue of mean removed gage (inch)

$a_r + a_\ell$ = rms value of right alignment plus rms value of left alignment (inch)

a_g/a_r = rms value of gage/rms value of right alignment

a_g/a_ℓ = rms value of gage/rms value of left alignment

a_g/a_m = rms value of gage/rms value of mean alignment

$\frac{a_g^2}{a_\ell^2 + a_r^2}$ = mean square value of gage/mean square of left alignment plus mean square of right alignment

These parameters were plotted along with gage, alignment, curvature and crosslevel. It was found that the moving point rms was useful to discriminate between typical and isolated alignment variations (Section 3.0).

Figure 5-5 shows an example where this descriptor is used to separate the isolated from typical alignment variations. As shown in Figure 5-5(a), the alignment includes an isolated variation in the form of a jog. The rms values of alignment in the vicinity of this variation are significantly larger than the values for typical variations (Figure 5-5(b)). The ratios of rms values as shown in Figure 5-5(c) are useful to study the relative magnitude of gage and alignment variations. Figure 5-5(c) shows large ratios at the beginning due to low alignment activity in this area.

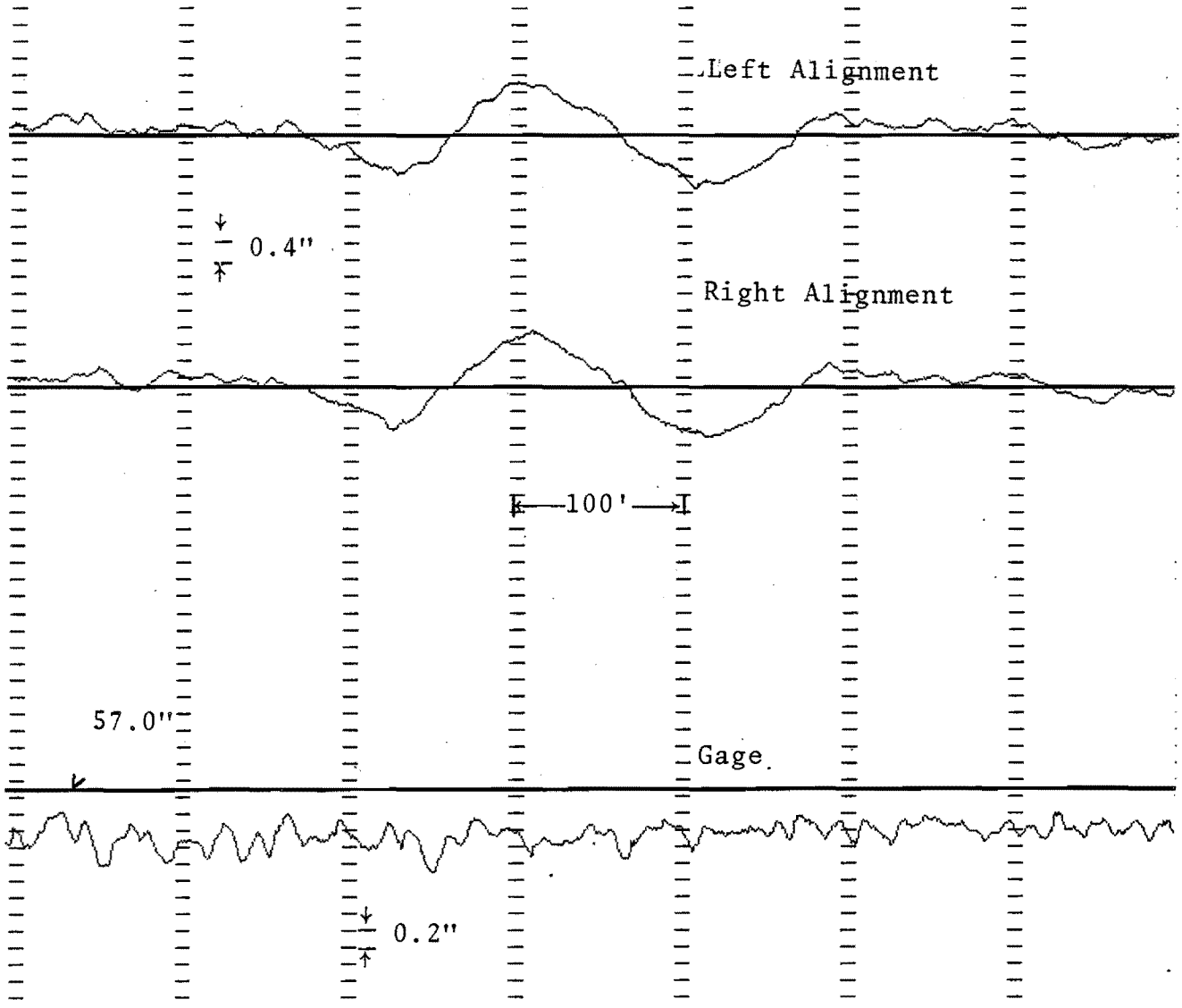

Figure 5-5(a). Typical and Isolated Alignment Variations, Measured Gage and Alignment

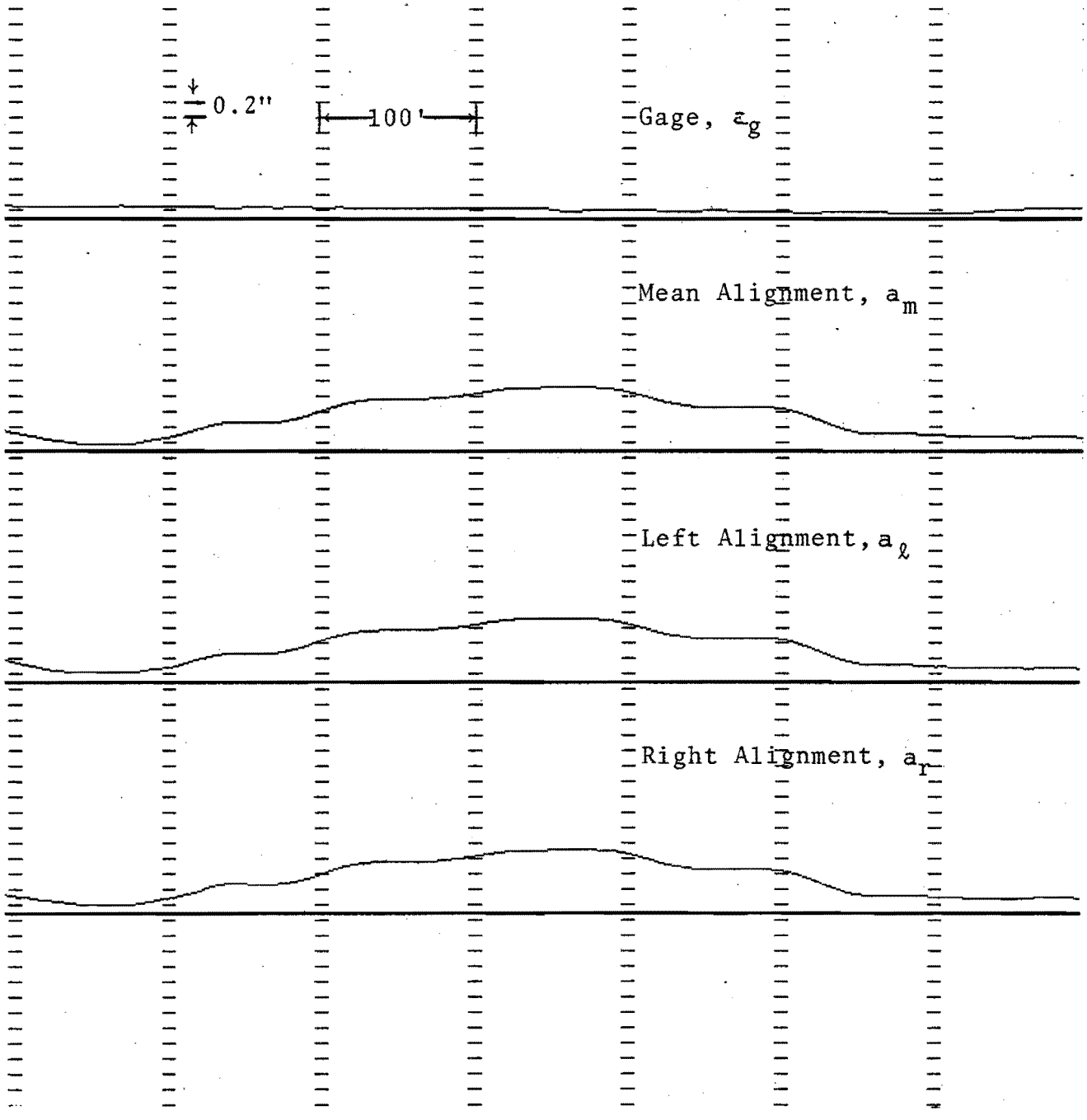

Figure 5-5(b). Typical and Isolated Alignment Variations, rms Variations of Gage and Alignment

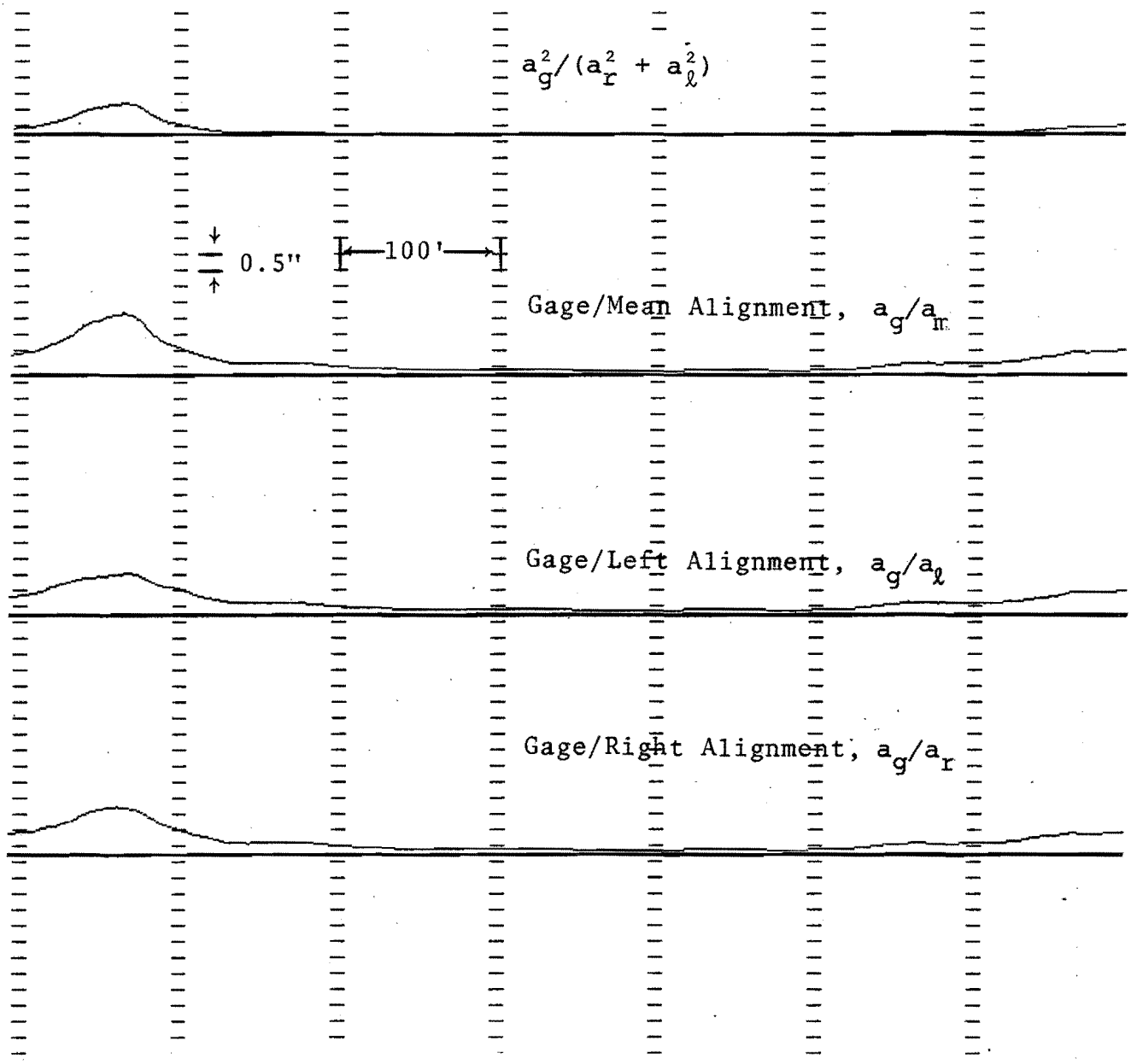

Figure 5-5(c). Typical and Isolated Alignment Variations, Ratios of rms Variations of Gage and Alignment

Figure 5-6 includes an isolated variation in gage in the form of a bump. Figure 5-6(b) shows significantly large rms values of gage in this vicinity. This is also reflected in the plot of ratios in Figure 5-6(c). The values of rms parameters for gage and alignment variations were recorded for Class 2 and 3 track. These values along with mean gage, curvature and crosslevel are tabulated in Appendix F.

Figure 5-7 is a plot of typical and isolated alignment variations as a function of curvature for Class 3 bolted track. Figure 5-8 shows the typical and isolated alignment variations for Class 2 bolted track as a function of E - e. Note that no consistent pattern is evident about the alignment variations either as a function of E - e or as a function of curvature. The rms values of gage, mean alignment and the ratios of gage and alignment variations were also plotted as a function of curvature and superelevation. No definite relationship was found between any of these parameters and either the curvature or superelevation.

Both Figures 5-7 and 5-8 show that the rms values for isolated variations are distinctly larger than the values for typical variations. Therefore, the 200-foot moving point rms descriptor can be used to distinguish between the typical and isolated alignment variations.

Table 5-2 gives the range of the rms descriptor values for Class 2 and 3 track. The average rms values for typical gage and alignment variations are given in Table 5-3. Average rms values for isolated variations are listed in Table 5-4. Note that these values are much larger than the corresponding values for typical variations.

5.1.4 SHORT WAVELENGTH VARIATIONS

The gage and alignment data were high-pass filtered to investigate the short wavelength variations. The long wavelength cutoff for this filter was approixmately 50 feet. The 200-foot moving point window was then used to calculate the rms gage and alignment variations. The rms values were plotted as a function of distance along the track and the analyses similar to the one described in Section 5.1.3 were conducted to analyze the short wavelength variations.

The rms values for both the gage and alignment were almost constant showing no effect of curvature or crosslevel. The average rms values for gage, high rail alignment, low rail alignment and mean rail alignment were 0.09, 0.09, 0.07 and 0.11, respectively.

Figure 5-9 shows the effect of filter on alignment variations. Note that the long wavelength isolated variation has been taken out by the filter. This is also indicated by the smaller rms values for short wavelength variations.

Figure 5-10 shows the rms value after filtering the data shown in Figure 5-5. The effect of the long wavelength isolated alignment variation (jog) has been removed and the rms values in this case are much smaller and constant throughout.

Figure 5-11 shows the rms values of short wavelength gage and alignment variations for the data shown in Figure 5-6. Again note that the effect of isolated gage variation (bump) is not noticeable any more and that the rms value of gage is constant throughout.

This section has shown that the scatter in rms values is mainly due to the long wavelength (50 - 200 feet) gage or alignment variations. In addition, the isolated variations are mainly the long wavelength variations.

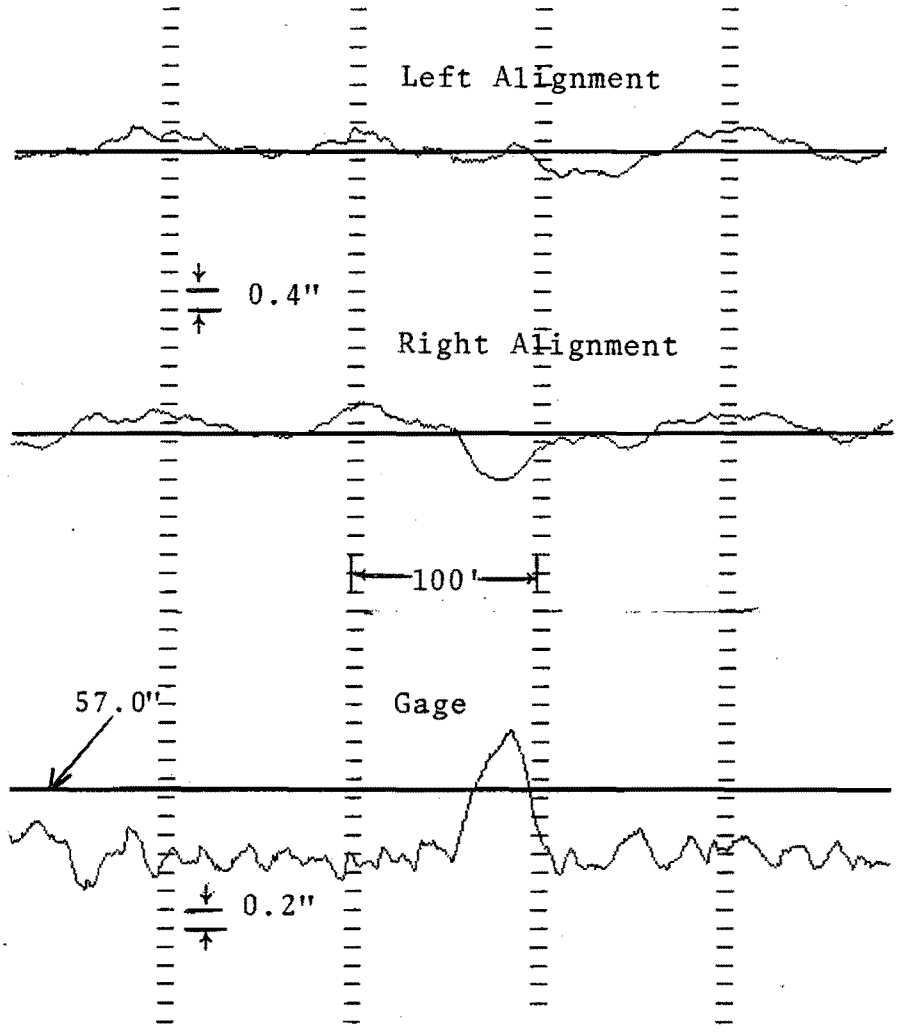

Figure 5-6(a). Typical and Isolated Gage Variations Measured Gage and Alignment

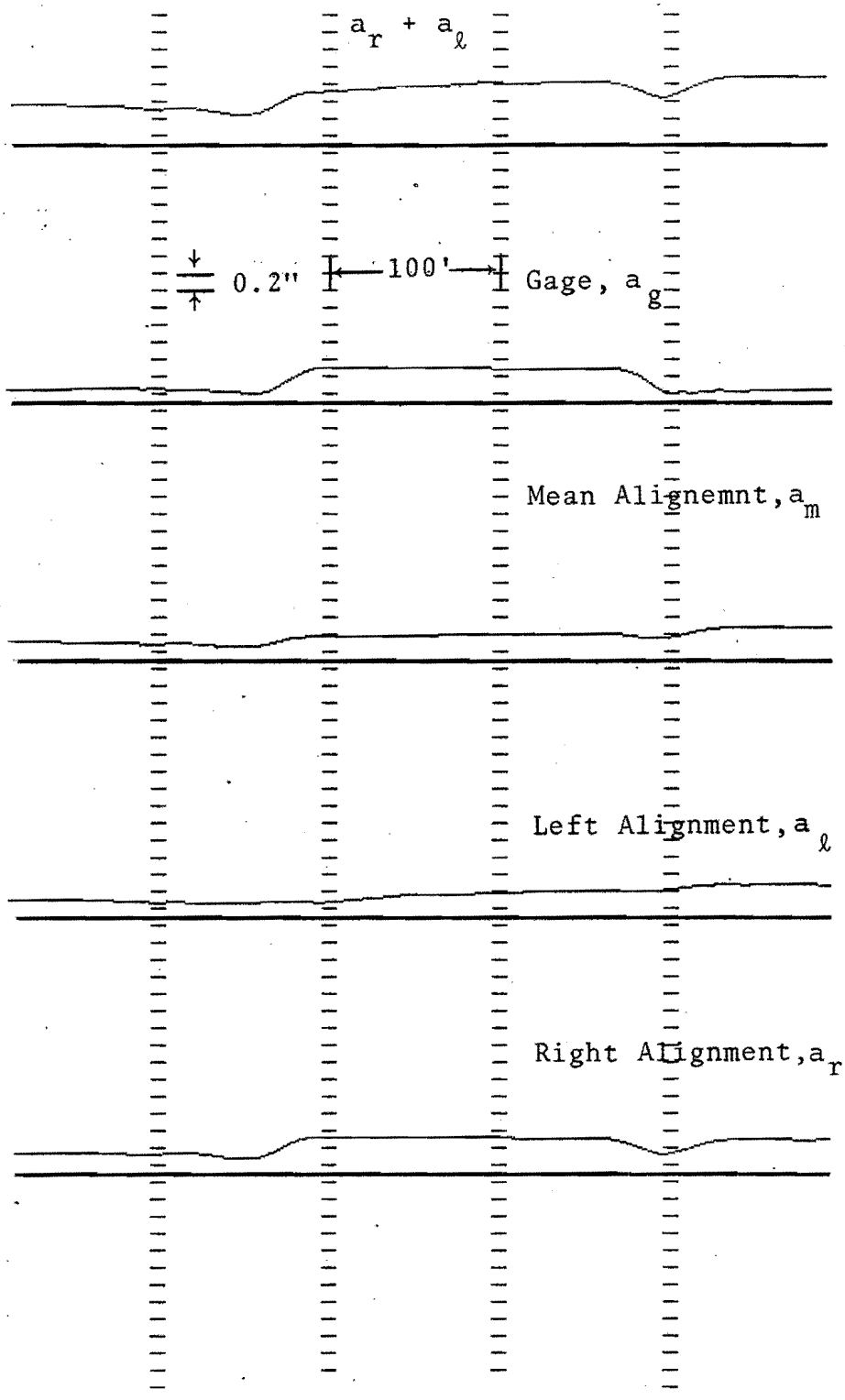

Figure 5-6(b). Typical and Isolated Gage Variations
rms Variations of Gage and Alignment

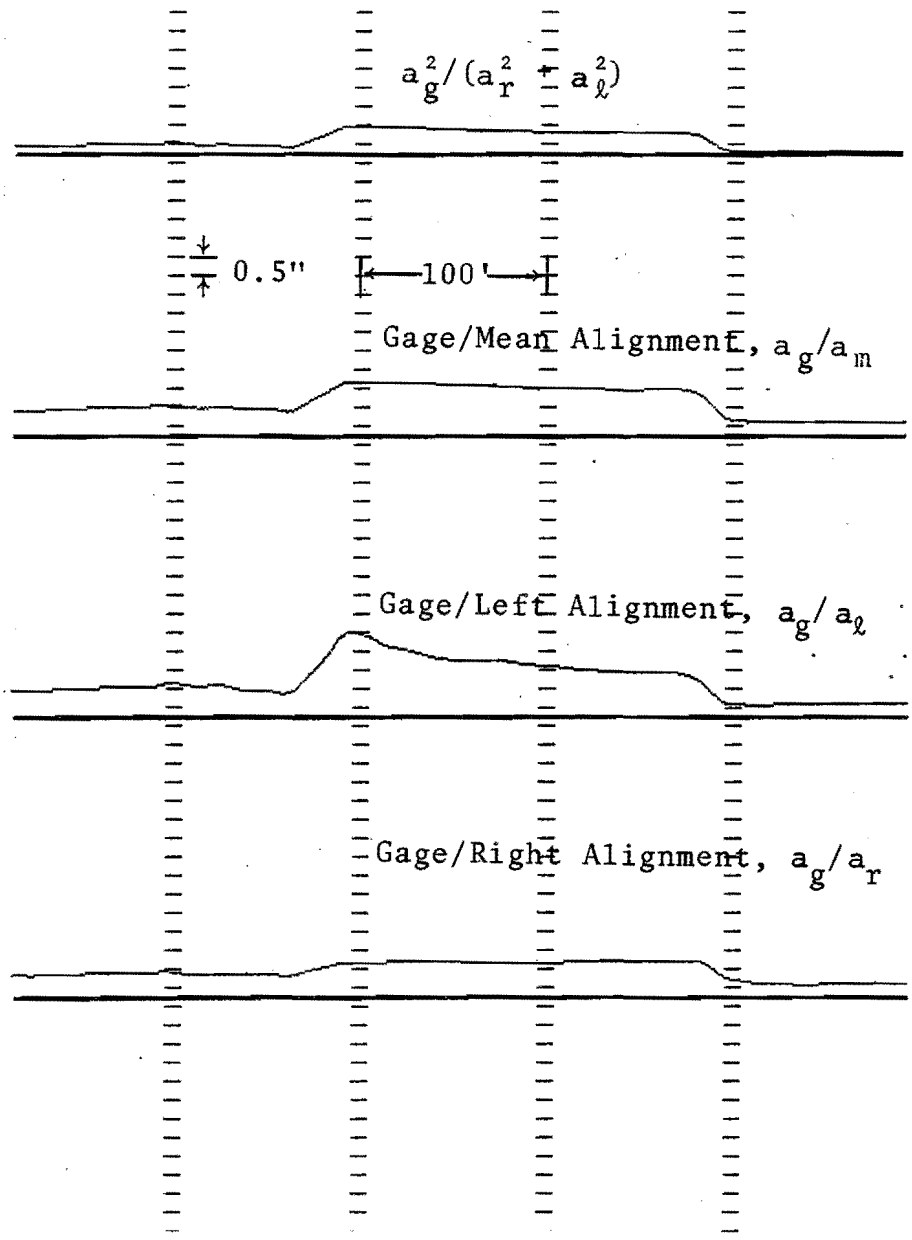

Figure 5-6(c). Typical and Isolated Gage Variations, Ratios of rms Variations of Gage and Alignment

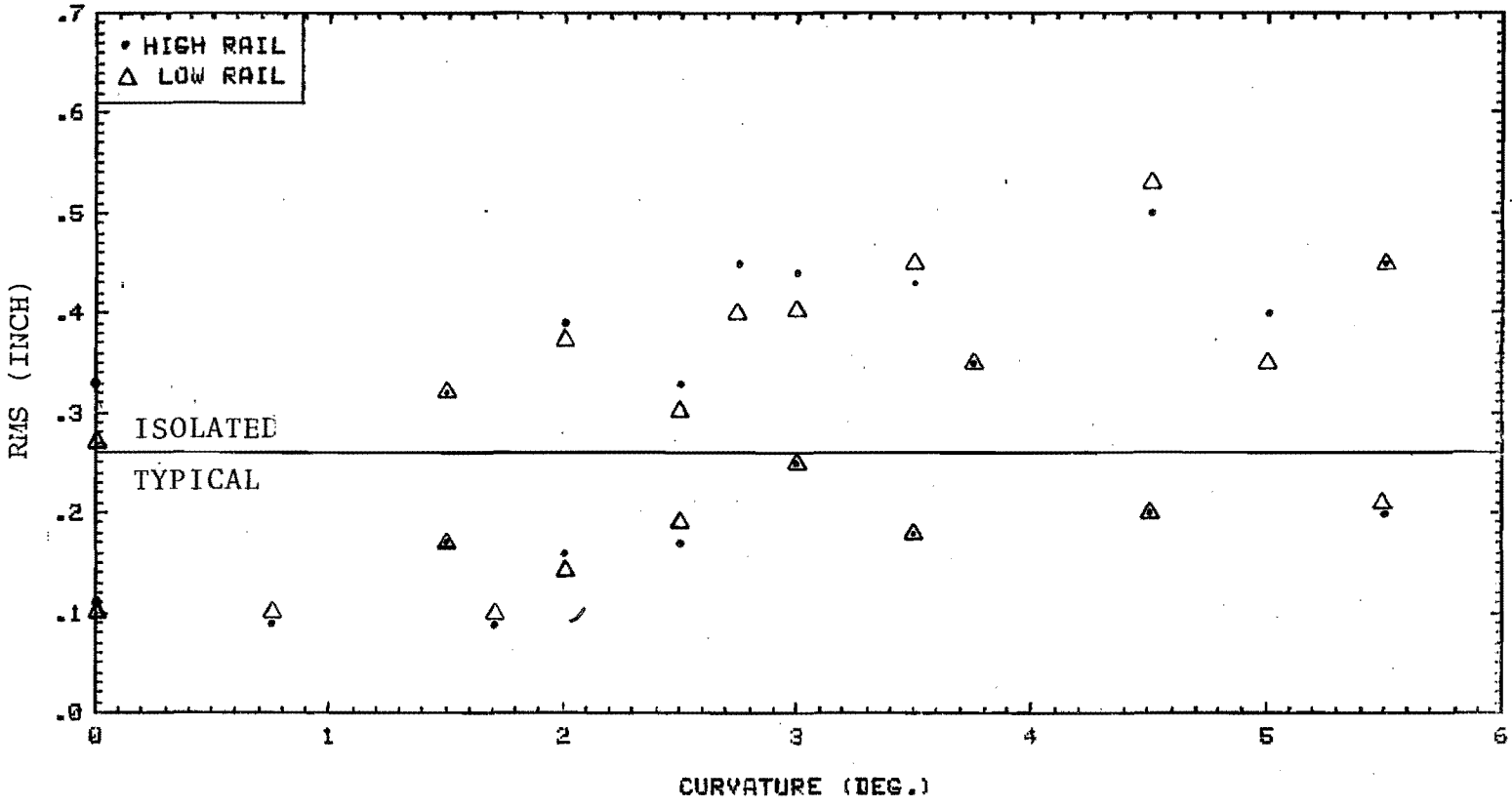

Figure 5-7. RMS Variations of Alignment as a Function of Curvature for Class 3 Bolted Track

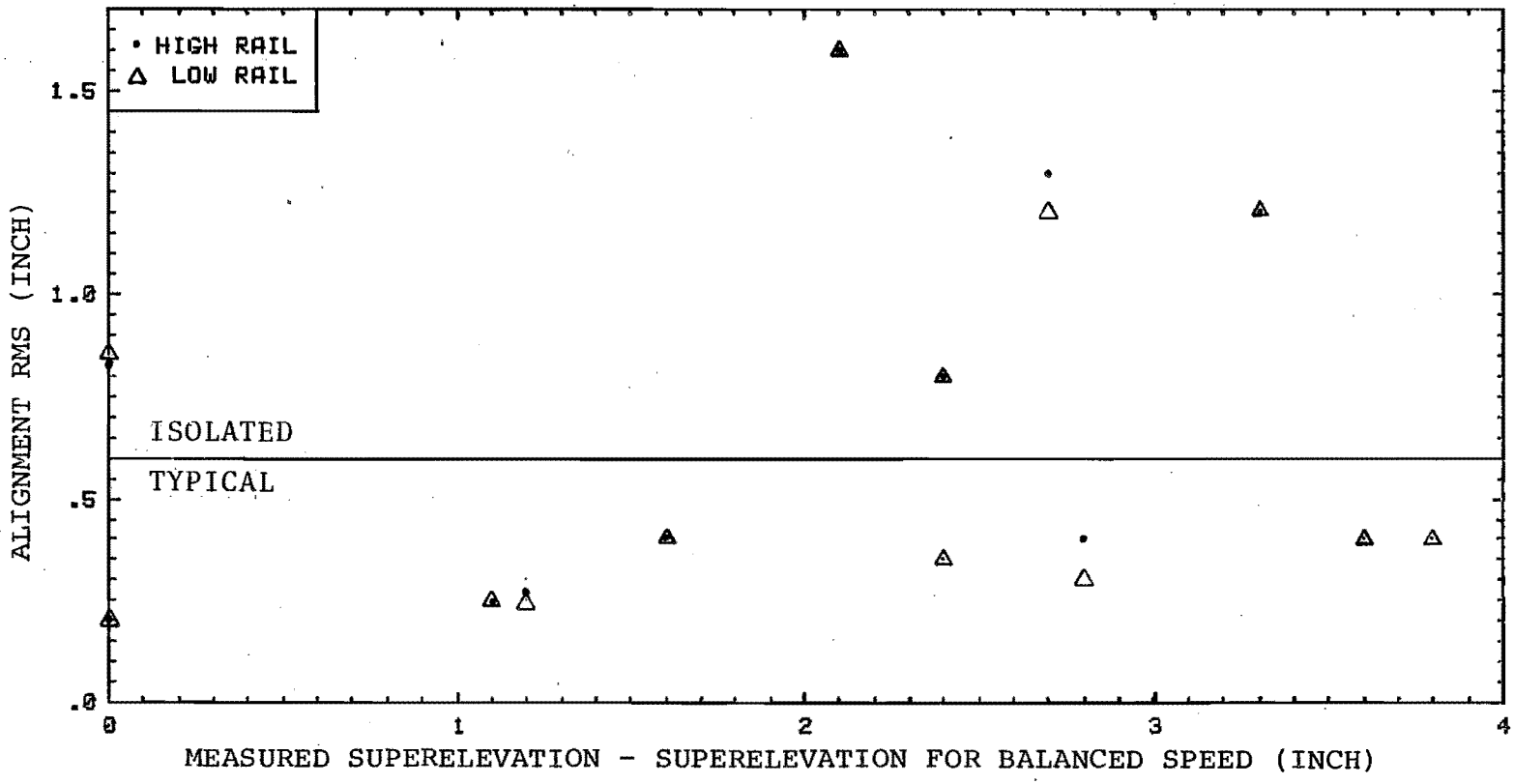

Figure 5-8. RMS Variations of Alignment as a Function of Superelevation for Class 2 Bolted Track

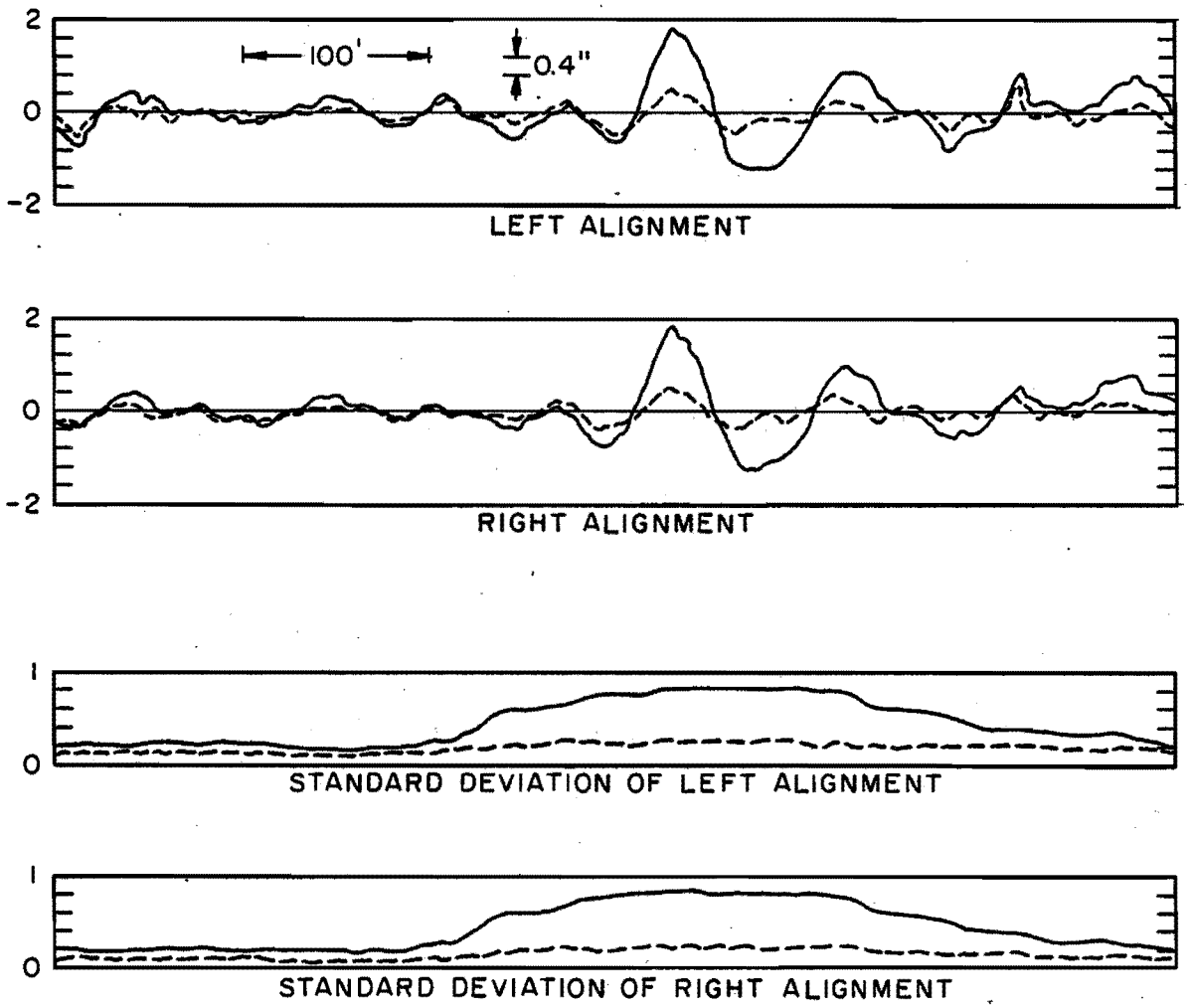

SOLID LINE - MEASURED VARIATIONS

DOTTED LINE - SHORT WAVELENGTH VARIATIONS (UP TO 50 FEET)

Figure 5-9. Comparison of Short and Long Wavelength Alignment Variations

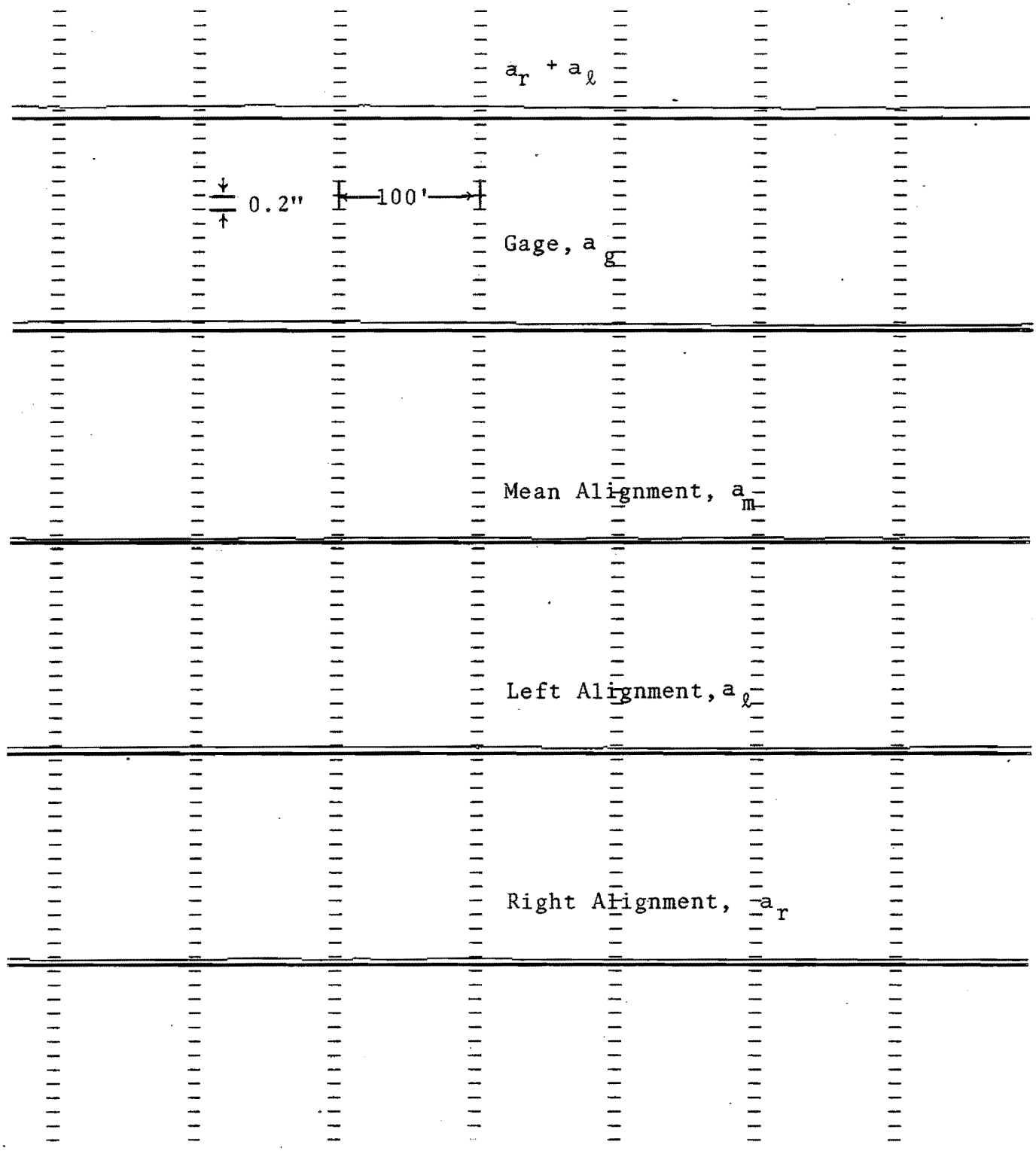

Figure 5-10. Short Wavelength rms Variations Corresponding to Data Shown in Figure 5-5

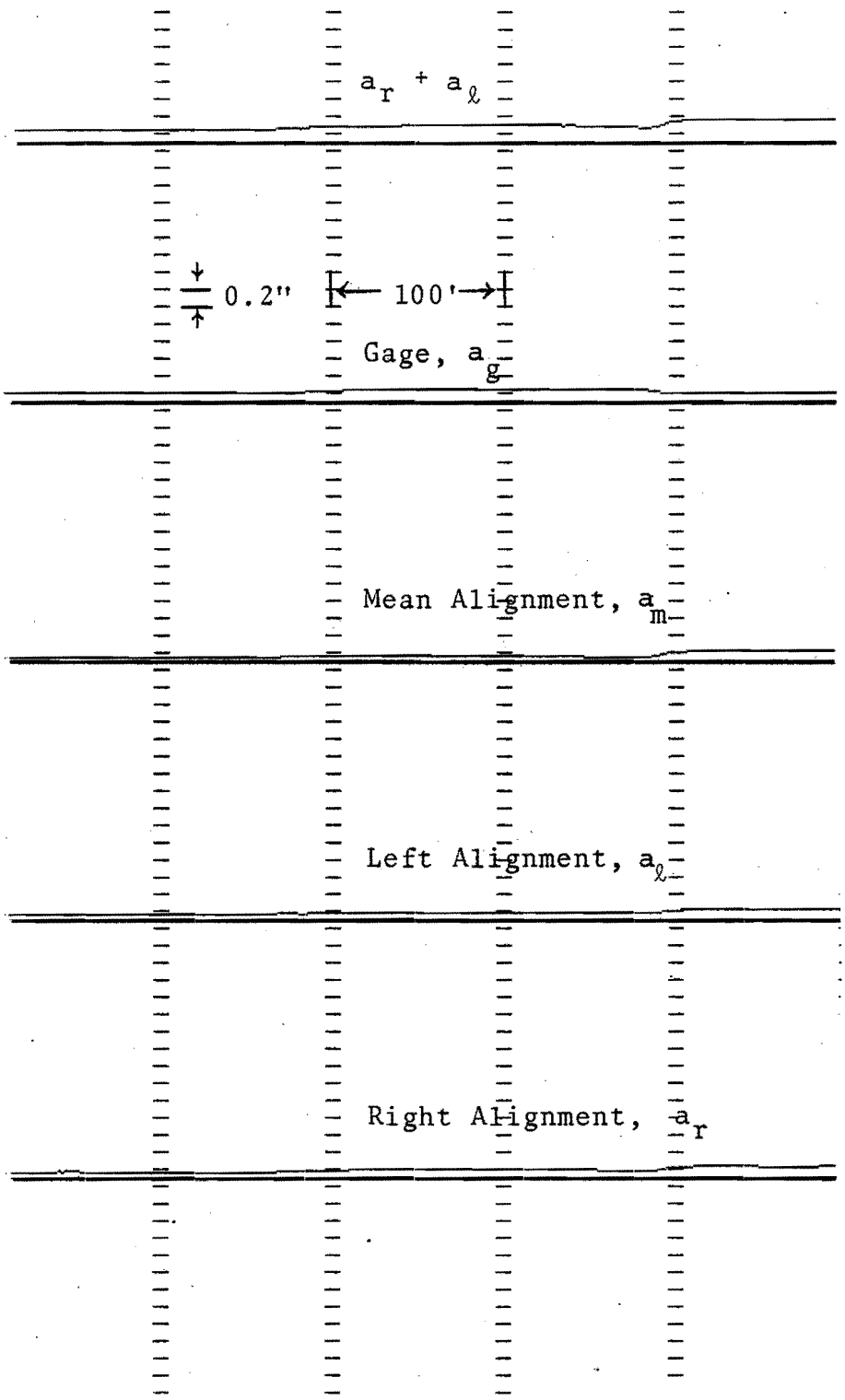

Figure 5-11. Short Wavelength rms Variations Corresponding to Data Shown in Figure 5-6

TABLE 5-2

RANGE OF RMS GAGE AND ALIGNMENT VARIATIONS* (INCH)

Track Class	Track Type	Minimum or Maximum	a_g	a_ℓ	a_h	a_m
2	Bolted	Minimum	0.10	0.20	0.20	0.20
		Maximum	0.30	1.60	1.60	1.60
3	Bolted	Minimum	0.07	0.10	0.10	0.10
		Maximum	0.35	0.65	0.60	0.65
3	Welded	Minimum	0.08	0.10	0.10	0.10
		Maximum	0.30	1.01	1.00	1.00
2,3	Large Curves Bolted	Minimum	0.10	0.10	0.15	0.12
		Maximum	0.25	0.80	0.80	0.80

*Calculated using 200-foot moving point window.

a_g = rms value of mean removed gage
a_ℓ = rms value of low rail alignment
a_h = rms value of high rail alignment
a_m = rms value of mean alignment

TABLE 5-3

AVERAGE RMS VALUES OF TYPICAL GAGE AND ALIGNMENT VARIATIONS* (INCH)

Track Class	Track Type	a_g	a_ℓ	a_h	a_m
2	Bolted	0.12	0.29	0.30	0.29
3	Bolted	0.11	0.13	0.14	0.13
3	Welded	0.11	0.13	0.12	0.12
2,3	Large Curves Bolted	0.17	0.22	0.21	0.21

*Calculated using 200-foot moving point window.

a_g = rms value of mean removed gage

a_ℓ = rms value of low rail alignment

a_n = rms value of high rail alignment

a_m = rms value of mean alignment

TABLE 5-4

AVERAGE RMS VALUES OF ISOLATED GAGE AND ALIGNMENT VARIATIONS* (INCH)

Track Class	Track Type	a_g	a_ℓ	a_h	a_m
2	Bolted	0.19	0.85	0.84	0.84
3	Bolted	0.16	0.37	0.38	0.37
3	Welded	0.13	0.35	0.35	0.35
2,3	Large Curves Bolted	0.19	0.58	0.54	0.55

*Calculated using 200-foot moving point window.

a_g = rms value of mean removed gage

a_ℓ = rms value of low rail alignment

a_n = rms value of high rail alignment

a_m = rms value of mean alignment

5.2 PROFILE

Sections of Class 2 and 3 track were processed to determine the difference between the surface variations of the low and high rail. These sections were divided according to the degree of curvature and rms values of profile were computed separately for the low and high rail. Only the data in the body of curves were used and the spirals were excluded from these analyses. Class 3 data were processed separately for the bolted and welded track. Analyses were also conducted separately for short wavelength profile variations dominated by joints in the bolted track.

Table 5-5 lists the surface variations of the low and high rail as a function of degree of curvature and superelevation. Note that the profile space curve represents the deviations from uniformity and has a mean of zero.

A study of Table 5-5 shows no apparent relationship between the surface variations and the superelevation. However, the surface variations appear to increase with the degree of curvature. This is especially true for the low rail variations. Furthermore, the surface variations of the low rail are slightly larger than those of the high rail for the bolted track. For the welded track, surface variations of the low and high rail are of similar magnitude.

As expected, the surface variations of Class 3 track are smaller than those of Class 2 track. Furthermore, the welded track sections are much smoother than the bolted track sections.

The rms value of short wavelength profile are much smaller than the values for overall profile variations. This implies that there are significant profile variations of wavelengths longer than 39 feet.

In summary, the profile variations of the low and high rail are of equal magnitude for the welded track. For class 2 and 3 bolted track, the low rail tends to have more surface variations than the high rail. Furthermore, the surface variations of the low rail increase with the degree of curvature.

5.3 SUMMARY AND CONCLUSIONS

Track geometry data were analyzed to determine the effect of curvature and superelevation on gage and alignment variations. Analyses were also conducted to determine the difference between the surface variations of the low and high rail. The following conclusions can be made based on these analyses.

The curvature has insignificant effect on gage variations in the data analyzed in this study. The curvature does not show any consistent effect on the magnitude of either rail alignment variations. On the average the alignment variations of the low and high rail are of the same order of magnitude.

Alignment variations tend to increase as train speeds reflect more unbalance of superelevation. In isolated cases, one rail may have more alignment variations than the other which can be associated with the operations at unbalanced speeds. However, no definite conclusions can be made from the analyses presented in this section regarding the difference between the alignment variations of the low and high rail as a function of superelevation.

The rms value calculated by using a 200-foot moving point window can distinguish between the typical and isolated variations. The average values of this descriptor both for the typical and isolated variations are given for Class 2 and 3 track.

TABLE 5-5

SURFACE VARIATIONS OF LOW AND HIGH RAIL

Section	Superelevation of High Rail (Inch)	Curvature (Degrees)	Profile Space Curve Variations		Short Wavelength* Profile Variations	
			rms of Low Rail Profile (Inch)	rms of High Rail Profile (Inch)	rms of Low Rail Profile (Inch)	rms of High Rail Profile (Inch)
Class 2 Bolted	0.0	0	0.23	0.23	0.16	0.16
	2.0	1	0.23	0.22	0.16	0.12
	3.0	2	0.24	0.22	0.17	0.12
	4.9	3	0.26	0.22	0.14	0.12
	3.0	4	0.26	0.23	0.21	0.16
Class 3 Bolted	0.0	0	0.15	0.14	0.12	0.11
	2.7	2	0.17	0.16	0.12	0.13
	4.2	4	0.20	0.15	0.15	0.12
	4.6	5	0.33	0.26	0.16	0.15
Class 3 Welded	0.0	0	0.08	0.08	0.06	0.06
	2.1	2	0.08	0.07	0.04	0.04
	3.1	4	0.13	0.13	0.07	0.07
	4.2	5	0.11	0.10	0.06	0.05

*Cut-off wavelength for the high-pass filter was approximately 50.

The surface variations of left and right rail are generally the same for the tangent track. In curves, the surface variations of the low and high rail are of the same order of magnitude for the welded track. For Class 2 and 3 bolted track, the low rail tends to have more surface variations than the high rail. Furthermore, the surface variations of the low rail increase with the degree of curvature.

A significant number of long wavelength variations (greater than 39 feet) are found both in surface and alignment. Isolated variations in alignment and profile are generally the long wavelength variations.

6.0 NEW TECHNOLOGY

A comprehensive review of work performed has revealed no patentable item produced under this effort. However, the work performed under this study significantly contributed to the state-of-the-art in the area of analytical descriptions of track geometry variations.

Analytical descriptions were developed both for typical and isolated track geometry variations. In addition, the relationships between track geometry parameters were developed in order to simulate the actual railroad operating conditions.

A frequency domain analysis program, FEDAL was developed and is fully operational. It accepts the data generated by FRA track geometry cars and generates auto-spectral densities, cross-spectral densities, coherence functions, and transfer functions. This program represents significant improvement over the previous such programs.

It is demonstrated that rms values calculated by using a 200-foot moving point window can be used as a descriptor for gage and alignment variations. This descriptor can distinguish between typical and isolated variations.

7.0 REFERENCES

1. Corbin, J. C., "Statistical Representations of Track Geometry," Volumes I & II, Report Nos. FRA/ORD-80/22.1 and FRA/ORD-80/22.2, National Technical Information Service, Springfield, VA, March 1980.

2. Hamid, A., et al, "Characterization of Relatively Large Track Geometry Variations," ENSCO Report, U.S. Department of Transportation, Office of Rail Safety Research, Washington, DC, October 1979.

3. Hamid, A., et al, "A Prototype Maintenance-of-Way Planning System," Report No. FRA/ORD-80-47.1, National Technical Information Service, Springfield, VA, Nov 1980.

4. Association of American Railroads, "Phase II Track Train Dynamic," R-380, 1978.

5. Hay, W., "Railroad Engineering," John Wiley & Sons, New York, 1953.

6. Kerr, A. D., "Railroad Track Mechanics and Technology," Pergamon Press, New York, 1978, pp. 79-140.

7. Association of American Railroads, "The Track Cyclopedia," Simmons-Boardman Publishing Corporation, Omaha, NE, 1978.

8. Corbin, J. C., "Statistical Characterization of Railway Track Behavior," ASME/IEEE, Joint Railroad Conference, Pittsburgh, IEEE Paper No. C74903-31A, April 1974.

9. Schoeneberg, K. W., "Rail Research--Problem Definition," Report No. R-120, AAR Research Center, Chicago, IL, March 1973.

10. Federal Railroad Administration, Track Safety Standards," reprinted from Railroad Track Structures as published in the Federal Register, February 1973.

11. Remington, P. J., Rudd, M. J., and Ver, I. L., "Wheel/Rail Noise and Vibration," Final Report (2 Volumes), UMTA-MA-06-0025-75-10 and UMTA-MA-06-0025-75-11, May 1975.

12. Otnes, R. K., and Enochson, L., "Digital Time Series Analysis," John Wiley & Sons, New York, 1972, p. 284.

13. Bloomfield, P., "Fourier Analysis of Time Series: An Introduction," John Wiley & Sons, 1976.

14. Bendat, J. S. and Piersol, A. G., "Engineering Applications of Correlation and Spectral Analysis," John Wiley and Sons, New York, 1980, p. 43-47.

15. Lee, H. S., and Weinstock, H., "Rail Car Harmonic Roll Response to Periodic Crosslevel Variations," Report No. WP-743-C-15-075, Transportation Systems Center, 1979, p. 14.

U.S. Department
of Transportation

**Research and
Special Programs
Administration**

Kendall Square
Cambridge, Massachusetts 02142

Postage and Fees Paid
Research and Special
Programs Administration
DOT 513

Official Business
Penalty for Private Use $300